UNITED STATES
DEPARTMENT OF THE INTERIOR
GEOLOGICAL SURVEY

ACOUSTIC-TELEVIEWER AND ACOUSTIC-WAVEFORM LOGS USED TO CHARACTERIZE DEEPLY BURIED BASALT FLOWS, HANFORD SITE, BENTON COUNTY, WASHINGTON

By F. L. Paillet

Open-File Report 85-419

Denver, Colorado

1985

UNITED STATES DEPARTMENT OF THE INTERIOR

DONALD PAUL HODEL, Secretary

GEOLOGICAL SURVEY

DALLAS L. PECK, DIRECTOR

For additional information, write to:

U.S. Geological Survey
Water Resources Division
Mail Stop 403, Box 25046
Denver Federal Center
Denver, Colorado 80225

For purchase, write to:

Open-File Services Section
U.S. Geological Survey
Box 25425
Denver Federal Center
Denver, Colorado 80225
(303) 236-7476; FTS 776-7476

CONTENTS

ILLUSTRATIONS

TABLES

CONVERSION FACTORS

Multiply SI units	By	To obtain inch-pound units
millimeter (mm)	0.03937	inch
centimeter (cm)	0.3937	inch
meter (m)	3.281	foot
kilometer (km)		mile
kilometers per second (km/s)	0.6214	miles per second
microsecond per meter (μs/m)	3.281	microseconds per foot

The following units are listed to define abbreviations:

revolutions per second (r/s)

megahertz (MHz)

kilohertz (kHz)

microsecond (μs)

ACOUSTIC-TELEVIEWER AND ACOUSTIC-WAVEFORM LOGS USED TO CHARACTERIZE DEEPLY BURIED BASALT FLOWS, HANFORD SITE, BENTON COUNTY, WASHINGTON

By F. L. PAILLET

ABSTRACT

Acoustic-televiewer and acoustic-waveform logs were obtained for a 400-meter interval of deeply buried basalt flows in three boreholes, and for shorter intervals in two additional boreholes located on the U.S. Department of Energy's Hanford Site in Benton County, Washington. Borehole-wall breakouts were observed in the unaltered interiors of a large part of individual basalt flows; however, several of the flows in one of the five boreholes had almost no breakouts. The distribution of borehole-wall breakouts observed on the televiewer logs correlated well with the incidence of core disking in some intervals, but the correlation was not always perfect. Breakout orientation could not be accurately determined from most of the televiewer logs because magnetic minerals in the basalt interfered with the operation of the down-hole magnetometer used to orient the logs. Various independent evidence indicated that borehole-wall breakouts were consistently located on the east and west sides of the boreholes. This orientation is consistent with previous estimates of the principal horizontal-stress field in south-central Washington, if breakouts are assumed to form along the azimuth of the least principal stress. The distribution of borehole-wall breakouts repeatedly indicated an interval of breakout-free rock at the top and bottom of flows. Because borehole-wall breakouts usually terminate at major slight-angle fractures, the data indicate that fracturing may have relieved some of the

horizontal stresses near flow tops and bottoms. Acoustic logs did not indicate that basalt in these breakout-free intervals was significantly different from other parts of flow interiors. Unaltered and unfractured basalt appeared to have a uniform compressional velocity of 6.0 $\pm$ 0.1 kilometers per second and a uniform shear velocity of 3.35 $\pm$ 0.1 kilometers per second throughout flow interiors. Acoustic-waveform logs also indicated that borehole-wall breakouts did not affect acoustic propagation along the borehole; so fracturing associated with the formation of breakouts appeared to be confined to a thin zone of stress concentration around the borehole. Televiewer logs obtained before and after hydraulic fracturing in these boreholes indicated the extent of induced fractures, and also indicated minor changes to pre-existing fractures that may have been enlarged during fracture generation. Televiewer logs were compared to the impression-packer images of induced fractures, illustrating the effects of vertical-scale compression and of generally lesser spatial resolution provided by the ultrasonic-televiewer imaging system.

INTRODUCTION

Many different measurement methods have been developed for characterizing the mechanical properties of rocks around boreholes to predict the response of rocks under various states of stress. These measurement methods include strain measurements during overcoring, laboratory tests on samples obtained by coring, and measurements made by lowering geophysical devices into boreholes. An especially useful approach involves the interpretation of rock performance under the stress concentrations introduced by the presence of a cylindrical borehole in competent rocks subjected to regional compressive stresses. McGarr and Gay (1978) and Zoback and Haimson (1982) review the extensive theory and application of hydraulic-fracturing techniques in interpretation of the state of stress. Bell and Gough (1979), Gough and Bell (1981), Plumb (1982), and Fordjor and others (1983) discuss the interaction between borehole-stress concentrations and regional stresses in the generation of borehole-wall breakouts and elliptical borehole cross sections. Zoback and others (1984) describe numerical calculations in which the shear-failure mechanism is applied to stress concentrations around an initially cylindrical borehole in rock subjected to nonequal principal stresses. The orientation and shape of predicted borehole-wall breakouts match detailed acoustic profiles of breakouts in several boreholes studied by those authors. Paillet (1983a) relates the apparent opening of induced fractures at the borehole wall to the stress-concentration mechanism in homogeneous granitic rocks under regional compression in the Canadian Shield. All of these studies indicate that the relationship between observed borehole-wall breakouts and the regional state of stress can provide much information about the mechanical properties of crystalline rocks.

In addition to the principal objective of characterizing the nature of fractured rock surrounding the boreholes at the study site, this report addresses four specific topics: (1) Use of continuous televiewer and other acoustic logs throughout the entire interval of interest to relate the detailed distribution and character of borehole-wall breakouts to the general geology of the borehole; (2) correlation of the distribution of borehole-wall breakouts on the continuous logs to observed drilling-induced damage observed on recovered-core sections; (3) application of continuous acoustic logs in the selection of specific intervals for hydraulic-fracture tests to correlate the induced fractures with pre-existing fractures; (4) determination of the extent of fracturing away from the borehole wall and the relationship between natural fractures and fracturing related to borehole-wall breakouts. Although the various acoustic logs described here cannot replace the information provided by core-sample analyses and hydraulic-fracturing tests, the continuous record of rock properties and the larger sample volumes provided by some of the acoustic-logging devices provide at least some information that is not available through the use of any other technique.

DESCRIPTION OF STUDY SITE

The boreholes used for this study are located on the Hanford Site, operated by the U.S. Department of Energy, in Benton County, Washington (fig. 1). Five boreholes located on various parts of the Hanford Site were selected for study because they were considered representative of a larger number of boreholes drilled in an ongoing study of the suitability of subsurface formations for the construction of a radioactive-waste repository. The location of the five boreholes is given in figure 1, and the types of logs run at various depth intervals are listed in table 1.

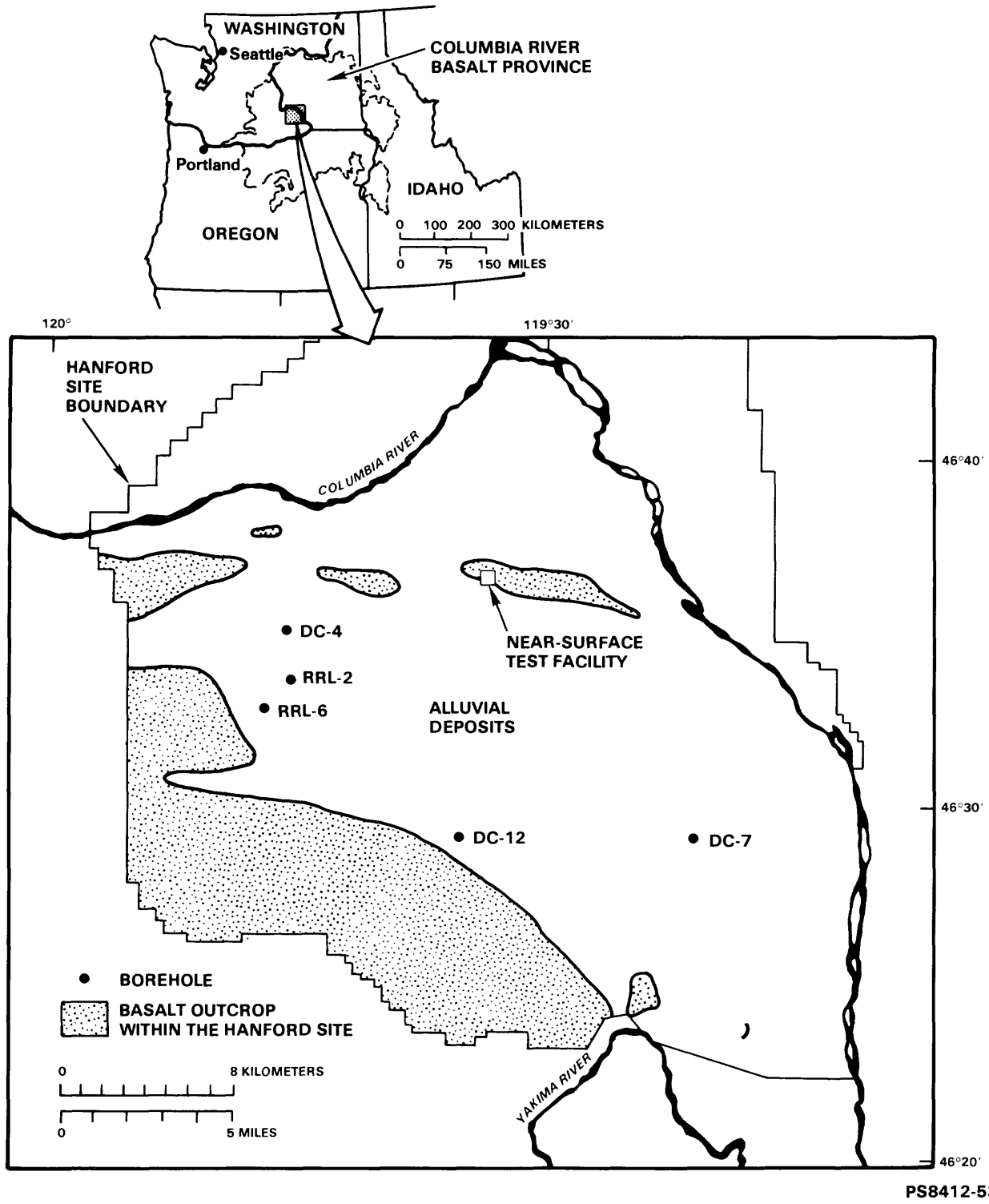

Figure 1. Map showing location of boreholes DC-4, RRL-2, RRL-6, DC-12, and DC-7.

Table 1.--Summary of logs and data for Hanford boreholes
[m, meters].

Borehole number	DC-4	RRL-2	RRL-6	DC-12	DC-7
Year drilled	1978	1982	1982	1981	1980
Total depth	1219 m	1211 m	1231 m	1358 m	1526 m
Casing depth	803.5 m	827 m	864.5 m	689 m	847 m
Dates logged	11/2-3/83 01/24/84	1/27/84	10/31-11/1/83 11/18/83 1/23/84	01/25/84	01/27/84
Caliper	1158-777 m	*	1219-823 m	1280-914 m	1158-782 m
Acoustic transit-time	1155-792 m	*	1219-838 m	*	*
Acoustic waveform	1152-792 m	*	1213-930 m	*	*
Televiewer	1189-803 m	1169-1140 m 1061-1049 m 994-914 m	1213-864 m	1256-908 m 872-779 m	1155-1116 m 1085-1053 m 983-933 m

*Logs not run

Correlation of flows comprising the Grande Ronde basalt member of the Columbia River Basalt Group (Swanson and others, 1979) identified in core holes drilled at the Hanford site are given in geologic sections constructed by Cross (1983). Although these flows do not constitute formally defined formations, the designations made by Cross (1983) are used here to facilitate comparison with previous work. One of the primary objectives behind the application of geophysics to this study site is the need to identify changes in character of basalt flows when they are encountered in boreholes drilled at different locations. The nature of these changes provides important checks on the ability to predict the rock quality index and mechanical properties of individual basalt flows that might be used to construct a repository. Therefore, many of the logs described in this study are presented for intervals corresponding to these informally designated basalt flows penetrated in the five different boreholes. Comparison of logs obtained in each of the five boreholes is presented along a line connecting the boreholes that trends southeasterly from borehole DC-4 to borehole DC-7. The five boreholes intersect multiple flows in the interval of interest, but the correlation given by Cross (1983) indicates that four major flows intersect all of the boreholes: the informally designated Rocky Coulee, Cohassett, McCoy Canyon, and Umtanum flows illustrated in figure 2. Core descriptions for the boreholes are taken from the descriptions given by Cross (1983). Four of the boreholes (RRL-2, RRL-6, DC-4, and DC-12) were boreholes with published core descriptions. The fifth borehole (DC-7) was a larger diameter, rotary-drilled borehole located within about 20 m of another core hole (DC-8) with a published core description. Depths used to define the tops and bottoms of individual flows are taken from those given by Cross (1983) even though the log response sometimes indicated that flow tops and bottoms might be picked at slightly different depths.

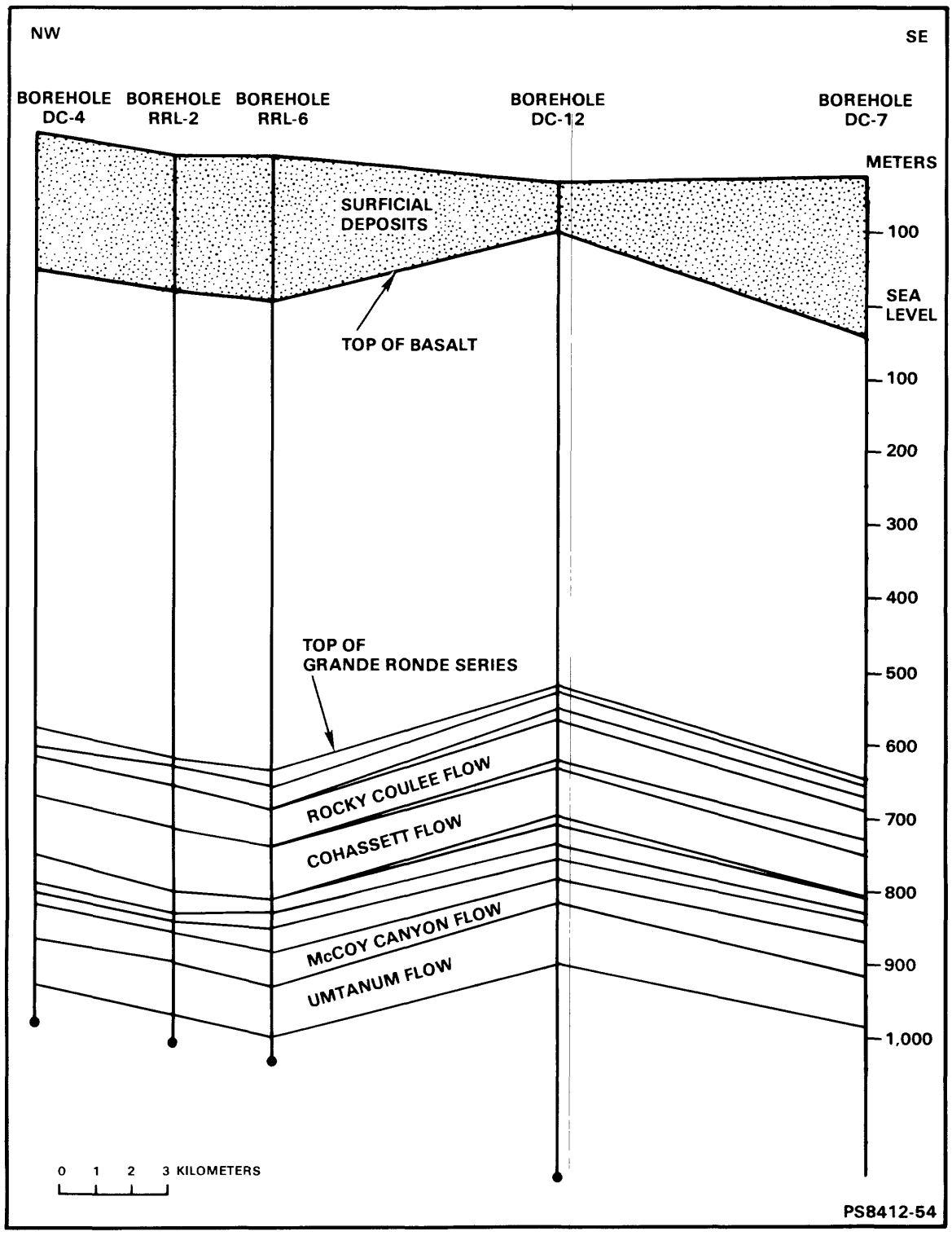

Figure 2. Geologic section showing correlation of basalt flows between boreholes and informal flow names given by Cross (1983).

An important feature of the core samples from all five boreholes is the condition denoted as "disking" by Cross (1983), which is a term referring to a tendency for core samples to break into thin disks with flat or slightly saddle-shaped surfaces. This core breakage is believed to be drilling-induced as a result of rapid stress relief of samples subjected to substantial in-situ stress. Therefore, the extent of disking on a core may be correlated with borehole-wall breakouts as described by Zoback and others (1984) and Bell and Gough (1979). Other important physical conditions of core samples include flow top and bottom rubble, flow top and bottom breccia, vesicular zones, and vuggy zones. Rubble is defined by Cross (1983) as "...friable, broken rock..." occurring in the "...upper, commonly vesicular zone..." of flows. Breccia is defined as "...brecciated, commonly glassy and/or altered...", with "...sub-rounded to angular clasts from a few millimeters to more than a meter in diameter." Vesicular zones are defined as those containing more than about 2 percent by volume of vesicles. Vuggy zones are defined as those zones similarly dominated by large vesicles with diameters greater than 1 cm. In cases where both small and large vesicles are present, the zone is denoted by the size that appears predominant on visual inspection.

The core descriptions note the presence of "tectonic" fractures in certain locations, which are defined as naturally occurring fractures attributed to tectonic movement. Some of these fractures appear partially filled with minerals or brecciated rock. The interiors of basalt flows also contain numerous fine fractures associated with the columnar cooling joints of the flows. These columnar joints can be observed in outcrops at several locations on the Hanford Site. Structure of the columnar jointing in the walls of the excavation at the Near Surface Test Facility (fig. 1) is illustrated in figure 3. The columnar structure appears as a series of approximately vertical joints producing irregular columns with joint spacing ranging from 10 to 100 cm. It is assumed that many of the irregular near-vertical fractures observed in the interiors of the basalt flows on the televiewer logs represent such columnar joints.

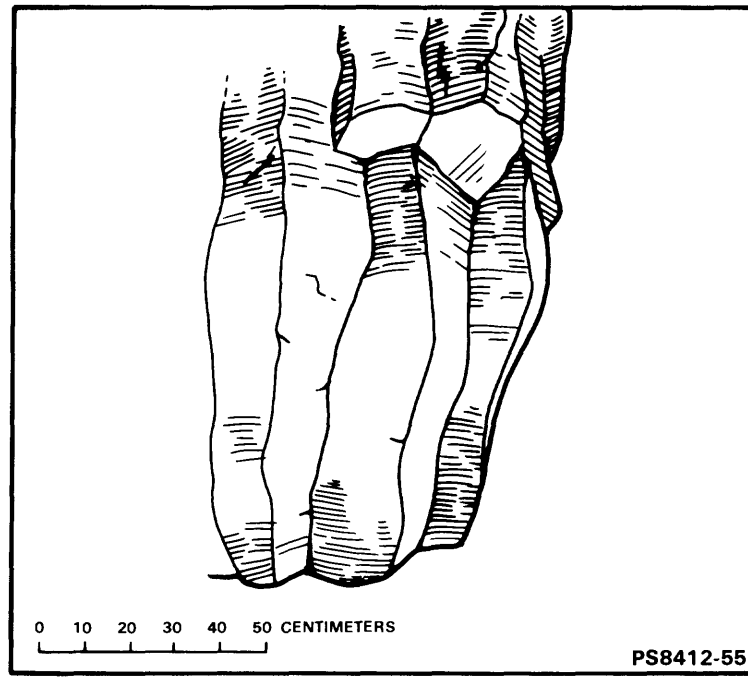

Figure 3. Sketch of basalt columns in flow center in wall of Near Surface Test Facility.

ACOUSTIC WELL-LOGGING EQUIPMENT

The two acoustic methods used in this study were acoustic televiewer logging and acoustic-waveform logging. The televiewer is an ultrasonic device that produces a photographic image of the pattern of acoustic reflectivity of the borehole wall. The televiewer system used for this investigation was based on a source transducer producing a pulsed acoustic beam of approximately 1.25 MHz with a diameter of about 5 mm. The televiewer beam scans the borehole at a rate of 3 r/s while the televiewer sonde is slowly pulled up the borehole. Detailed descriptions of the televiewer logging system and a discussion of the imaging techniques used in the processing of televiewer logs are given by Zemanek and others (1969). A typical example of the use of televiewer logs in the interpretation of fractured crystalline rocks is given by Keys and Sullivan (1979). Magnetic minerals present in the borehole wall at Hanford caused a large proportion of televiewer logs to be incorrectly oriented. This problem will be described in detail in subsequent sections of this report. All televiewer logs presented here are given without orientation with the exception of those cases where the orientation of televiewer logs is discussed in the text.

A major drawback in the use of televiewer logs to characterize fractured rocks is the inability to probe rocks surrounding the borehole where in-situ conditions have not been affected by drilling and local stress concentrations. Acoustic-waveform logs using frequencies less than a few tens of kilohertz provide much better rock penetration; these logs may be used to distinguish between drilling-induced fractures and naturally conductive fractures (Paillet, 1983a). The generalized approach can be compared to the performance of a local seismic-refraction survey within the borehole, as described by Paillet and White (1982). The acoustic-logging system used in this study is described in more detail by Paillet (1980). This system has an energy source producing a relatively narrow acoustic bandwidth centered on 34 kHz.

Seismic properties of rocks are usually interpreted in terms of the critically refracted compressional and shear waves arriving at the acoustic receivers (White, 1965). These waves are considered to have a depth of investigation on the order of one wavelength into the rock surrounding the borehole. Source-to-receiver spacings normally are designed to provide a few wavelengths of travel path. The exact depth of investigation is difficult to document in the most general case; however, numerical experiments repeatedly indicate that a small zone of altered rock around the borehole will produce a measurable difference in refracted-wave speed when the zone width begins to approach one acoustic wavelength (White and Zechman, 1968; Chan and Tsang, 1983). If typical basalt velocities of 6.1 km/s for compressional waves and 3.3 km/s for shear waves are used for these calculations, the refracted seismic waves used in this study should provide depths of investigation greater than 17 cm (compressional) and 10 cm (shear).

ACOUSTIC-TELEVIEWER LOGS

The televiewer-logging system produces a photographic image of the amplitude of acoustic energy reflected off the borehole wall. This acoustic character represents a different physical property than the optical appearance of core, so that a comparison between the appearance of core samples in photographs and the televiewer log provides considerable information about properties of the rock surrounding the borehole. Several examples on the textures of the televiewer logs and the corresponding core samples are illustrated in figures 4 to 8.

A section of televiewer log from borehole RRL-6 having uniformly high borehole-wall reflectivity is compared with the corresponding section of core showing uniform, dark-gray basalt in figure 4. The contact of similar high-reflectivity texture on the televiewer log with much lower reflectivity rock is illustrated in figure 5. This contact corresponds to a change in core appearance from uniform dark-gray basalt (fig. 4) to red-brown, mottled core, representing brecciated and altered basalt in one of the core-top intervals described by Cross (1983). Correspondence between low borehole-wall reflectivity and altered or brecciated flow tops and bottoms appears to be a very reliable indicator of the extent of unaltered-flow interiors. This observation was confirmed by subsequent analysis of other geophysical-log data.

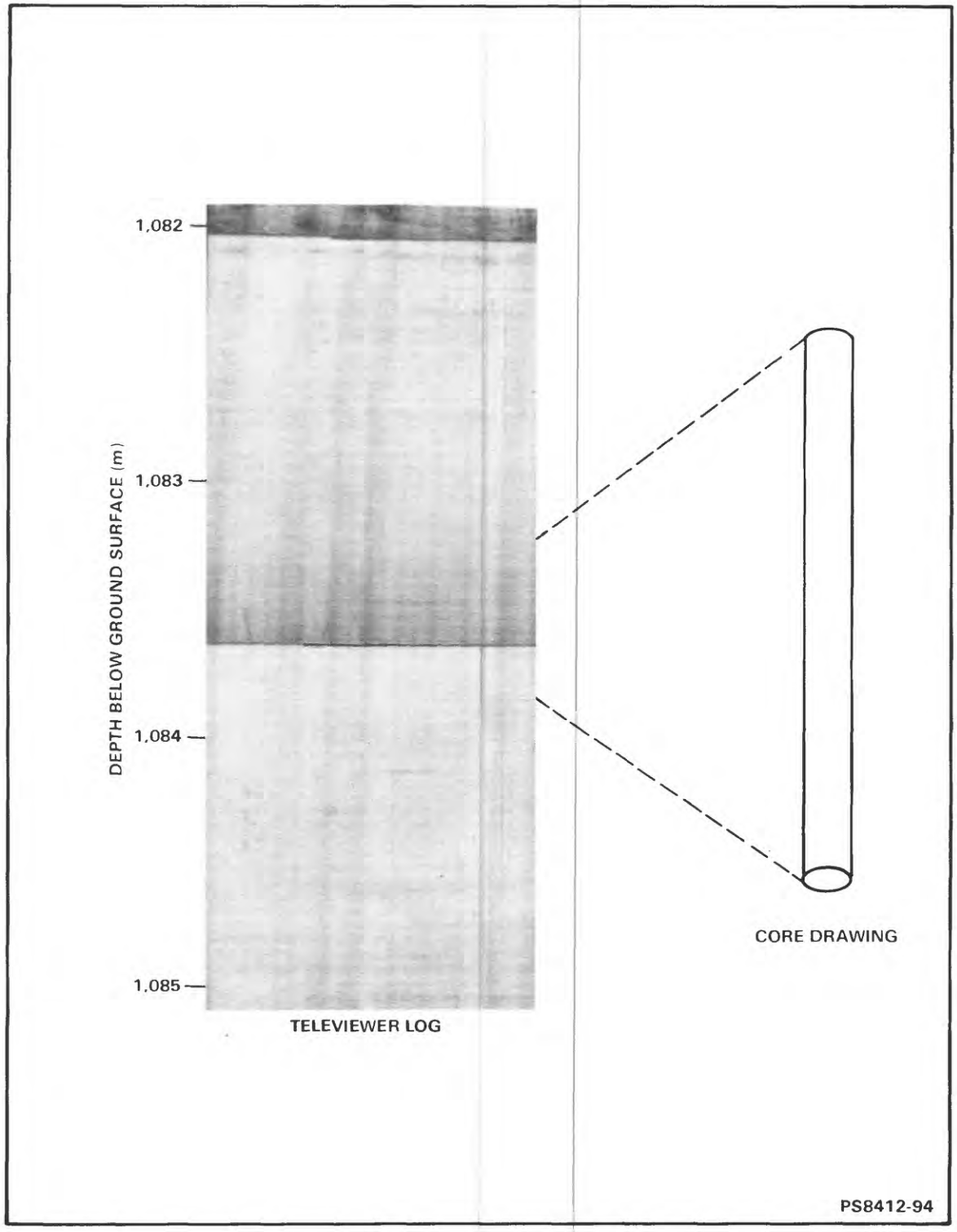

Figure 4. Comparison of televiewer log and core photograph for interval of uniform unfractured and unaltered basalt in borehole RRL-6.

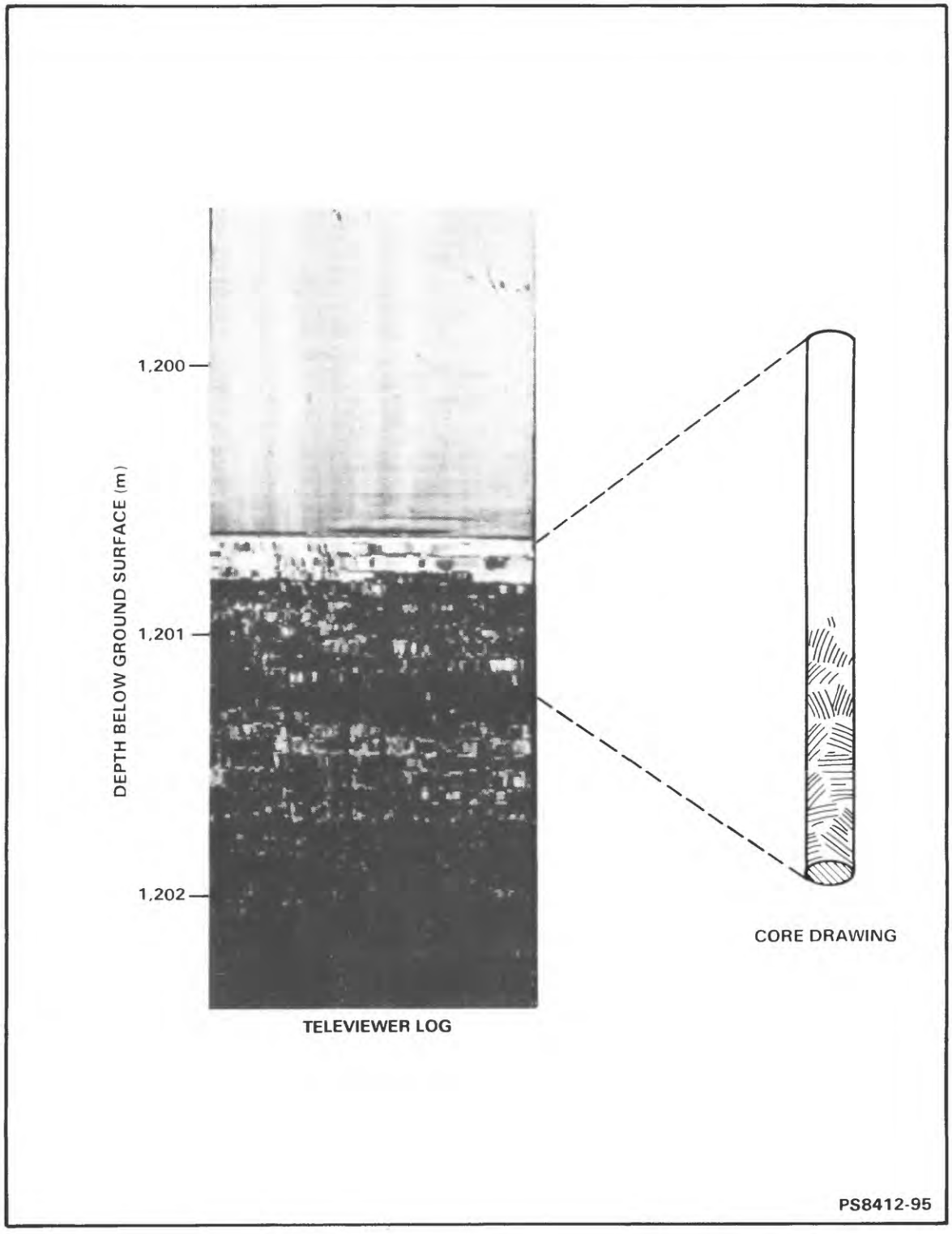

Figure 5. Comparison of televiewer log and core photograph for the contact between bottom of unaltered basalt flow and top of altered and brecciated flow in borehole RRL-6.

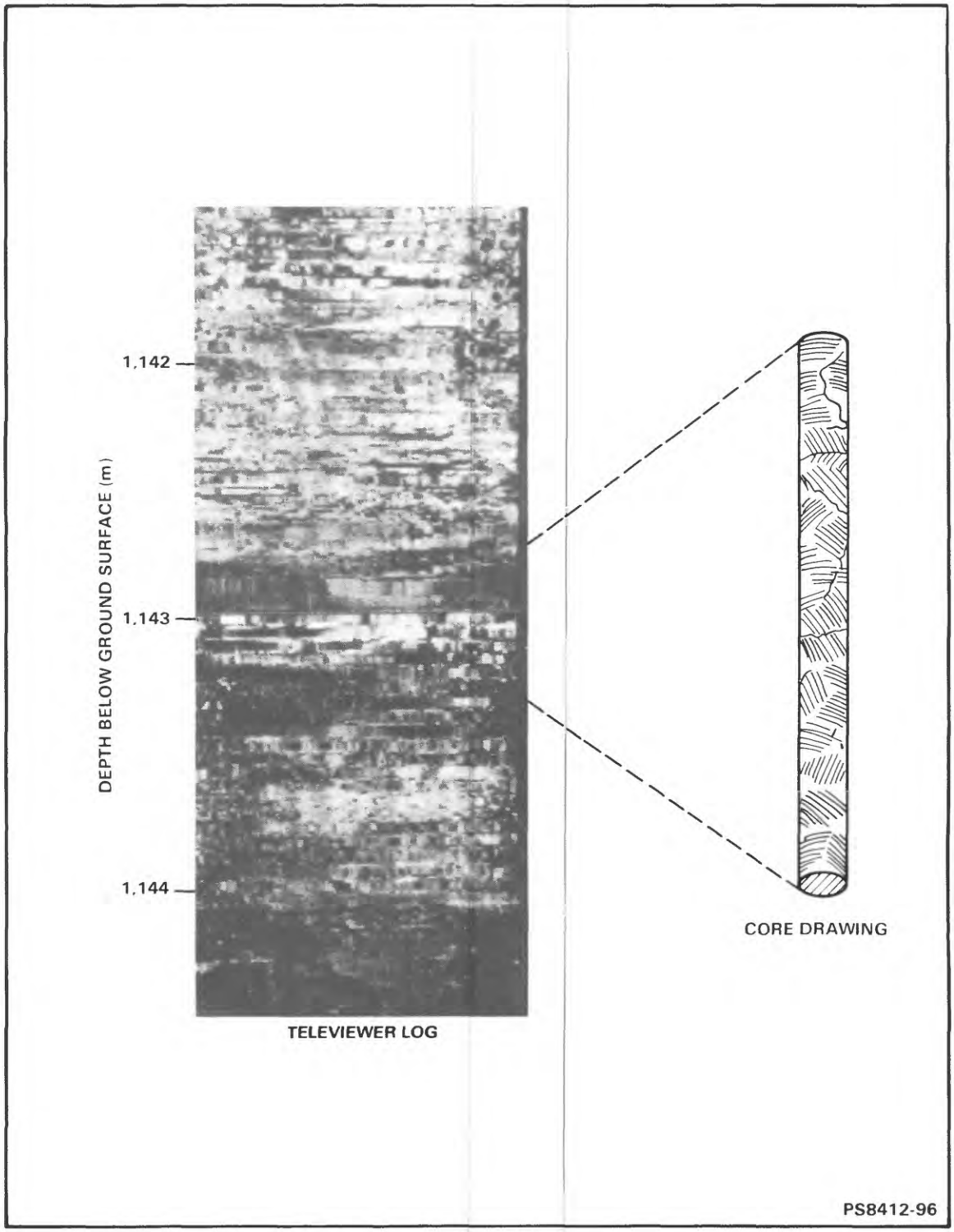

Figure 6. Comparison of televiewer log and core photograph for interval of very altered and brecciated basalt in borehole RRL-6.

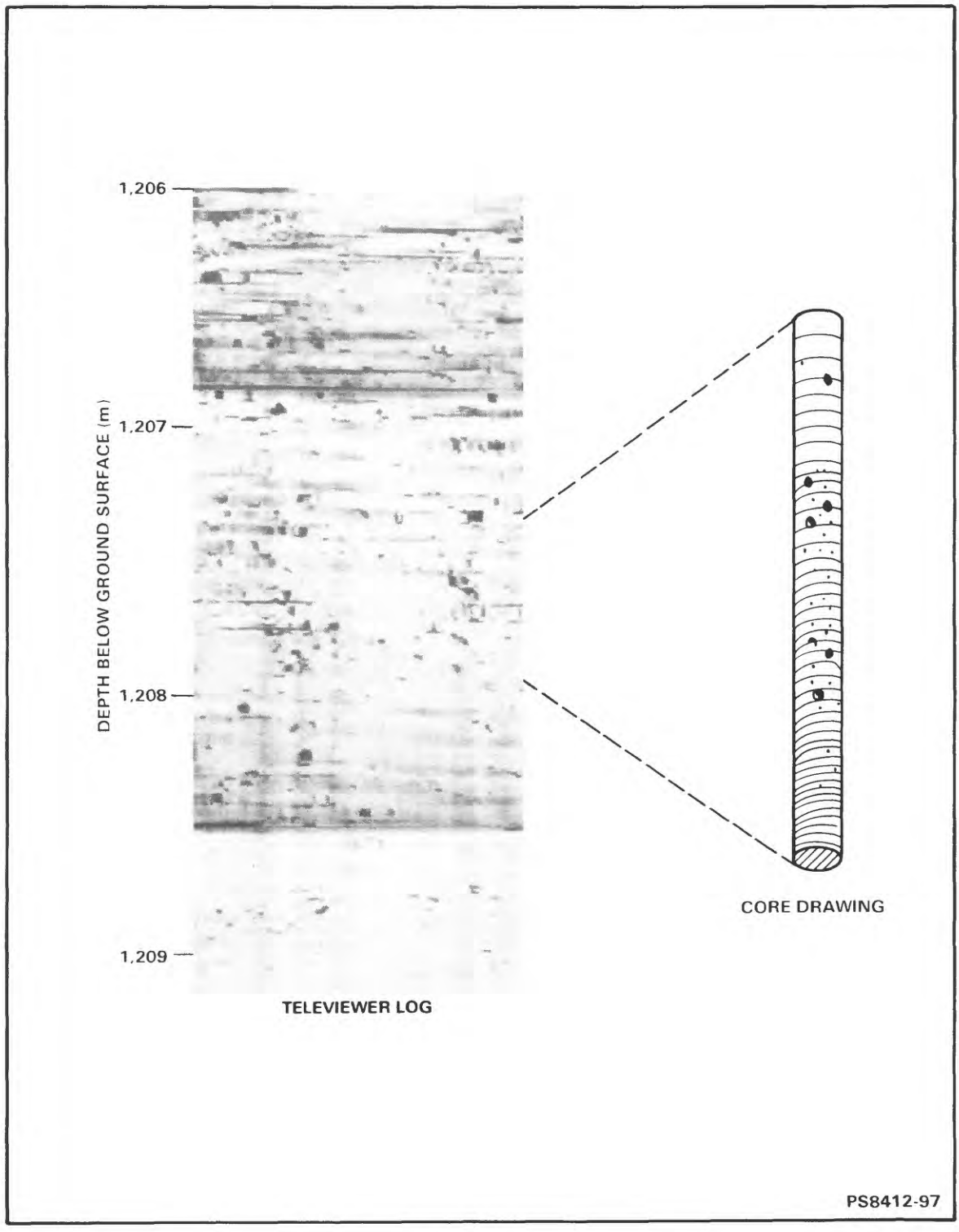

Figure 7. Comparison of televiewer log and core photograph for interval in borehole RRL-6 where striations on televiewer correspond to undulations on the surface of core.

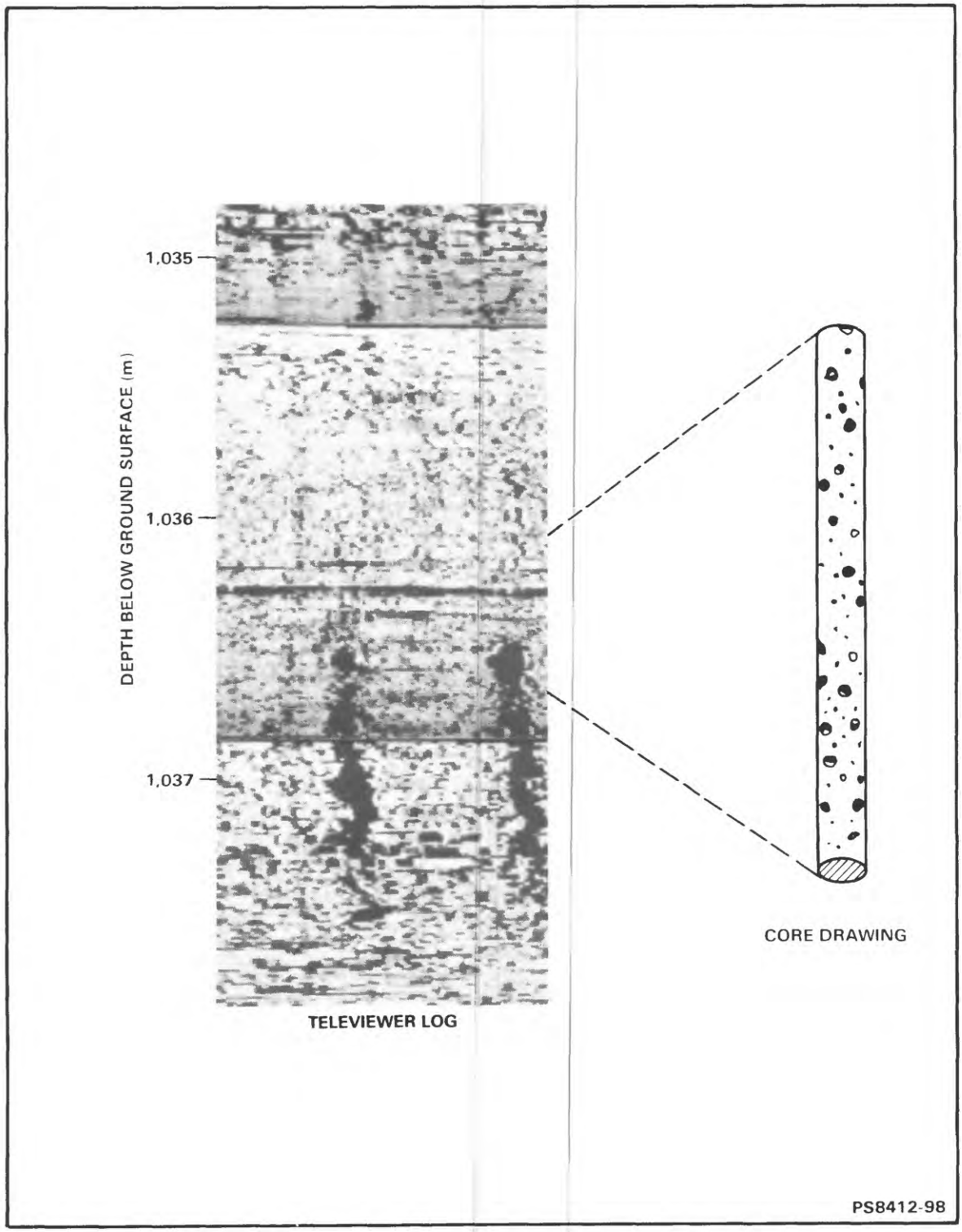

Figure 8. Comparison of televiewer log and core photograph for vuggy interval on borehole RRL-6.

The relatively soft altered rock in the intervals of low acoustic reflectivity is indicated by the presence of striations on the borehole wall (fig. 6), which generally result from the repeated passage of hydrologic test equipment and logging tools. Some intervals of televiewer log have faint diagonal stripes that appear to correspond to undulations on the surface of the core samples. Similar stripes on televiewer logs obtained in unfractured granite were described by Davison and others (1982). In that case, diagonal undulations, or rifling, of the borehole wall and associated irregularities on the surface of core samples were attributed to a spiral motion during drilling produced by excess weight on the drill stem. A similar situation may have caused the appearance of the televiewer log and core sample in figure 7. Vesicular and vuggy intervals in the boreholes also were apparent on the televiewer logs. A representative interval of televiewer log in a vuggy part of a flow, along with the corresponding interval of core, is illustrated in figure 8. Various textures on televiewer logs illustrated in figures 4 to 8 provide a relatively complete sample of the variation in televiewer-log character related to lithology and fractures in the five boreholes.

Televiewer logs run in parts of the five boreholes are illustrated in figures 9 to 18. The logs in each figure represent reduced interpretations of the original televiewer logs in a format that allows comparison of televiewer logs for large depth intervals. These figures compare the appearance of the borehole wall in each of the boreholes for individual flows within the Grande Ronde series described by Cross (1983). The figures allow comparison of unaltered flow interiors where they intersect each borehole, indicating the distribution of fractures and borehole-wall breakouts. Televiewer logs were compared to core descriptions for all five boreholes, and to core photographs for the three boreholes with most complete televiewer logs (RRL-6, DC-12, and DC-4). This comparison was used to determine corrections needed to relate depths on U.S. Geological Survey logs to depths given on core photographs. This correction was determined by identifying at least 10 distinctive fractures and abrupt lithology changes on both televiewer logs and core photographs.

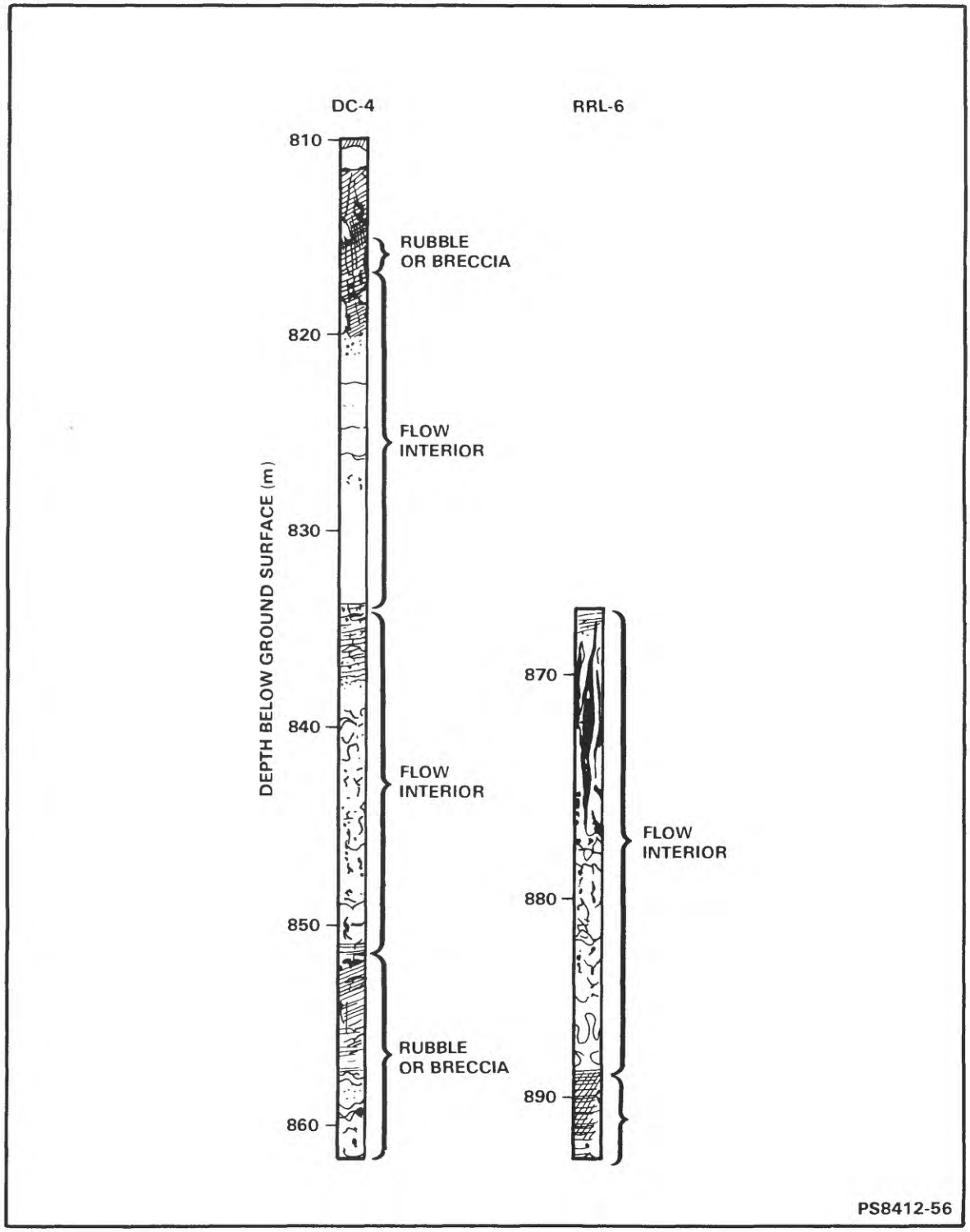

Figure 9. Televiewer logs of uppermost flows of Grande Ronde series.

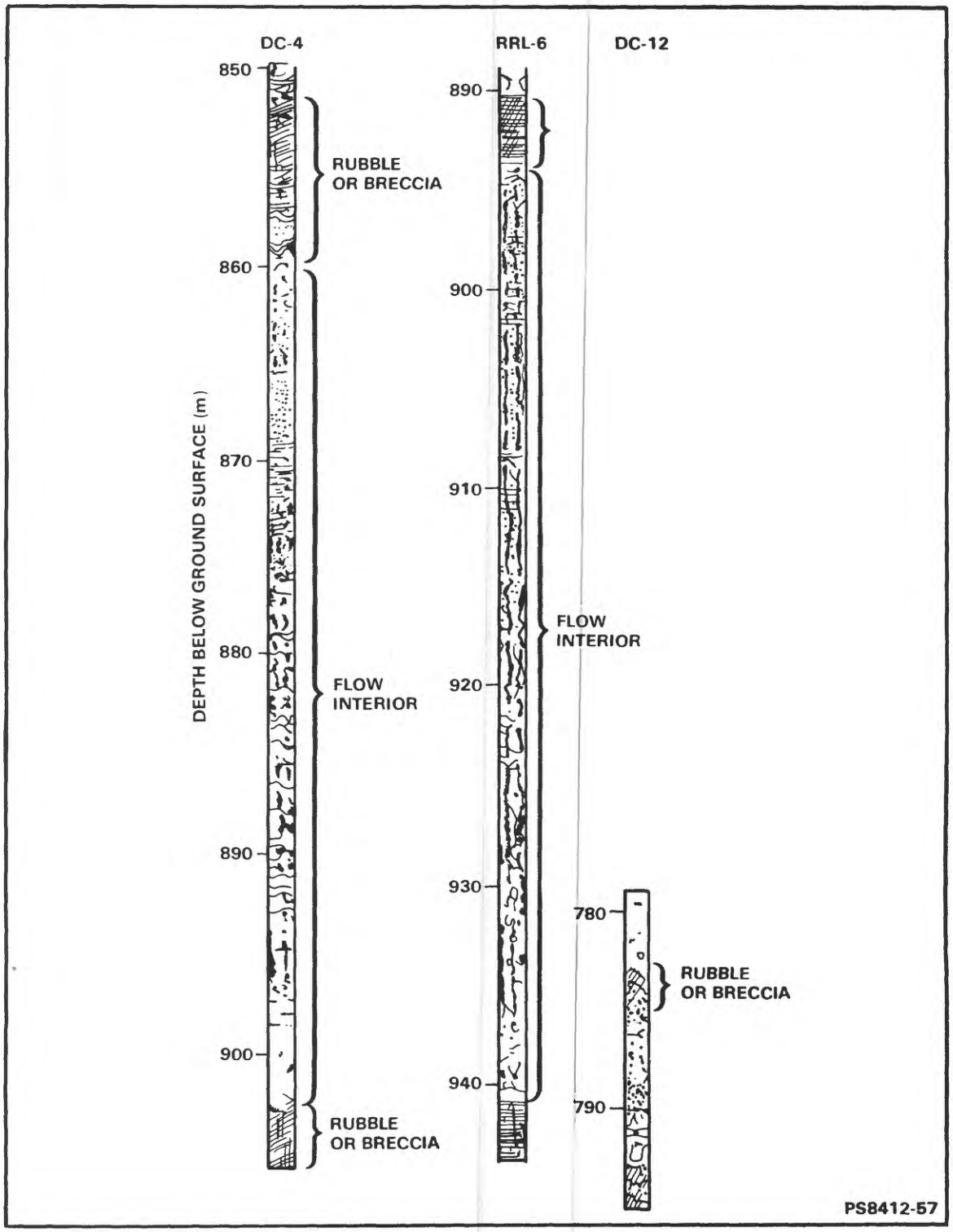

Figure 10. Televiewer logs of the Rocky Coulee flow.

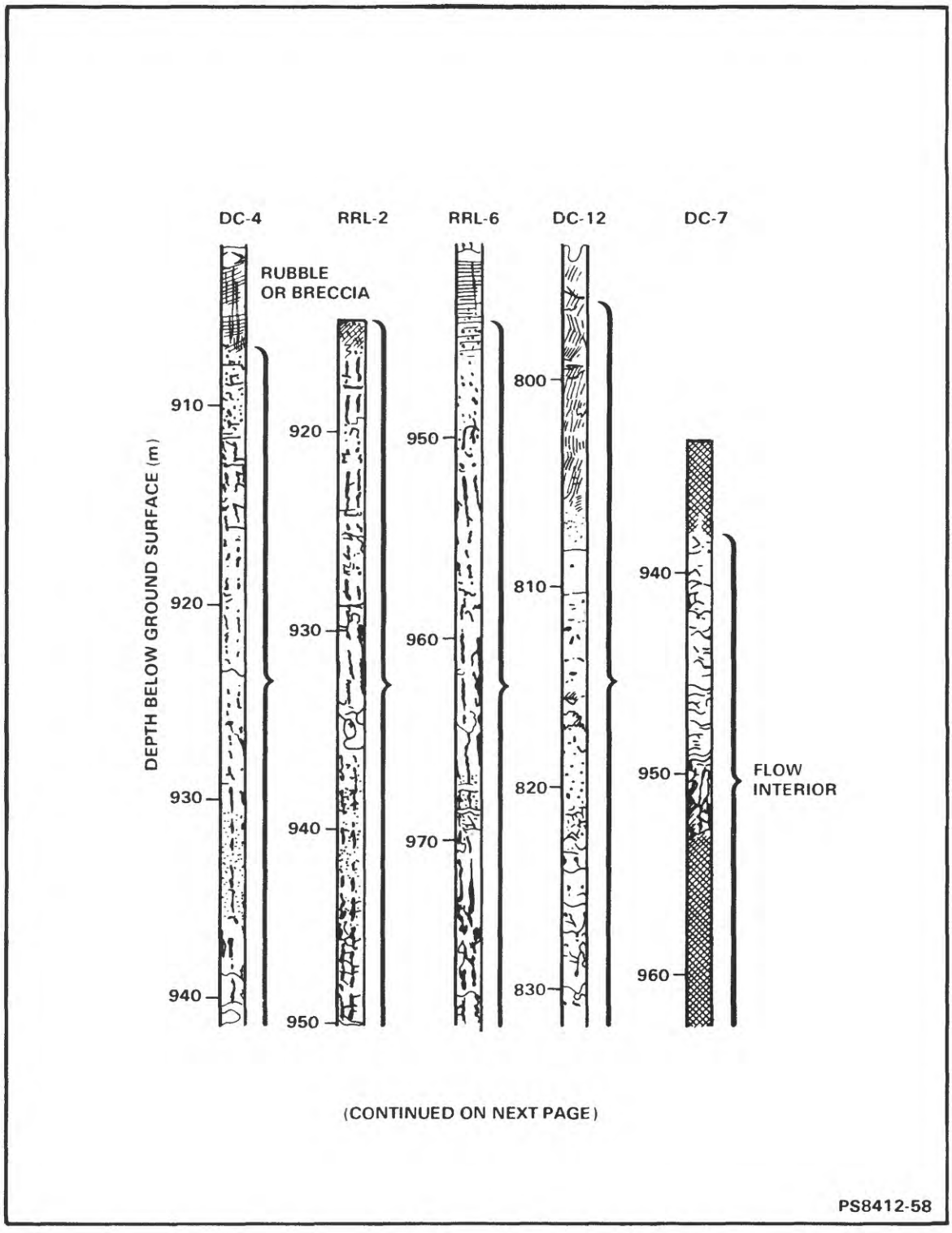

Figure 11. Televiewer logs of the upper part of the Cohassett flow.

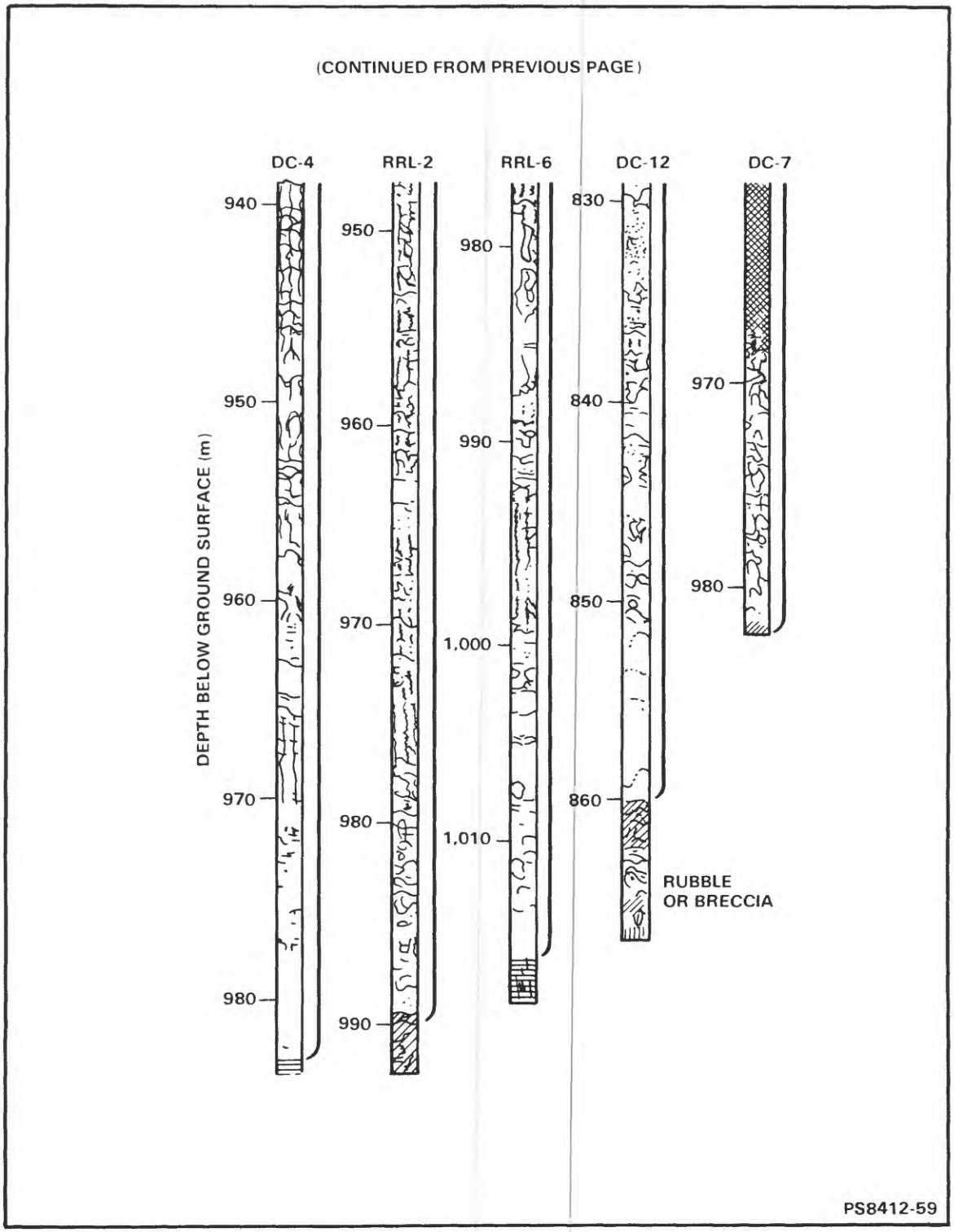

Figure 12. Televiewer logs of the lower part of the Cohassett flow.

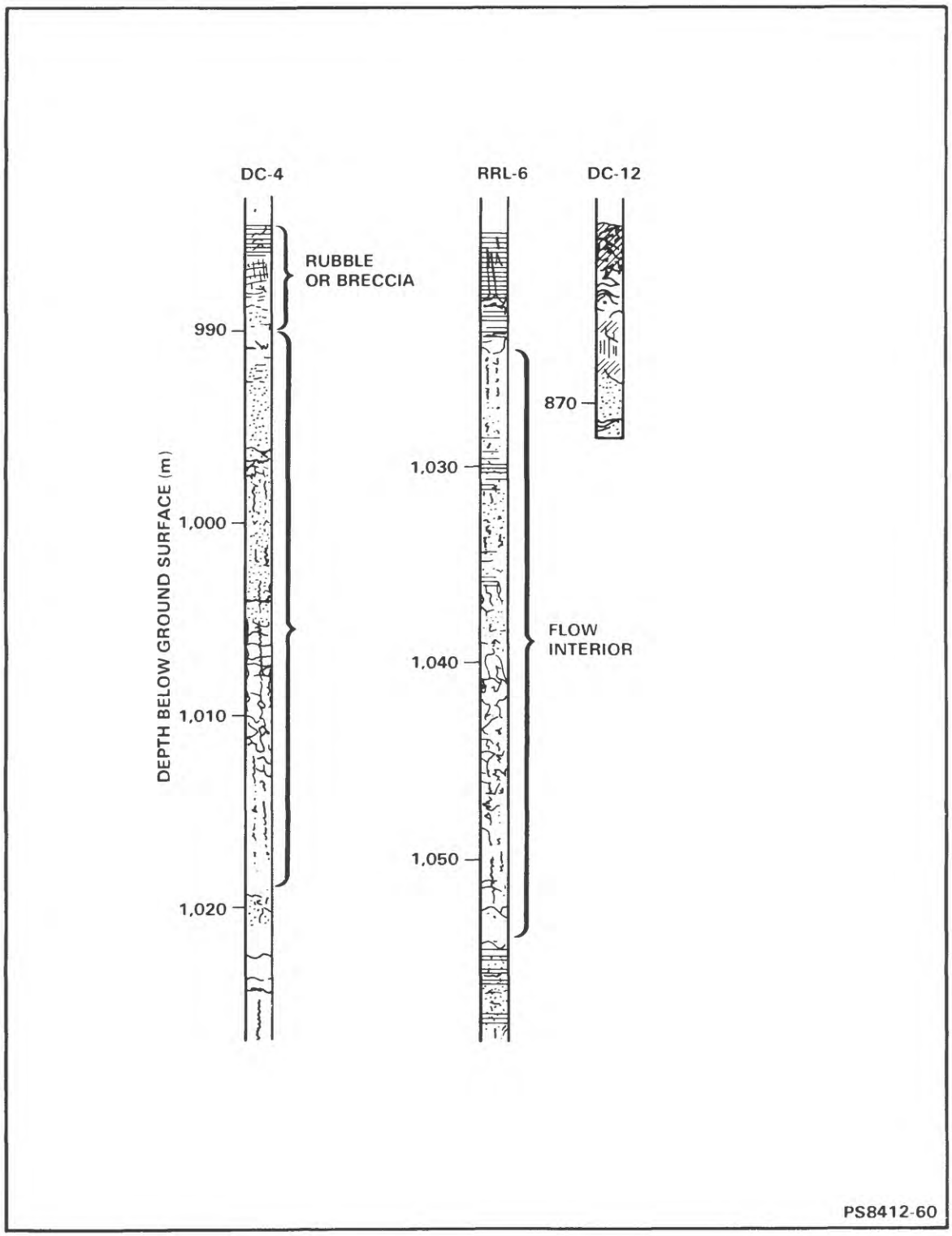

Figure 13. Televiewer logs of flows below bottom of the Cohassett flow.

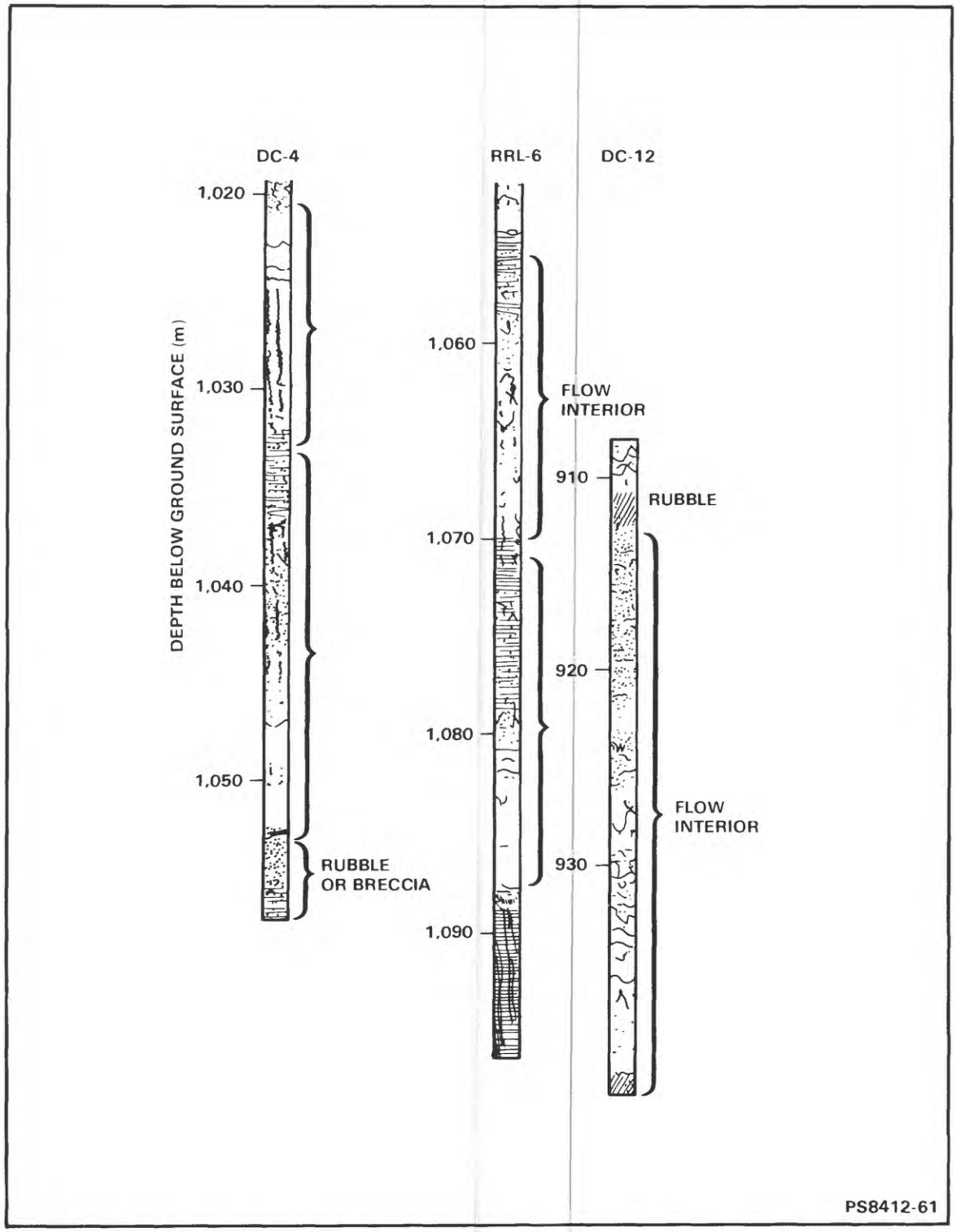

Figure 14. Televiewer logs of flows above the top of McCoy Canyon flow.

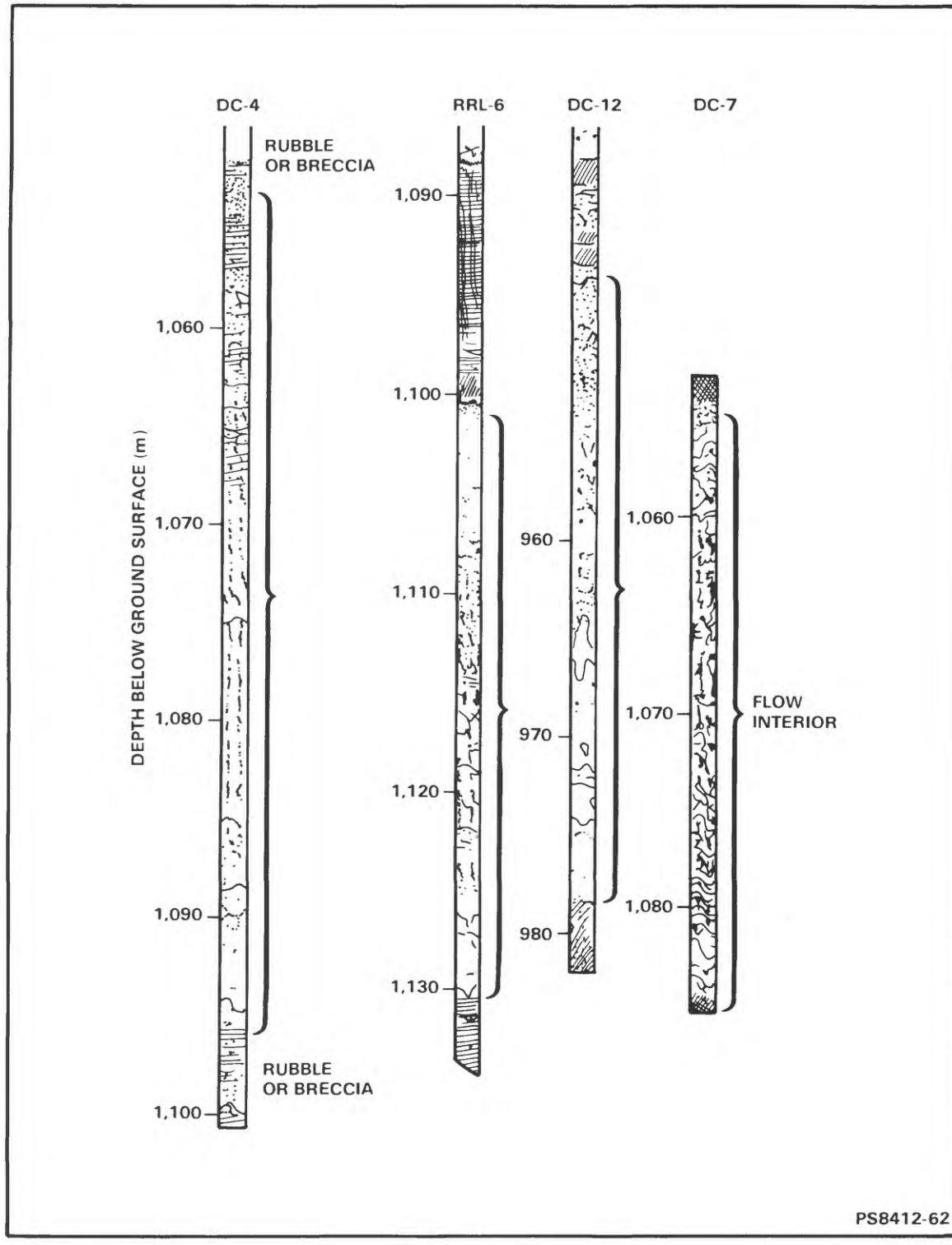

Figure 15. Televiewer logs of the McCoy Canyon flow.

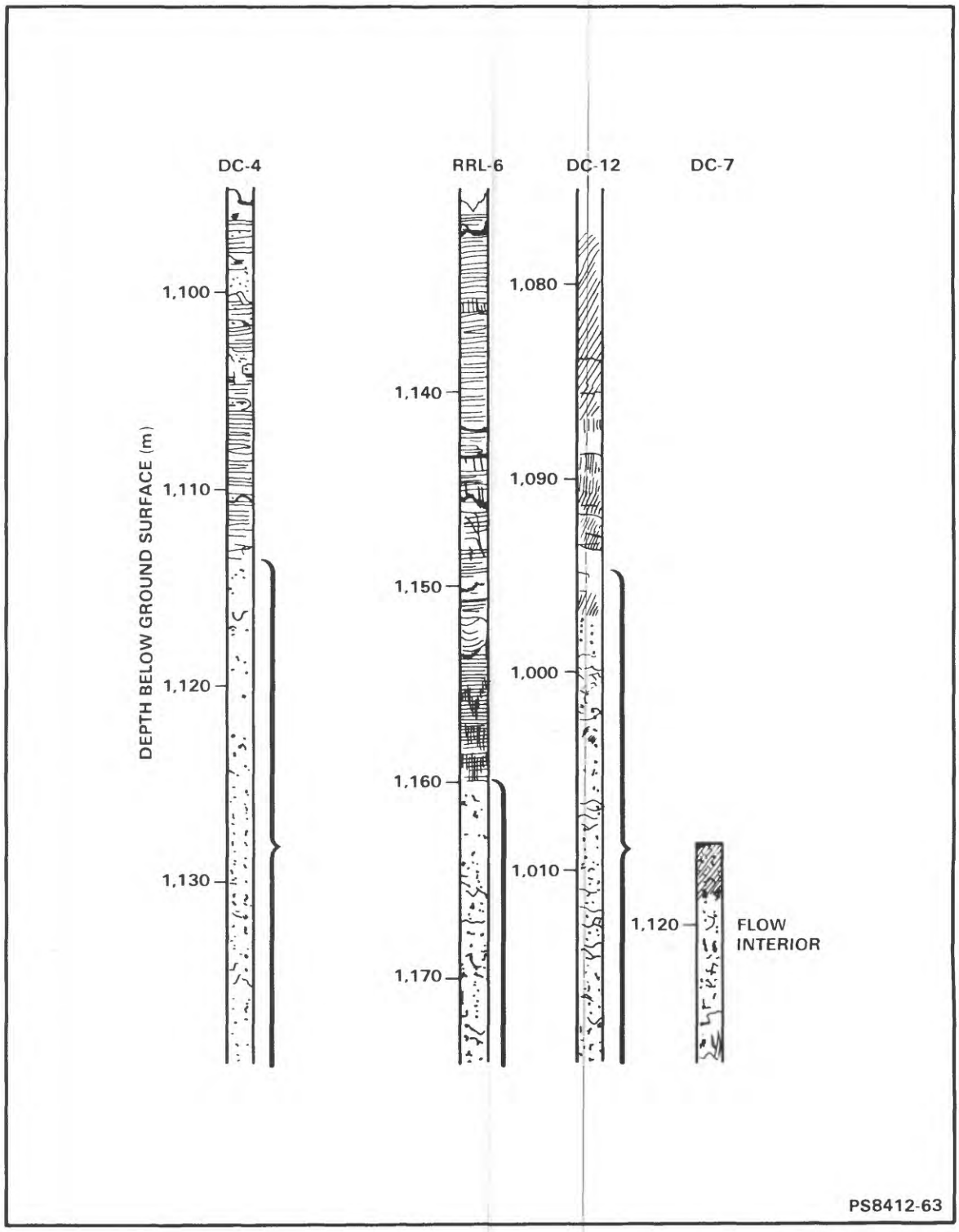

Figure 16. Televiewer logs of upper part of the Umtanum flow.

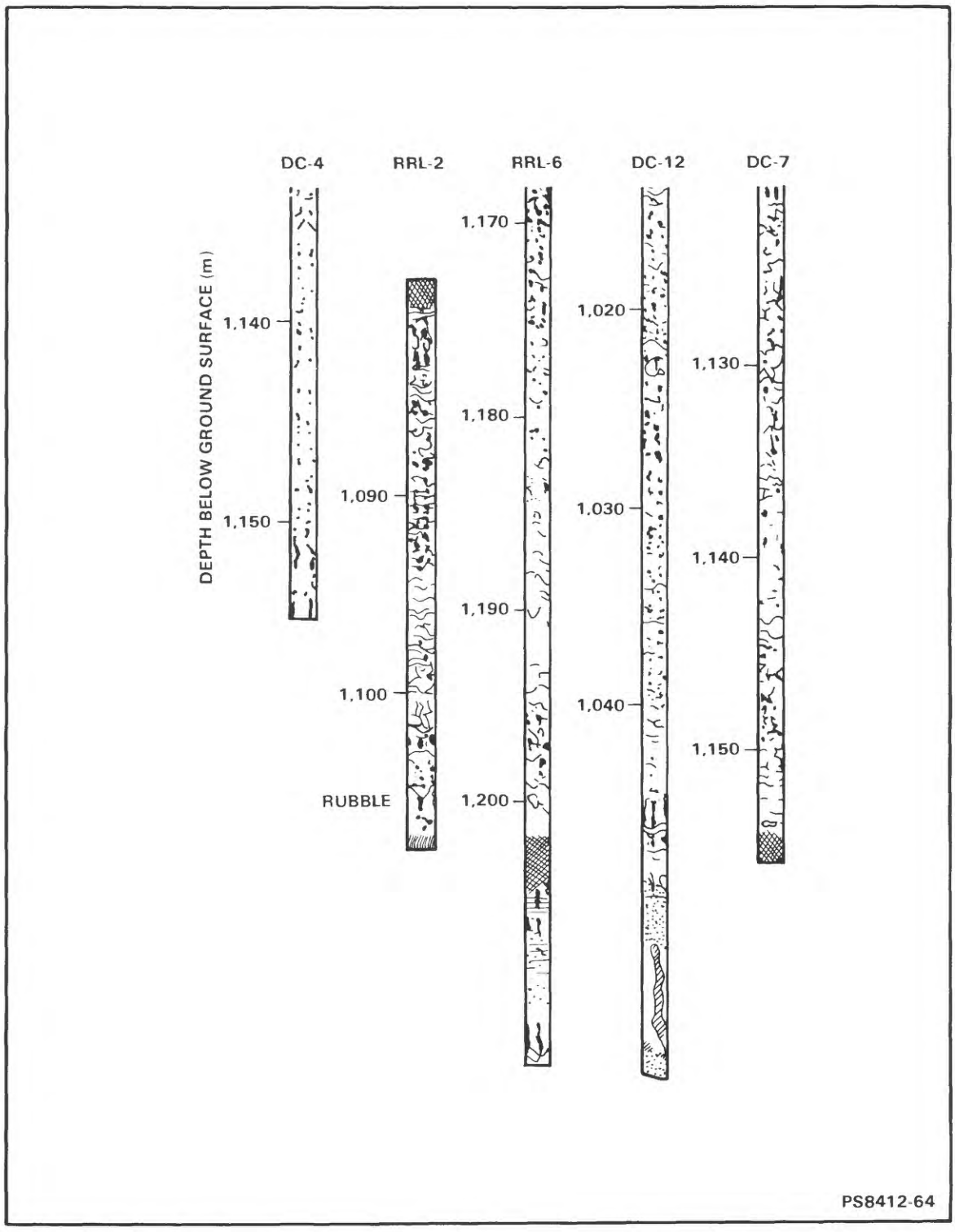

Figure 17. Televiewer logs of the lower part of the Umtanum flow.

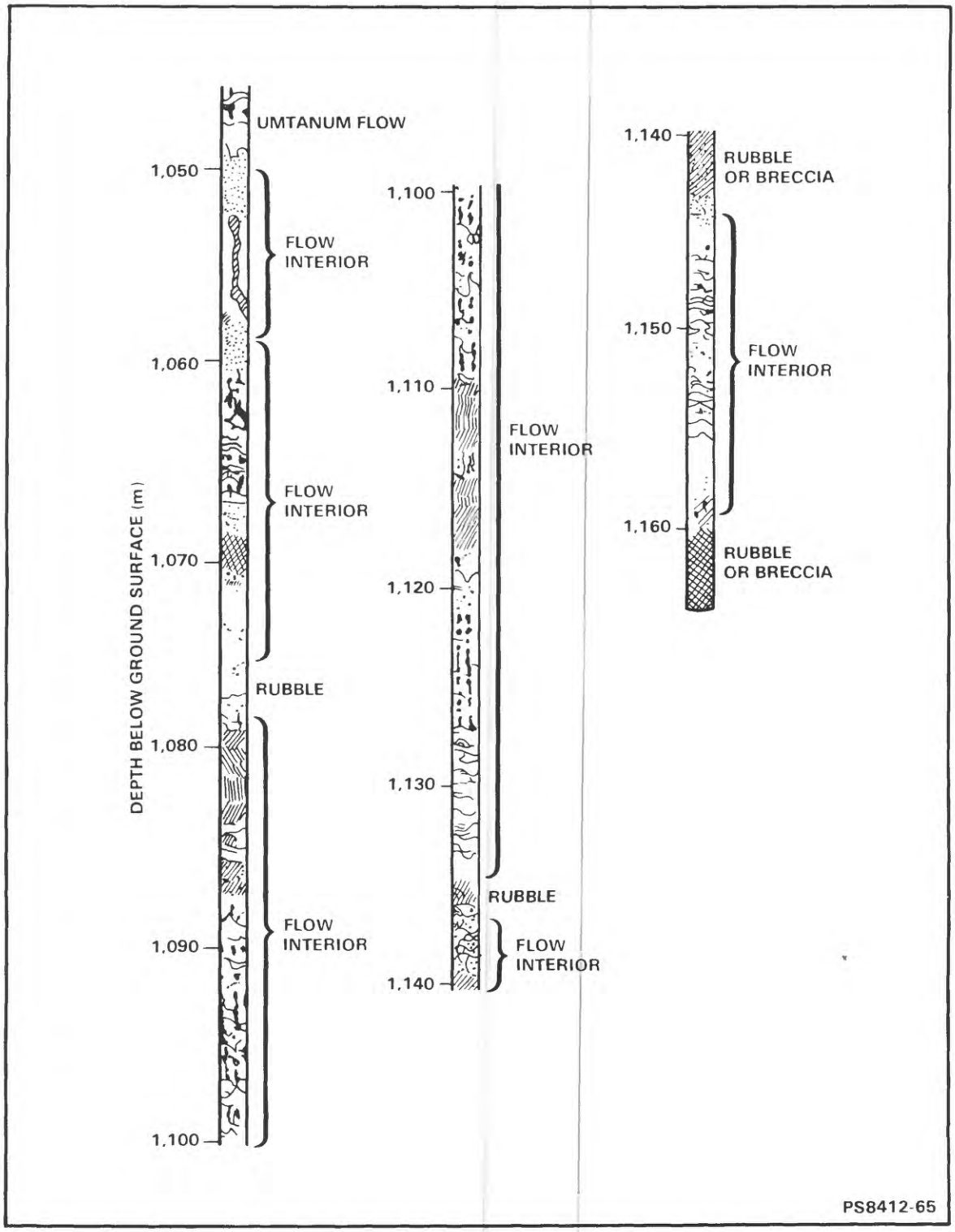

Figure 18. Televiewer logs of flows in borehole DC-12 below base of Umtanum flow.

Three examples of these correlations are given in figures 19 to 21, where isolated natural fractures present in the core samples are compared to natural fractures appearing on the televiewer logs. The comparisons in figures 19 to 21 also serve to illustrate the relationship between the character of the fractures intersecting core and the appearance of the fractures on the televiewer logs. The exaggerated horizontal scale of the televiewer log decreases the apparent dip of the fracture plane. The dip (ϕ) of the fracture may be calculated from the ratio of the vertical distance within which the fracture intersects the borehole (h) to the borehole diameter (d):

$$\phi = \tan^{-1} (h/d) \qquad (1)$$

Note that this calculated dip angle is given with respect to a plane perpendicular to the borehole, and needs to be corrected to account for deviation of the borehole from vertical. The apparent dip of the three fractures indicated on the core samples in figures 19 to 21 agrees with the calculated dip angles determined from the televiewer logs.

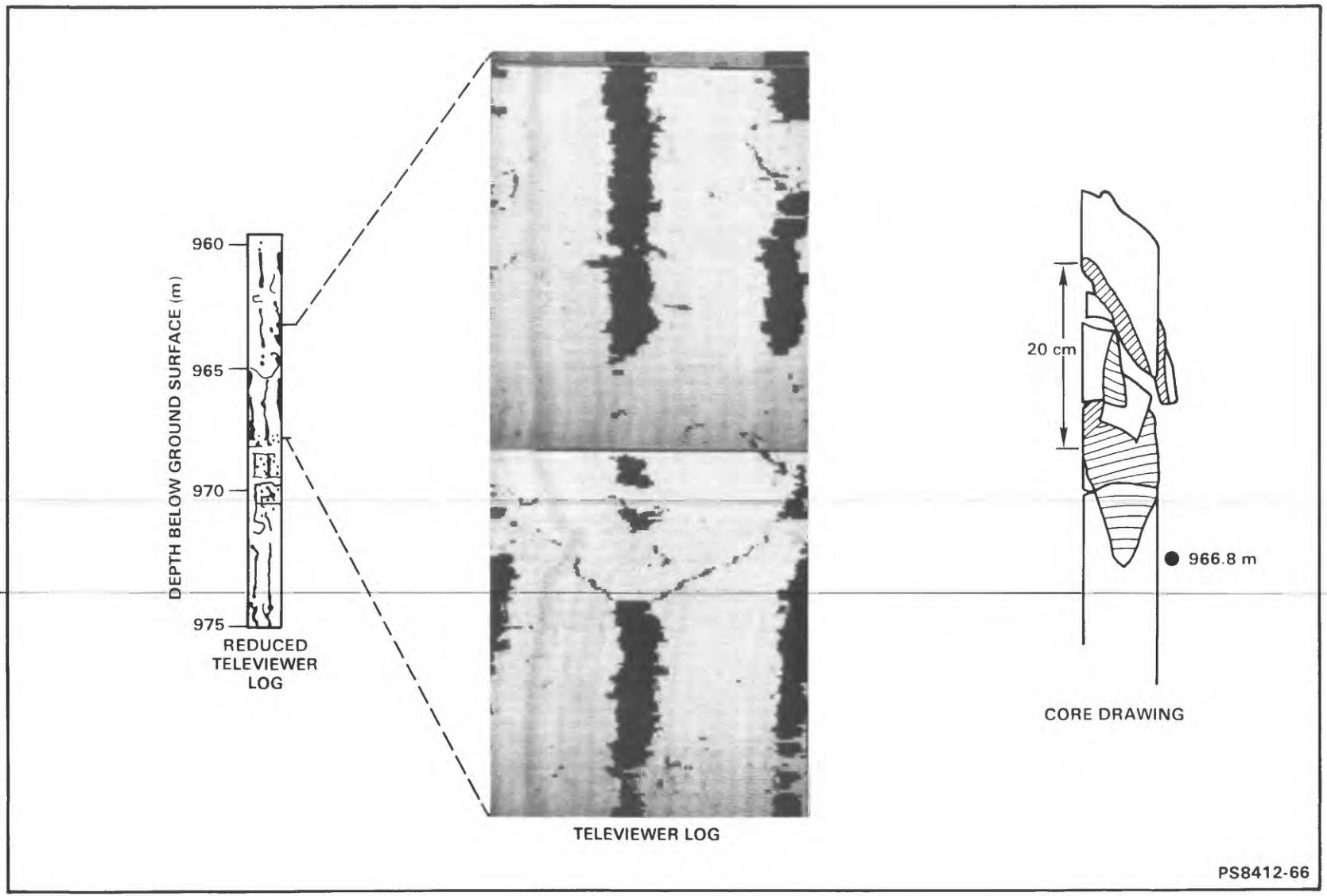

Figure 19. Televiewer log and core photograph of isolated fracture in borehole RRL-6.

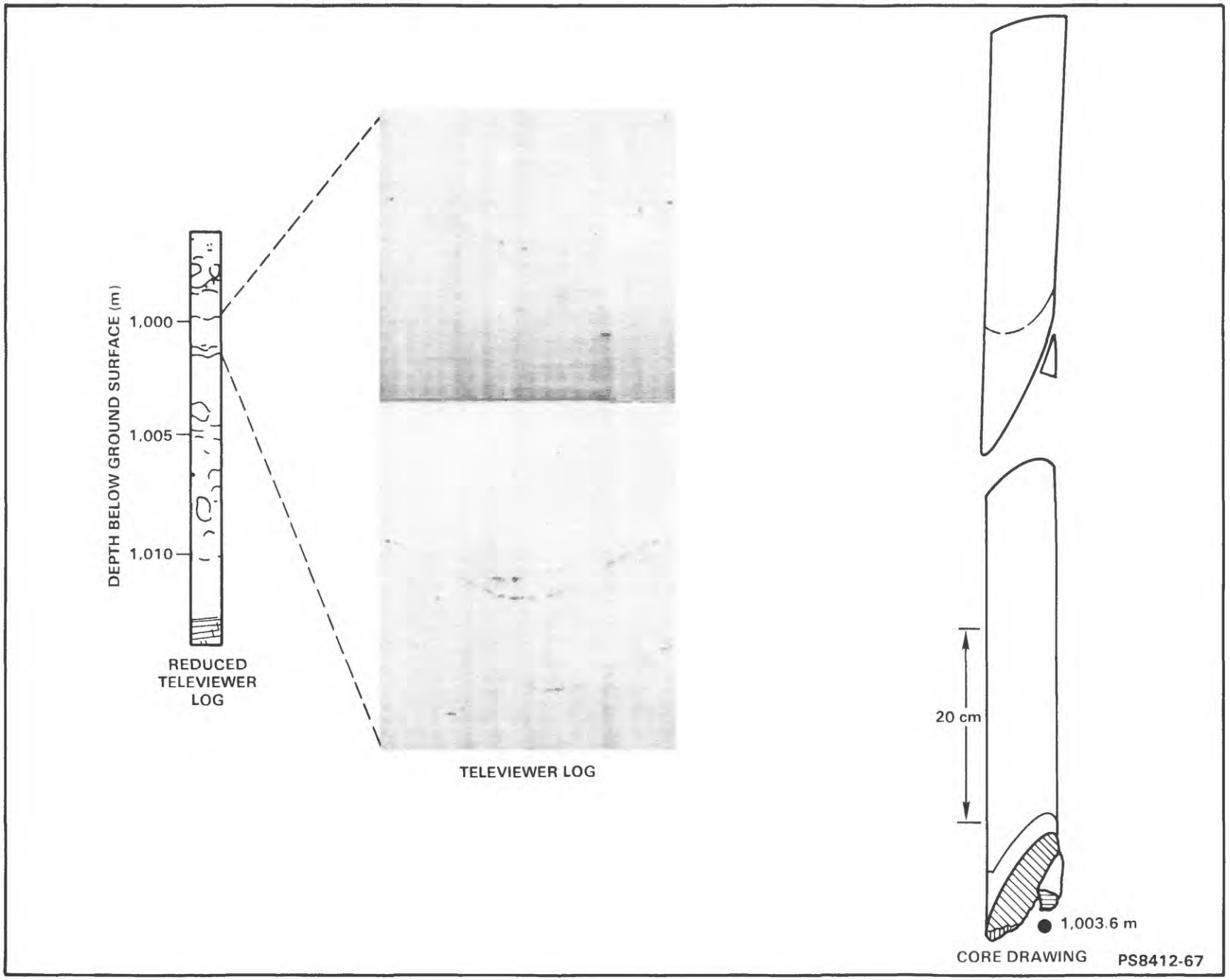

Figure 20. Televiewer log and core photograph of pair of closely spaced fracture in borehole RRL-6.

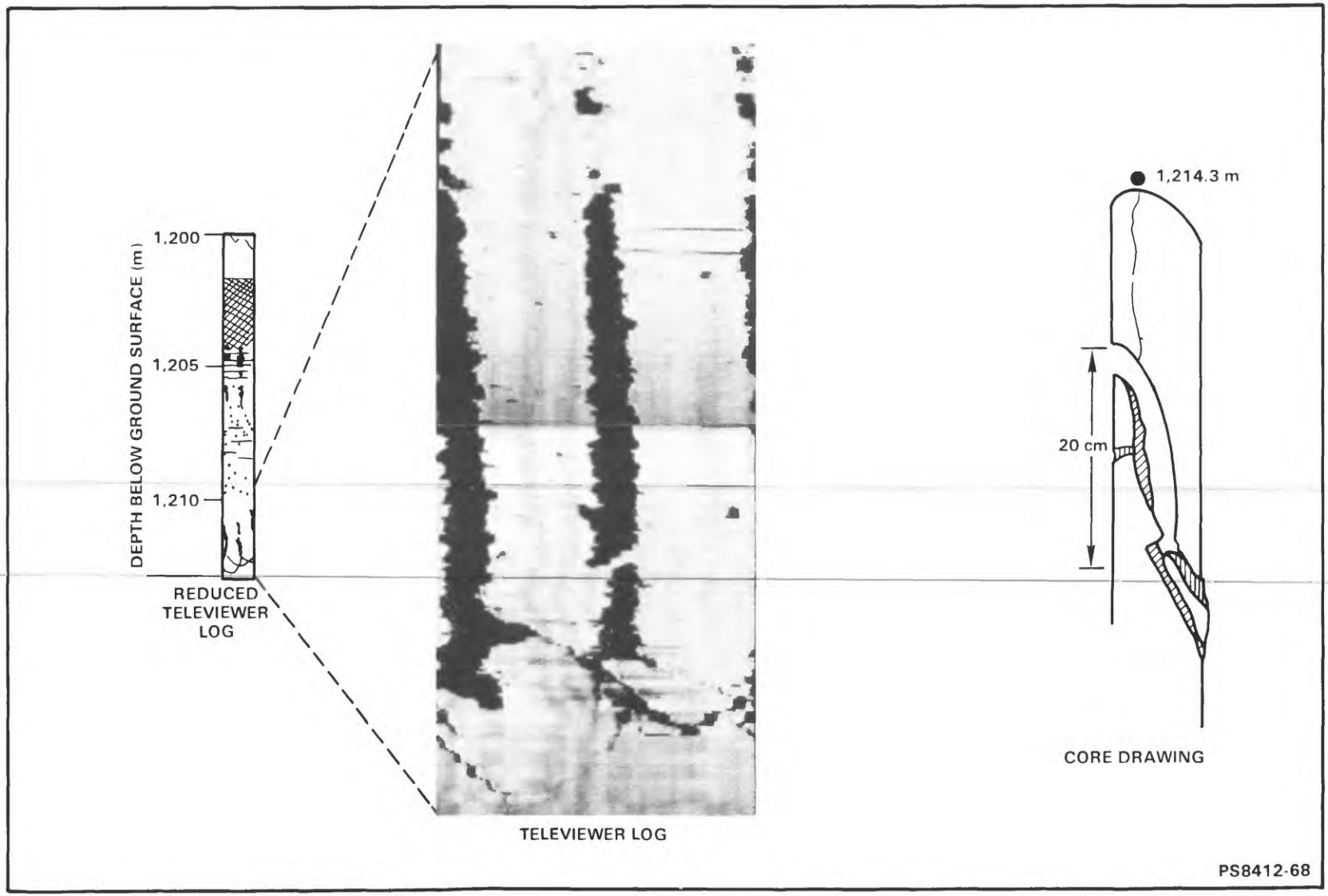

Figure 21. Televiewer log and core photograph of two intersecting fractures in borehole RRL-6.

The correlation of isolated fractures and bed boundaries on the televiewer logs with corresponding features on the core photographs indicate that approximately 1.5 m should be added to the depths given on the televiewer log for borehole RRL-6, and approximately 1.0 m added to the televiewer logs for boreholes DC-4 and DC-12, to make the depths logs correspond to the core photographs. This correction appears constant throughout the interval illustrated in figures 19 to 21, and probably represents a difference in depth reference for logs and core. All U.S. Geological Survey logs were referenced at ground level, whereas the core may have been determined from the kelly bushing on the drilling rig. A large number of isolated fractures could not be identified on the more limited intervals of televiewer logs for boreholes RRL-2 and DC-7, but a similar correction of approximately $\pm$1.0 m was assumed to make these televiewer logs correspond to core. Almost all detailed comparisons between core and acoustic logs were restricted to the three boreholes where a consistent depth correlation between core and televiewer logs was established.

Although the primary emphasis in this study is placed on the use of acoustic-televiewer and acoustic-waveform logs in the characterization of basalt, acoustic transit-time and caliper logs also were run in some of the boreholes. Caliper logs were run in boreholes RRL-6, DC-4, and DC-7, because these boreholes had been left capped for a period of time, and it was uncertain whether the boreholes were open all the way to the bottom. The risk to more expensive logging tools did not seem great, but the relatively inexpensive caliper logging system was used first whenever time permitted. The acoustic transit-time logs were run because the same acoustic-logging system was being used to generate acoustic-waveform logs, and the acoustic transit-time log could be used in the characterization of fractures (Pickett, 1963). The acoustic transit-time and caliper logs obtained in boreholes DC-4 and RRL-6 are shown in figure 22. The caliper logs in boreholes DC-4 and RRL-6 indicated some minor hole-diameter increase associated with the interbeds, and with certain flow interiors where the caliper arms intersected some of the borehole-wall breakouts. The caliper log for the larger diameter, rotary-drilled borehole DC-7, however, indicates that the interbeds and brecciated flow tops and bottoms correspond to hole enlargements. The borehole diameter within the flow centers averages about 22 cm, but the diameter increases to beyond the 40-cm limit of the fully opened caliper arms in the interbed intervals.

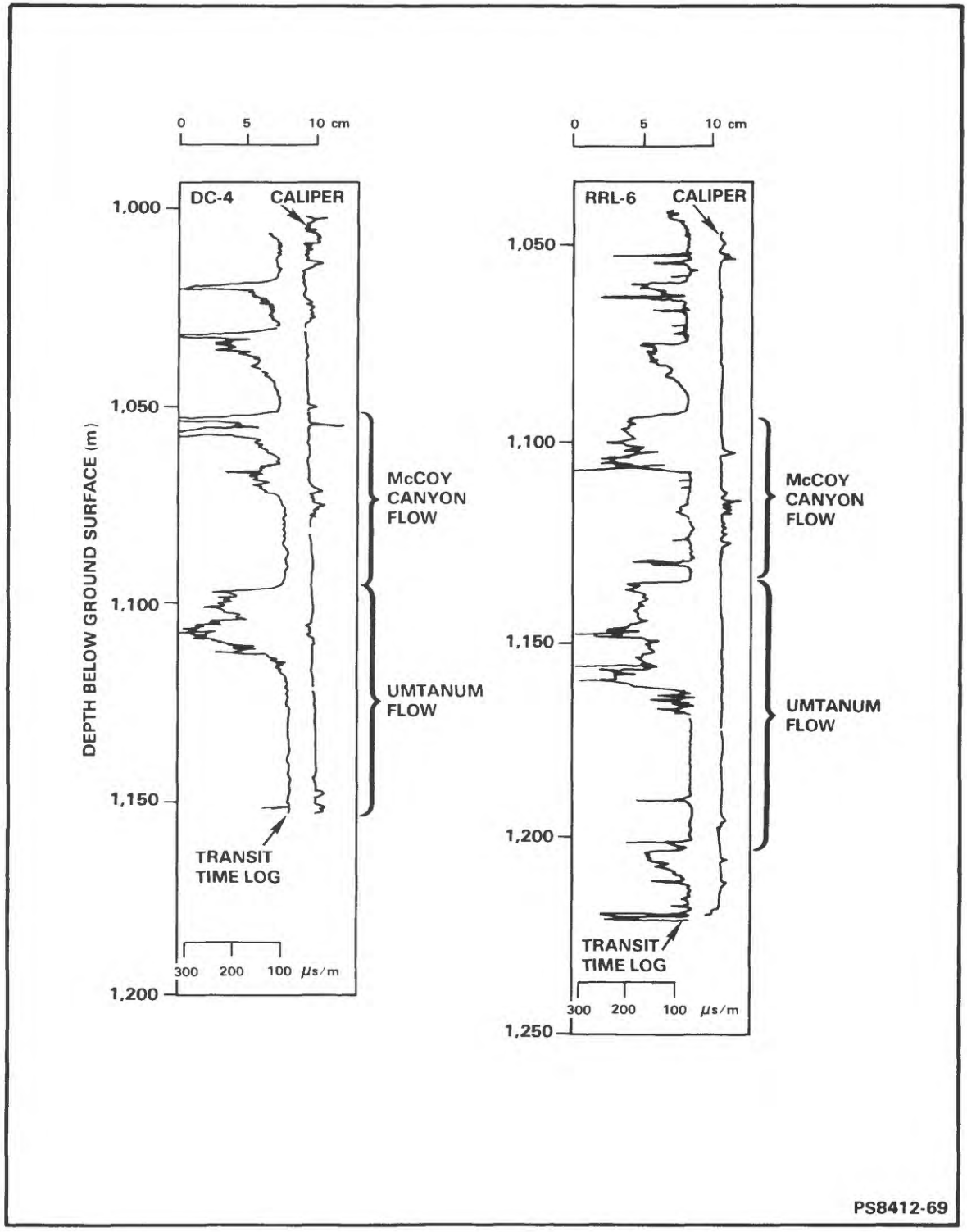

Figure 22. Acoustic transit-time and caliper logs for borehole DC-4 and RRL-6.

The acoustic transit-time logs indicate the abrupt differences between the unaltered basalt of the flow interiors and the much softer altered basalt of the brecciated flow tops and bottoms. Two representative sections of the acoustic transit-time log in RRL-6 and DC-4 were selected for detailed comparison with the televiewer log (fig. 23 and 24). These two intervals were selected to illustrate acoustic transit-time response to altered flow tops, vesicular zones, and borehole-wall breakouts. The abrupt transition between high acoustic reflectivity of flow interiors and low reflectivity of flow tops and bottoms corresponds very closely with an abrupt change in acoustic transit-time.

The representative section of caliper log for borehole DC-7 in figure 25 also indicates the large contrast in physical properties between the highly reflective flow interiors and the altered rock of the flow tops and bottoms. In that rotary-drilled borehole, the relatively soft rock of the flow tops, bottoms, and interbeds was washed out to a very large diameter, so that the abrupt increase in borehole diameter corresponds very closely with the change in acoustic reflectivity. It is important to note that the transitions between altered rock and the flow interiors did not always appear to coincide with the limits given by Cross (1983). This appeared to be true, even when the corrections for systematic differences in depth scale between the U.S. Geological Survey logging equipment and the core were accounted for. For example, the top of the Cohassett flow in borehole DC-12 is given as 794 m by Cross (1983), corresponding to 793 m on the televiewer log, but the transition between solid-flow interior and low reflectivity altered rock appears to be somewhere below 805 m (fig. 8). Similarly, the top and bottom of the flow labeled Grande Ronde Flow 15 on the core log for borehole DC-12 do not appear to have been correctly picked in figure 18.

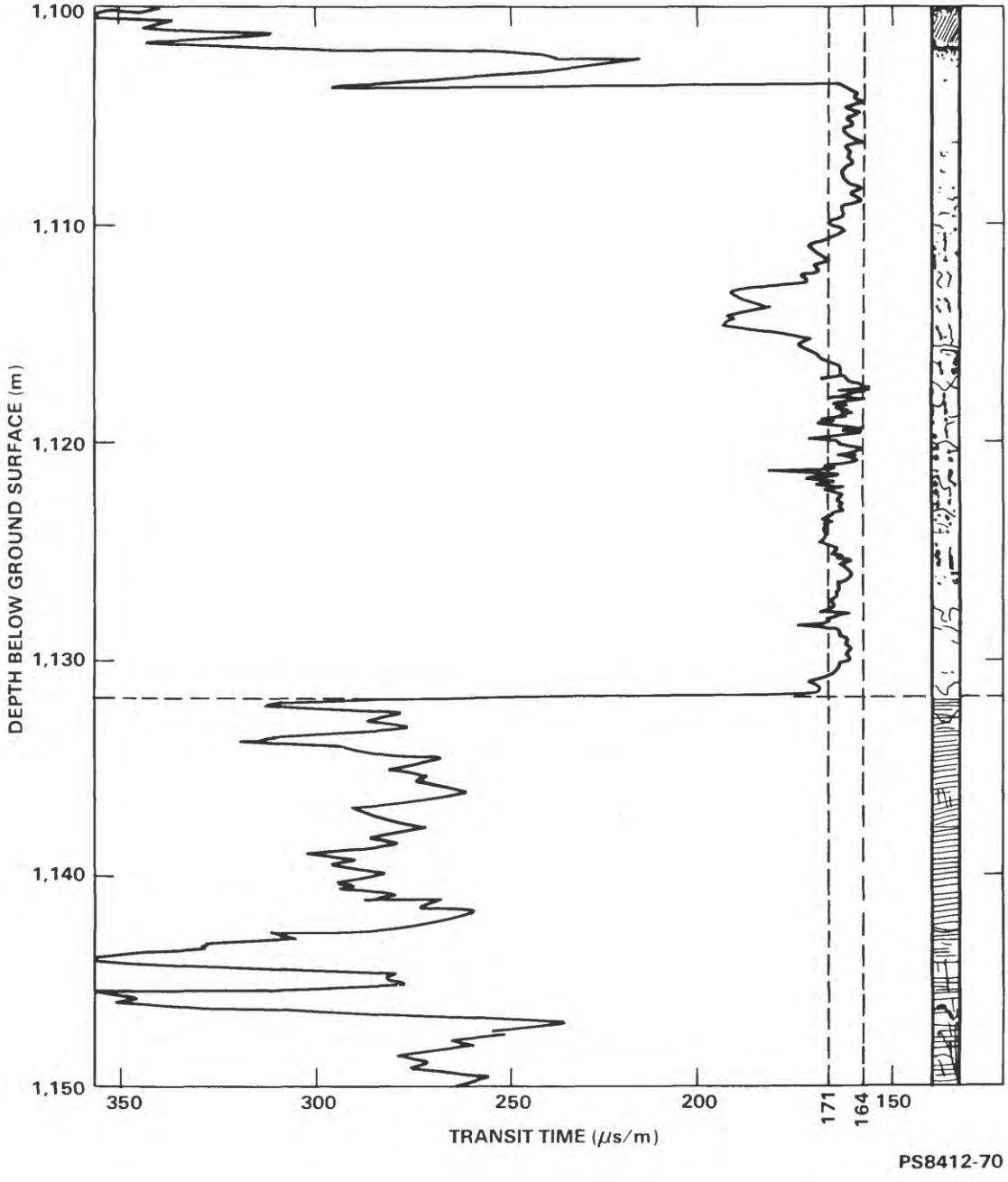

Figure 23. Acoustic transit-time and televiewer logs for representative interval in borehole RRL-6.

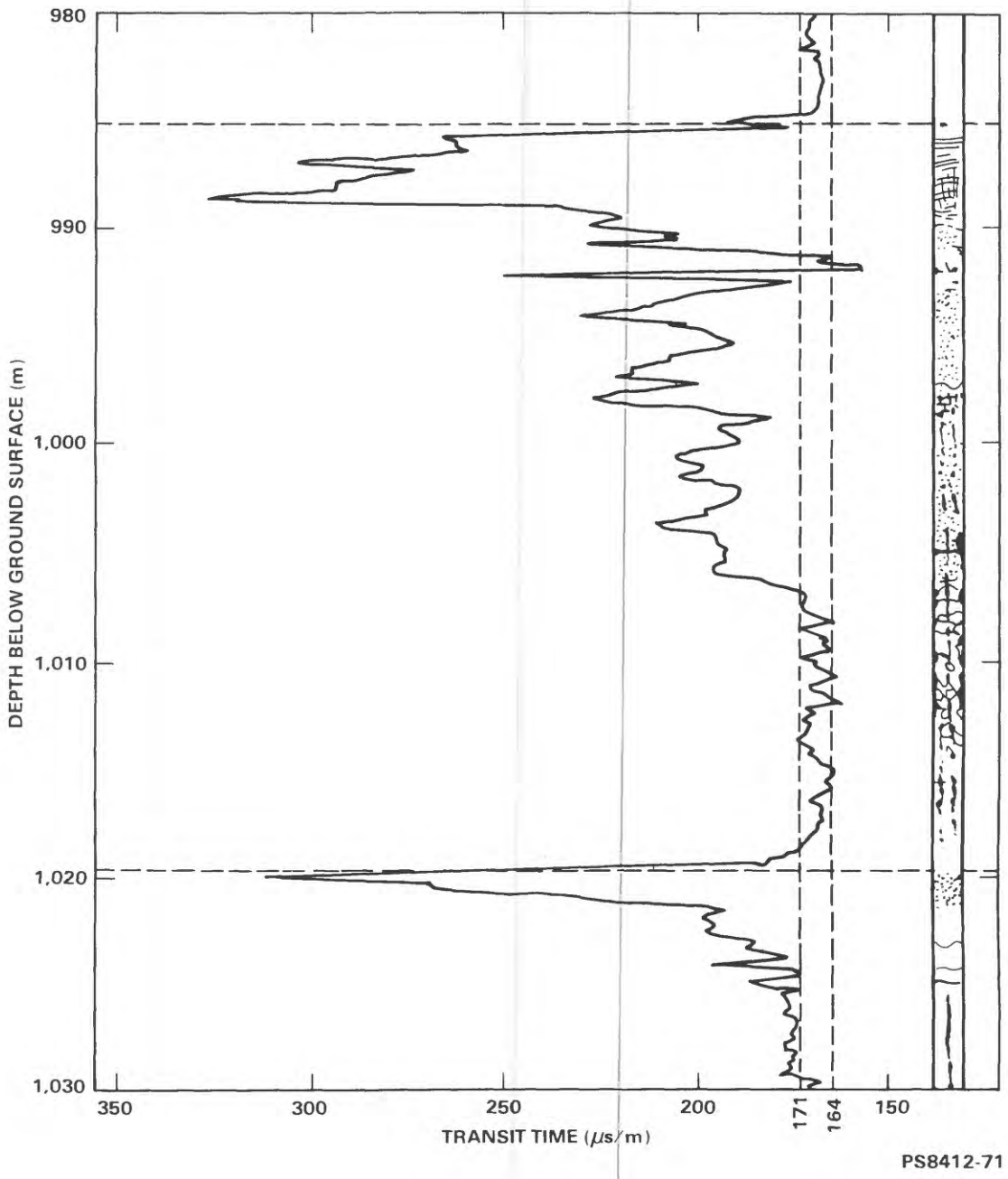

Figure 24. Acoustic transit-time and televiewer logs for representative interval in borehole DC-4.

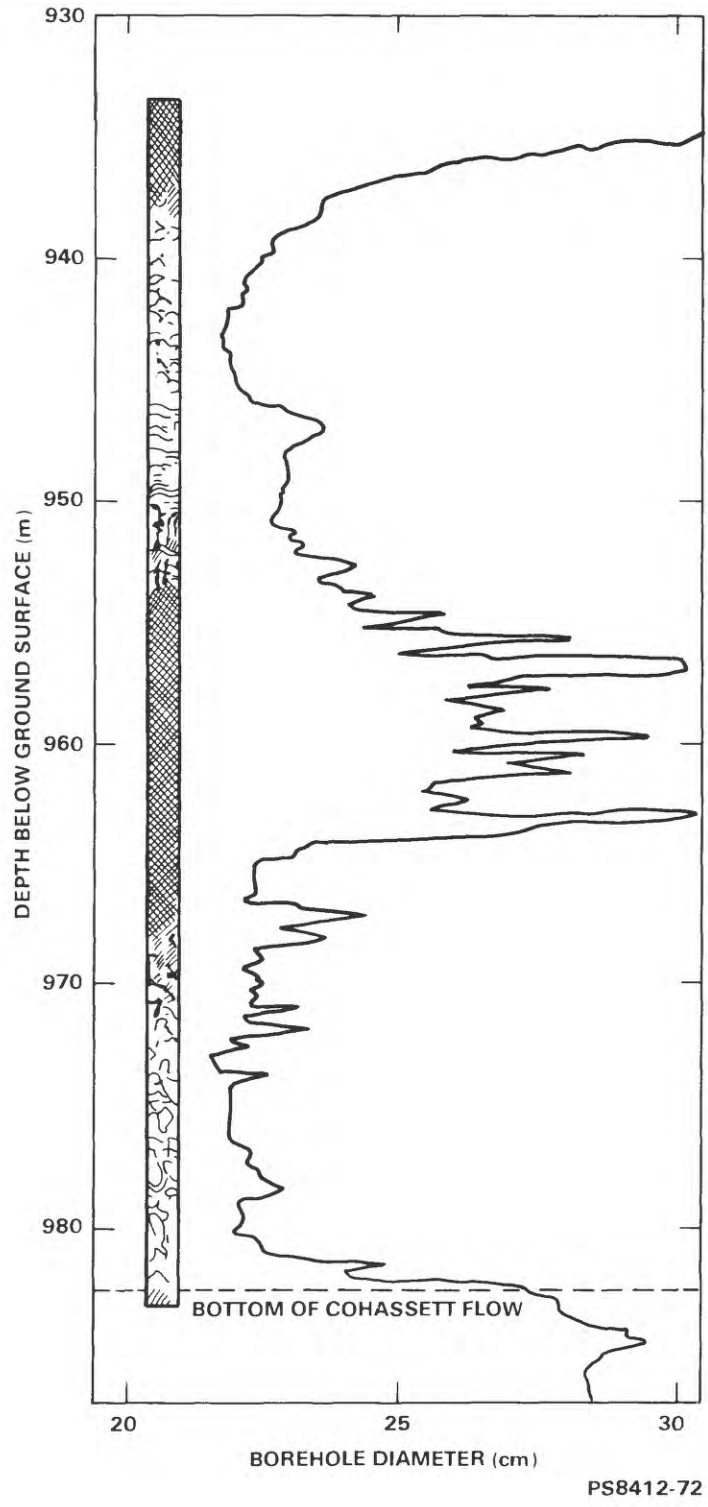

Figure 25. Televiewer and caliper logs for representative interval in borehole DC-7.

The comparison between acoustic transit-time logs and televiewer logs in figures 23 and 24 provide useful information about the character of flow interiors. The transit-time logs indicate that the solid basalt of the flow interiors has a compressional velocity of about 6.1 $\pm$ 0.1 km/s or an acoustic transit-time of 165 $\pm$ 5 μs/m. The slight variation in the log values around 165 μs/m probably results from the acoustic log having been run uncompensated. Most commercial acoustic transit-time logs are run using the average of transit times measured from top and bottom of the logging tool. This procedure partially averages out the effects of borehole-wall irregularities.

Although much of the logging literature indicates that acoustic transit-time logs are insensitive to the presence of fractures, and that acoustic logs can be calibrated in terms of matrix porosity rather than total porosity (Pickett, 1963), acoustic transit-time logs can be sensitive to open horizontal fractures. This sensitivity results from the fact that an open fracture perpendicular to the borehole axis must be crossed by all acoustic signals propagating from source to receiver. Paillet (1980, 1983c) demonstrated that attenuation of acoustic signals propagating across open fractures can sometimes be related to fracture permeability. Several of the fractures indicated on the televiewer logs in figures 23 and 24 appear to produce significant anomalies in acoustic transit time.

Distribution and Character of Borehole-wall Breakouts

The overview of the televiewer logs in figures 9 to 18 provides a qualitative indication of the extent of breakouts in the boreholes. Breakouts are indicated by the large, vertically continuous or discontinuous dark areas such as the typical example identified in figure 10. These figures show that the breakouts generally are confined to the interior of the flows. The vertical extent of breakout appears to vary greatly from flow to flow, and within some flows from one borehole to the next. For example, there are few breakouts in the Umtanum flow in borehole DC-12 than in boreholes RRL-6 and DC-4. The breakouts appear quite variable in character, alternating from nearly continuous, as in the lower part of figure 26A and the upper part of figure 26B, to highly discontinuous as in figure 26C. The nearly continuous breakouts appear to occur in intervals where the basalt is especially free of fractures and vugs, whereas the discontinuous breakouts are associated with the presence of multiple fine fractures. These fractures may have relieved stress at some points along the borehole wall preventing the formation of breakouts by the shear-failure mechanism described by Zoback and others (1984). In contrast, the many fine fractures associated with some of the discontinuous breakouts may represent fractures produced during breakout formation, and may not extend away from the borehole. The televiewer logs also indicated a repeated tendency for breakout-free intervals to occur at the tops and bottoms of flows. An example is the short interval at the bottom of the Cohassett flow illustrated at the top of figure 24. Many of the intervals of continuous or

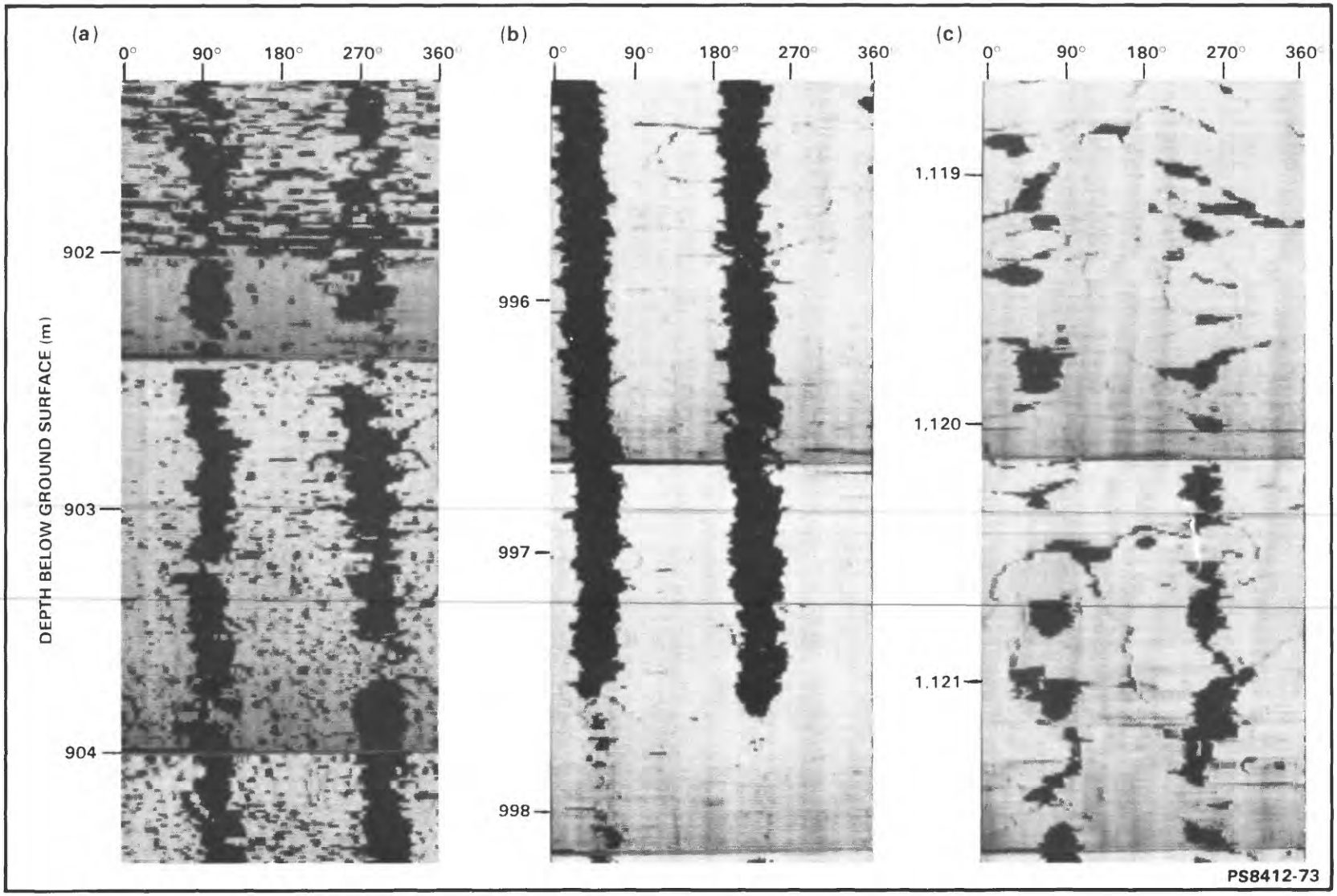

Figure 26. Televiewer logs showing examples of continuous and discontinuous borehole-wall breakouts in borehole RRL-6.

nearly continuous breakouts terminate at fractures or sets of fractures. Several examples are given in figure 27. Many of these breakout-terminating fractures occur at a moderate angle to the individual flows, and may have produced local stress relief near the flow margins.

The extent of borehole-wall breakouts in three boreholes where many meters of continuous televiewer logs were made (boreholes RRL-6, DC-4, and DC-12) is compared in figure 28 to the extent of core disking as reported in the core descriptions given by Cross (1983). This figure indicates that both wall breakouts and core disking are confined to the interior, unaltered parts of individual flows. Both disking and borehole-wall breakouts were much more extensive in boreholes DC-4 and RRL-6 than in borehole DC-12. Because the two boreholes with extensive breakouts and disking are relatively close together (fig. 1), similarity of televiewer logs from the two boreholes could have been anticipated. The much more limited televiewer logs from the other two boreholes (borehole RRL-2, located between boreholes RRL-6 and DC-4, and borehole DC-7) indicate that at least some breakouts are present, although not enough televiewer logs were run to make a detailed comparison.

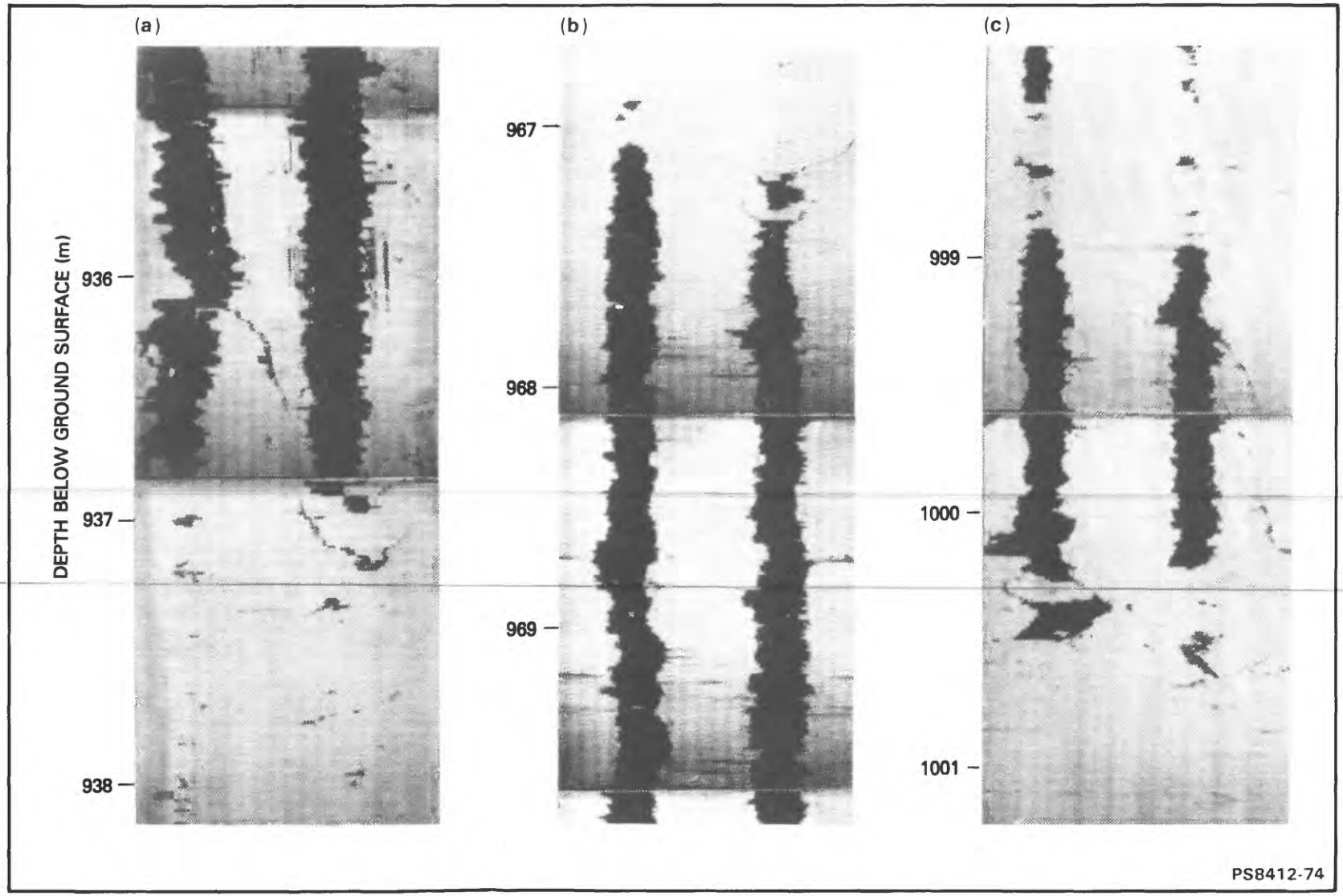

Figure 27. Televiewer logs showing examples of borehole-wall breakouts terminating at oblique natural fractures: (A) borehole RRL-6; (B) borehole DC-4; and (C) borehole RRL-6.

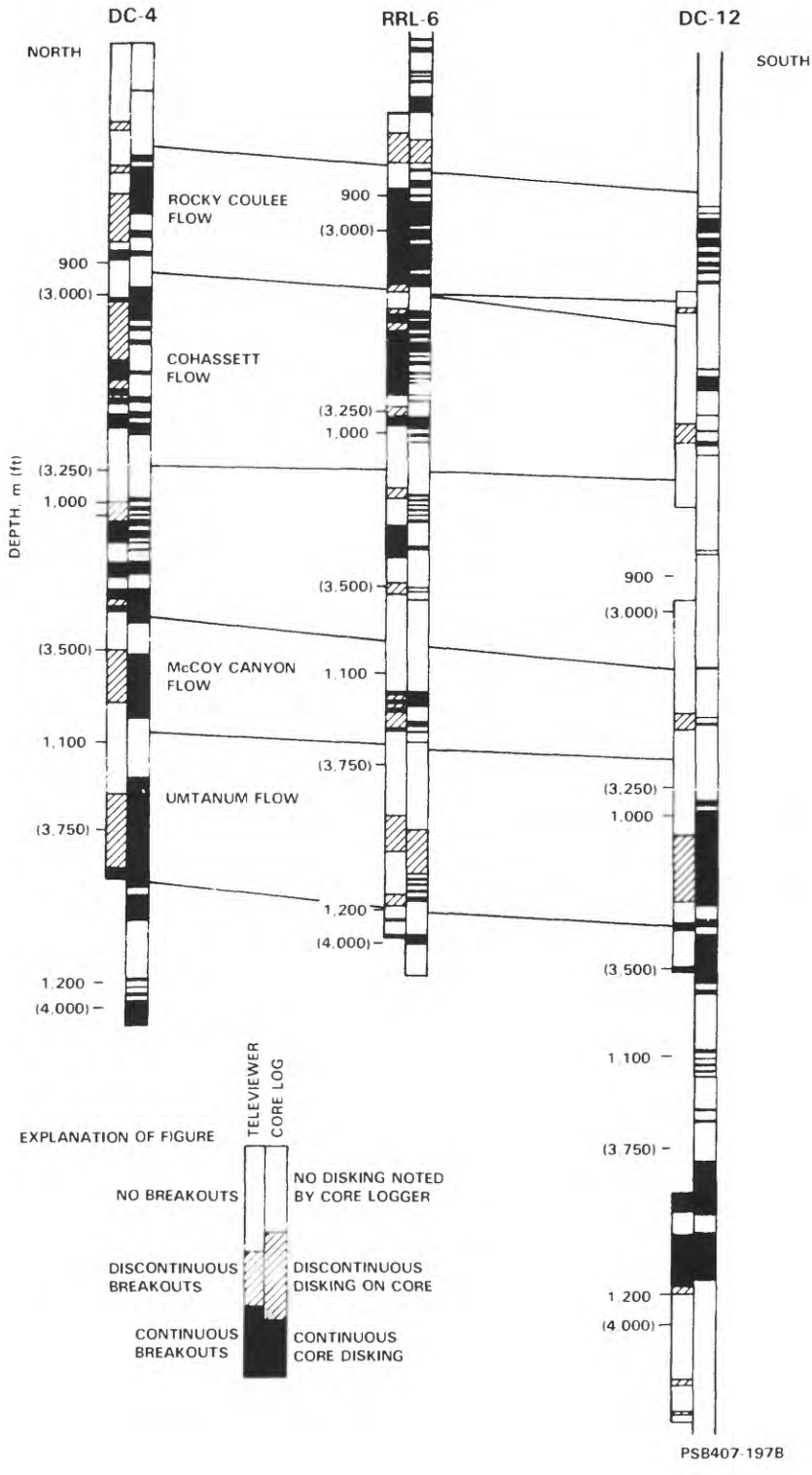

Figure 28. Correlation of borehole-wall breakouts on televiewer logs with disking on core logs in boreholes DC-4, RRL-6, and DC-12.

Although the televiewer was very effective in characterizing the extent of borehole-wall breakouts, several problems were encountered in using the televiewer to determine the orientation of these breakouts. The problems were caused by relatively large concentrations of ferromagnetic minerals in the basalt. The televiewer-logging system orients borehole-wall images with respect to the local geomagnetic field. The logging sonde uses a down-hole magnetometer to measure the azimuth of the local component of magnetic field perpendicular to the borehole axis. When the borehole is deviated from the vertical or there is a significant component of dip associated with the local geomagnetic field, the correct orientation of the televiewer log can be obtained by the methods given by Kierstein (1984) and Lau (1983). In many of the boreholes at the Hanford Site, the relatively large concentration of ferromagnetic minerals in the basalt produced significant local deviations in magnetic field measured by the magnetometer in the televiewer system. In a few cases, the local variations were so severe that the televiewer system would not function in the compass mode, and oriented logs could not be obtained. In many more cases, the local variations in magnetic field produced a recognizable distortion on the televiewer-log image. The distortion effect was not severe in borehole RRL-6, and most televiewer logs were oriented in this borehole.

The televiewer logs for the larger diameter borehole DC-7 also were free of distortion, and were run oriented. In this case, the effect of larger borehole diameter appeared to alleviate the effect of ferromagnetic minerals on the televiewer log. This may have been an indirect effect, because the larger diameter boreholes were not used for hydrologic testing, and a magnetized drill stem was never lowered into these boreholes. The drill stem being used to lower hydraulic-test equipment into the Hanford boreholes was highly magnetized. Because the magnetized drill stem was not rotated during the hydraulic tests, the field imposed by the drill stem may have reoriented the domains within the ferromagnetic minerals, greatly aggravating the distorting effect of these minerals on televiewer logs. Televiewer logs can be run with orientation determined by an internal mark rather than by the magnetometer. Because the orientation of the logging tool in the borehole is unknown, the actual orientation of televiewer logs run in the "mark" mode is undetermined. The slow-spiral motion of the centralized logging tool as the sonde is moved uphole changes the apparent orientation of the televiewer log, but this regular change in orientation does not greatly distort the televiewer log. A typical example of an oriented televiewer log from borehole RRL-6, showing image distortion by local concentrations of ferromagnetic minerals is given in figure 29. An interval of televiewer log in borehole DC-4, where variations in the local magnetic field had a pronounced distorting effect on the log is shown in figure 30A. This oriented log can be compared to the log of the same interval run in the "mark" mode (fig. 30B). In this repeat log, no distortion occurs, but the orientation of the features indicated on the log is unknown. In most cases where televiewer-log resolution was important, such as attempts to identify very faint induced fractures, televiewer logs were run in the "mark" mode to increase resolution.

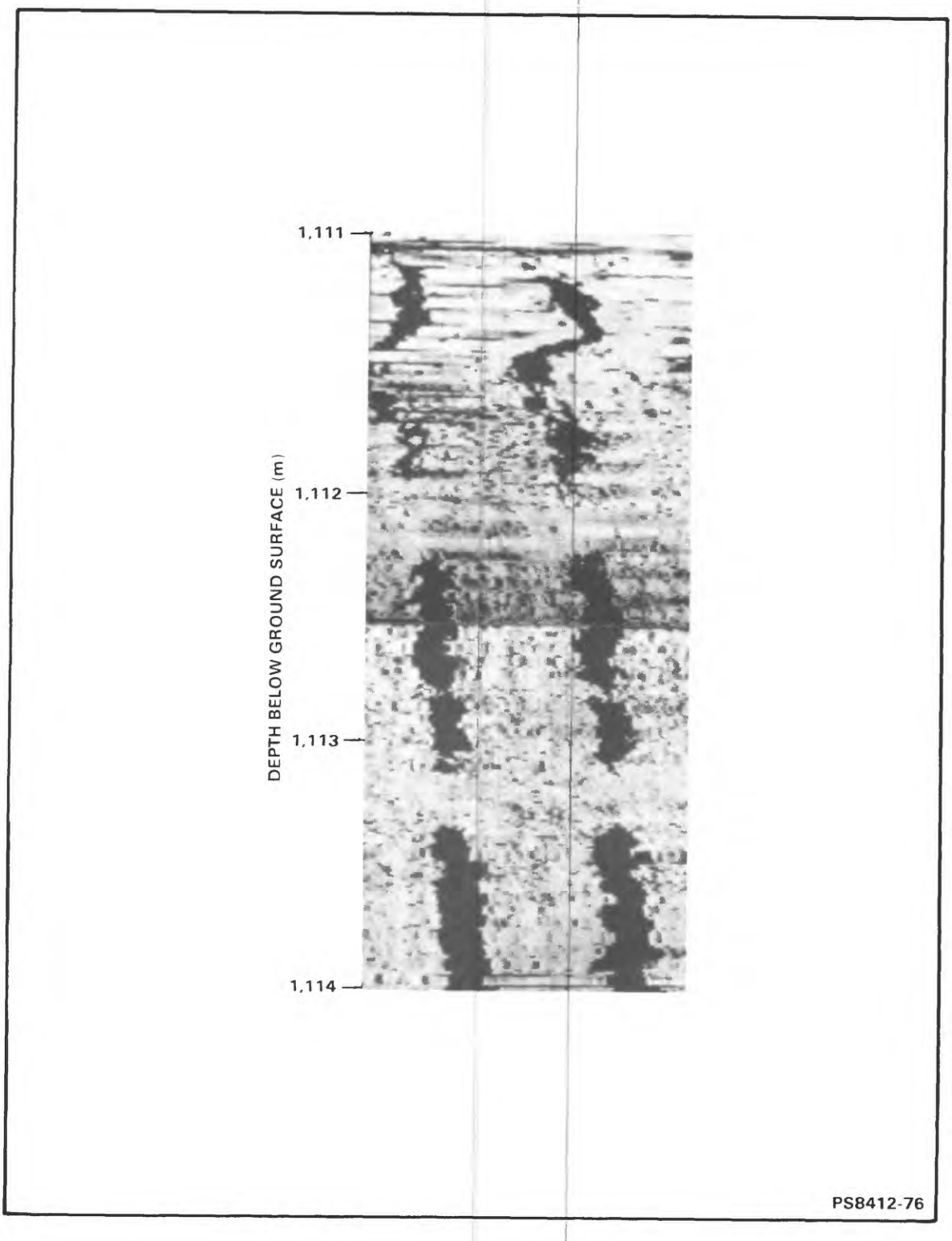

Figure 29. Televiewer log for interval in borehole RRL-6 where ferromagnetic minerals in the borehole wall have produced severe distortion of the oriented log image.

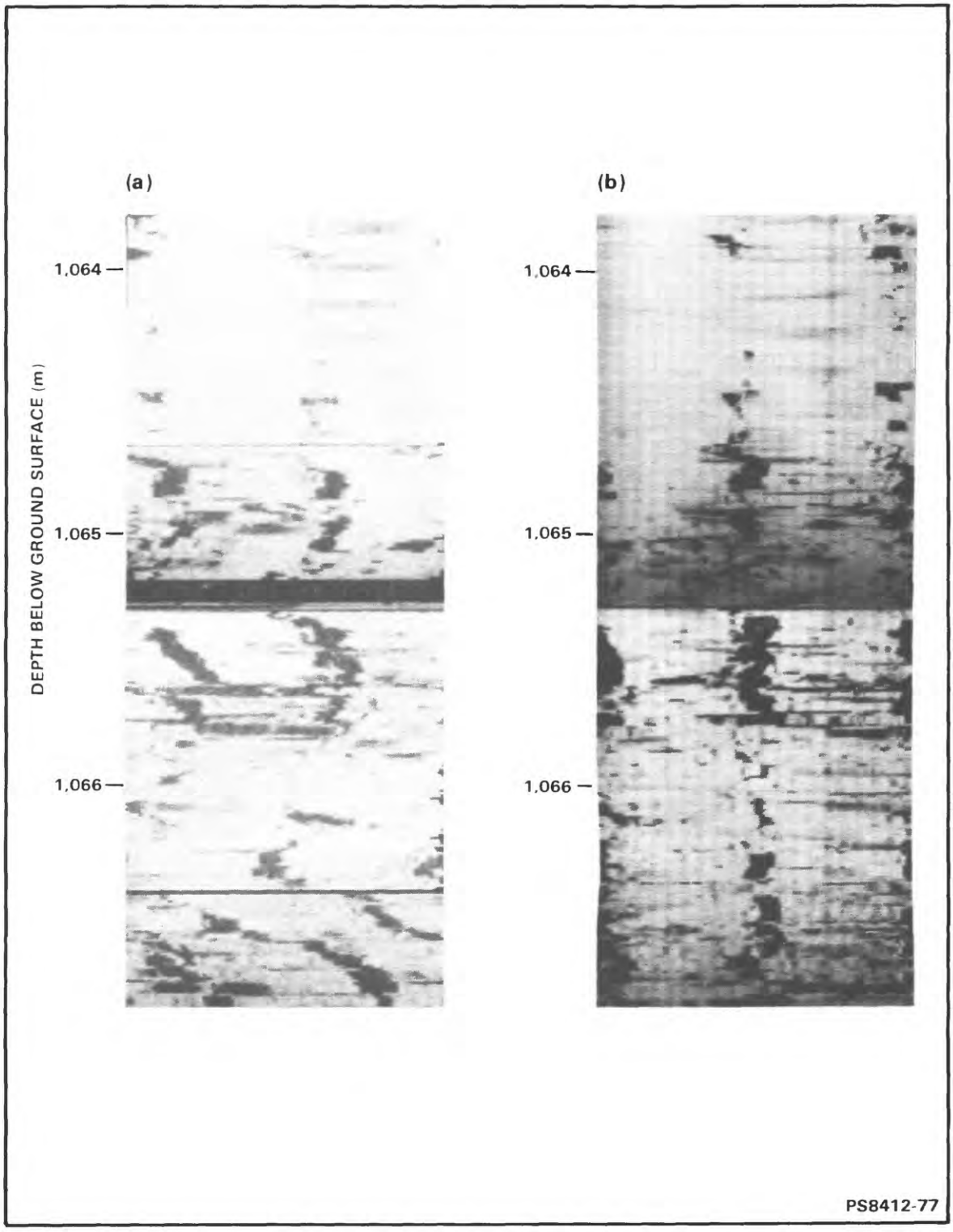

Figure 30. Comparison of televiewer logs for interval in borehole DC-4: (A) with severe distortion of image by ferromagnetic minerals, and (B) unoriented.

All of the existing theory on the production of borehole-wall breakouts indicates that these breakouts should have an orientation determined by the regional tectonic stress (Zoback and others, 1984). If regional stress does not vary along the length of the borehole, and borehole breakouts are parallel to the direction of least horizontal principal stress, then the orientation of breakouts should be consistent along the entire borehole. The televiewer logs illustrated in figures 9 to 18 show an apparent drift in breakout orientation with depth.

The possibility that local magnetic anomalies may have affected apparent orientation leads one to question whether this variation in borehole-wall-breakout orientation is real. The breakouts indicated on impression packers obtained in boreholes DC-4 and RRL-6 were consistently close to east and west. This orientation agrees with the estimated regional principal-stress field given by McGarr and Gay (1978) and Zoback and Zoback (1980) under the assumption that mean azimuth of breakouts is parallel to the direction of least principal horizontal stress (Zoback and others, 1984). The variable breakout orientations obtained in borehole RRL-6 (fig. 26) can be compared with the breakouts obtained on the oriented impression packers and in the rotary-drilled borehole DC-7 (fig. 31). The unreliability of orientations obtained in borehole RRL-6 also was indicated by apparent changes in borehole orientation, detected when the magnetized drill stem had been lowered into the borehole between televiewer runs. For example, there were large changes in apparent orientations of breakouts for certain intervals in borehole RRL-6 on televiewer logs made before and after hydraulic testing. These considerations collectively indicate that the borehole-wall breakouts illustrated in figures 9 to 18 have a consistent east-west orientation.

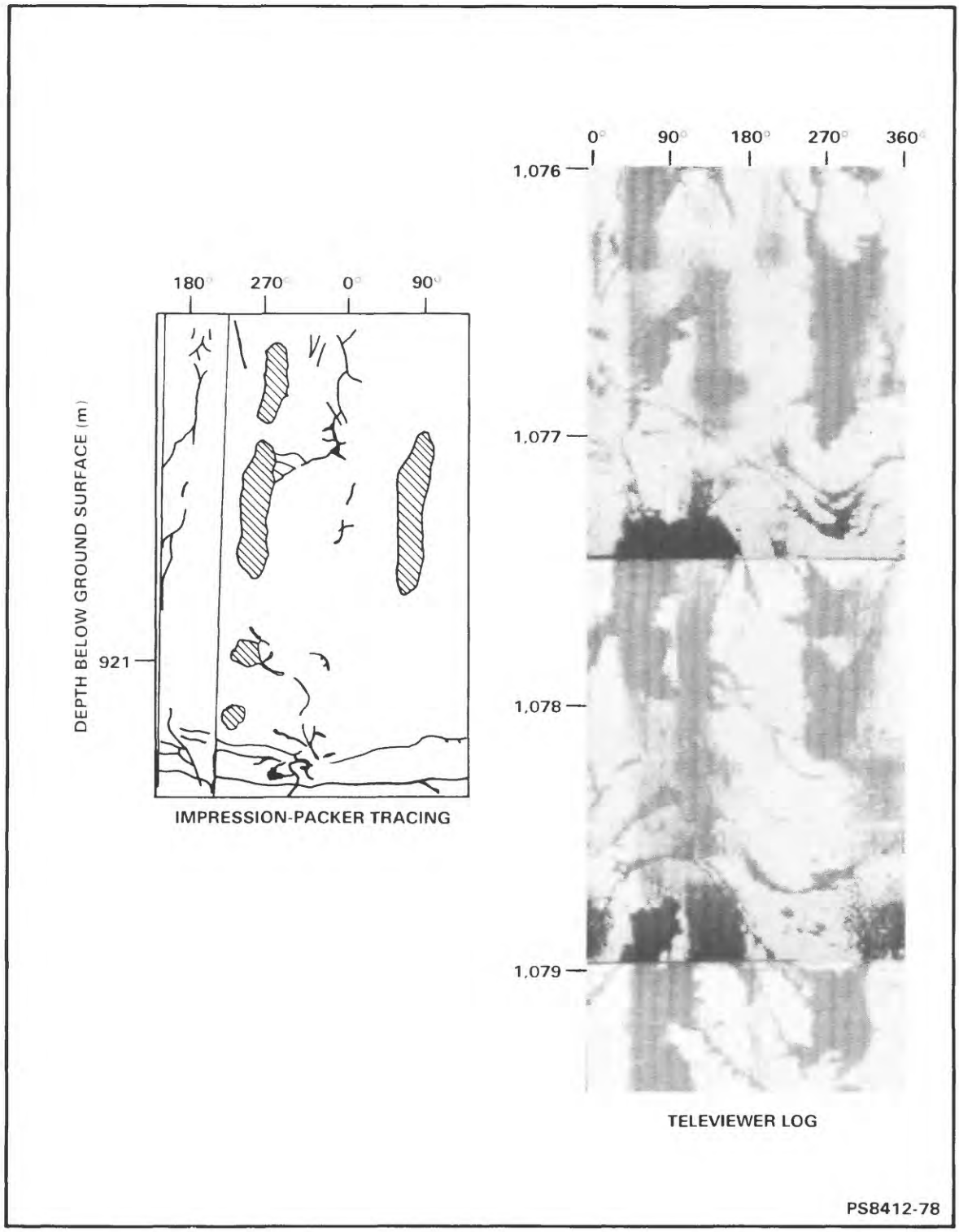

Figure 31. Orientation of borehole-wall breakouts in impression-packer tracings and orientations of breakouts on televiewer log for borehole DC-7.

The borehole-wall breakouts indicated in figures 9 through 18 appear to have formed immediately or shortly after the boreholes were drilled. Additional breakouts might have been forming during this study because an angular piece of basalt fell onto the logging tool during the televiewer logging of borehole DC-4 and became trapped between the tool body and the borehole wall. The rock chip jamming against the tool body caused the televiewer sonde to become stuck in place. When the tool was eventually freed, the rock chip was firmly lodged in the soft transducer window on the televiewer. The shape of the rock chip resembles the shape of many of the breakouts (fig. 32). The small piece of rock may have been dislodged by passage of the centralizing bowsprings attached to the televiewer, but the chip could have been released by spontaneous spalling of the borehole wall. For this reason, a representative interval in this well was relogged with the televiewer 45 days after the original televiewer logs illustrated in figures 9 through 18 were obtained.

A typical comparison of televiewer logs in borehole DC-4, run before and after the 45-day test period is illustrated in figure 33. Both logs were run in the "mark" mode, but the second set of logs has been rotated to a comparable orientation.

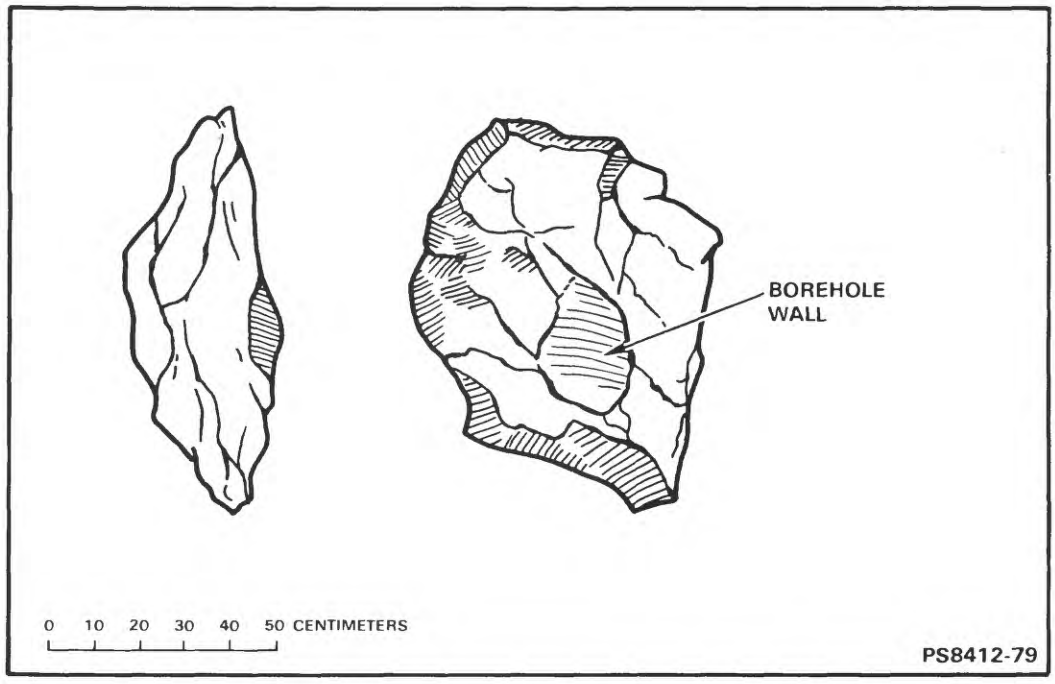

Figure 32. Sketches of angular piece of basalt that lodged in televiewer tool during logging of borehole DC-4; this fragment may have been produced by a typical borehole-wall breakout.

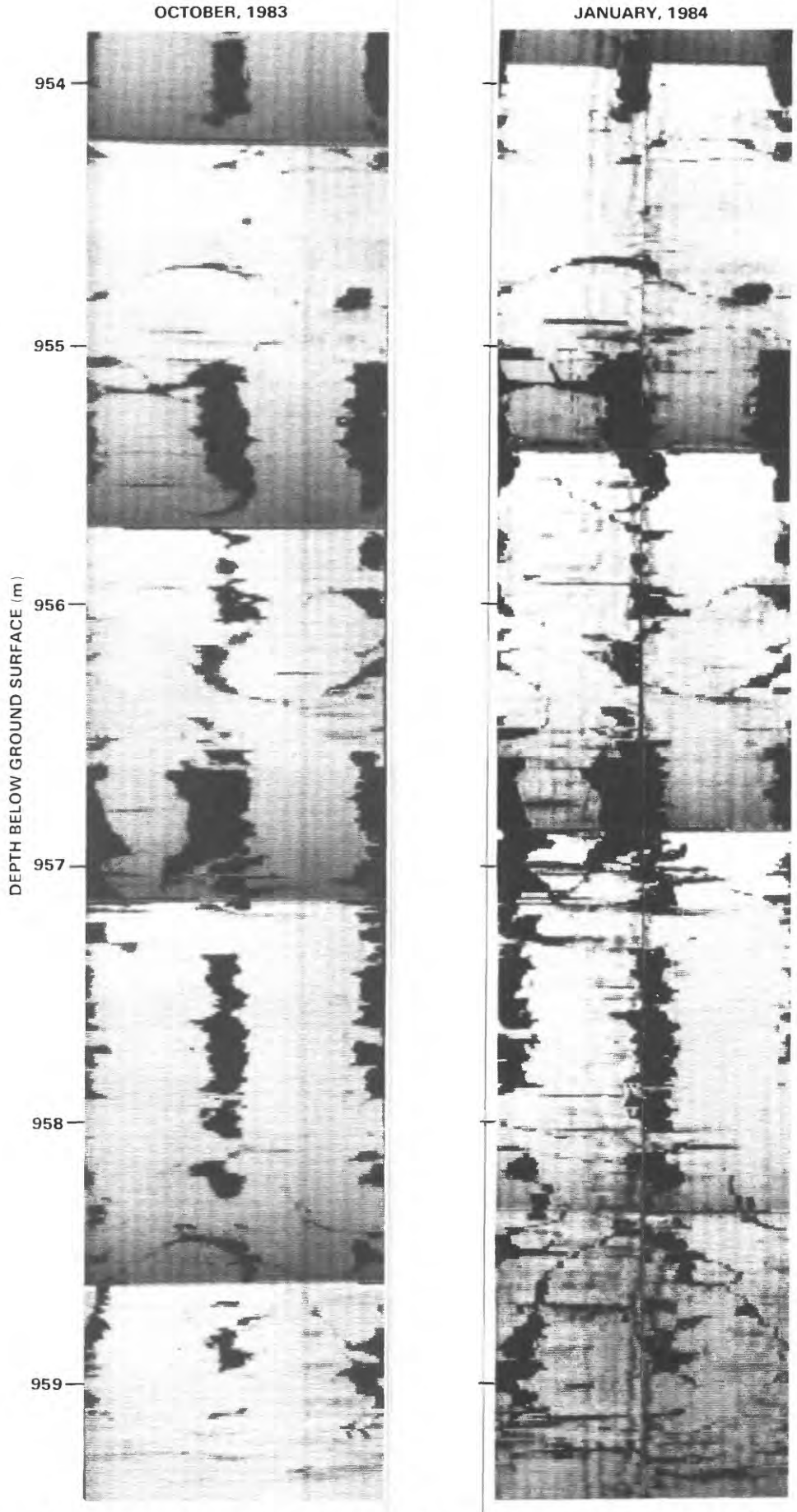

Figure 33. Comparison of televiewer logs for a representative interval in borehole DC-4 obtained before and after 45-day test period.

Acoustic Characterization of Induced Fractures

One of the objectives of this study is the use of acoustic logs before and after hydraulic fracturing stress measurements to assist in the characaterization of hydraulically induced fractures in borehole RRL-6 and DC-4. Hydraulic facturing (McGarr and Gay, 1978; and Zoback and Haimson, 1982) is considered the only widely accepted method for determining the local state of stress at depth. Orientation of the stress field is determined by measuring the orientation of fractures induced by pressurizing intervals within the borehole. Measurement of the induced fractures usually is accomplished by means of impression packers that produce an impression by forcing a soft material such as semicured rubber against the borehole wall. When properly used, impression packers produce a finely-detailed image of the pattern of fractures intersecting the borehole wall. However, impression packers are very time consuming to use, and they can provide only a very limited interval of borehole per run. The acoustic-borehole televiewer provides a continuous image of the borehole as indicated on figures 9 to 18, but the resolution in the televiewer log is substantially less than that given by optical-imaging devices (Davison and others, 1982).

Televiewer logs were run before hydraulic fracturing in boreholes DC-4 and RRL-6 to assist in selecting intervals for hydraulic fracturing, and to verify that fractures later identified as induced were not present prior to fracturing. The long intervals of borehole-wall breakouts presented a major problem in the selection of intervals for hydraulic fracturing. The breakouts could prevent packers from seating properly, and minor fracturing associated with the formation of breakouts might affect the orientation at which induced fractures would form at the borehole wall. Even if packers could be seated in intervals containing breakouts, the effective enlargement of the borehole could perturb the theoretical model of the borehole-stress-concentration field used to interpret in-situ stresses. Initial consideration was, therefore, given to identifying short intervals of borehole without such breakouts. In order to save time, televiewer logs were run at one gain setting, which was a compromise for average reflectivity, so that reflectivity in short intervals of unfractured basalt appeared especially high. The resolution of very fine fractures would have been somewhat better if these highly reflective intervals had been run at a lower gain, but this would have degraded the logs from most of the other intervals.

Although televiewer logs are much faster to run than impression packers, the televiewer is still a relatively slow geophysical device in comparison to other well-logging equipment. In order to permit the logging of large intervals in boreholes RRL-6, DC-4, and DC-12, televiewer logs initially were run at the reduced scale of about 25 cm of borehole per 1 cm of log. After initial televiewer logging, intervals for hydraulic fracturing were selected, and selected intervals fractured according to established procedures. The fractured intervals were relogged with the televiewer on an expanded scale of 12.5 cm of borehole per 1 cm of log. All post-fracturing logs were run in the "mark" mode and with gain adjusted to maximize apparent resolution of the finest scale fractures in each individual fracture zone. Only during attempts to identify fractures did it become apparent that televiewer gain should have been significantly decreased for the prefracture logging in order to ensure detection of fractures and other features as faint as the induced fractures. In that case, the resolution of the larger fractures would have been degraded because less acoustic energy would be available to penetrate into fracture openings. It is, therefore, important that prefracture logging be performed at two gain settings. One gain would be set for optimum resolution, whereas the other would be at a lower setting judged to provide optimum resolution of the fractures. This would require two separate televiewer-logging runs, doubling time requirements, or decreasing the length of borehole logged by one-half if hole time is fixed by scheduling contraints.

A total of 11 hydraulic fractures was induced in boreholes DC-4 and RRL-6 on the basis of impression-packer images of the fractures, although various technical criteria appeared to invalidate pressure records obtained from some of these fractures. Three of these fractures were induced in borehole DC-4; eight fractures were induced in borehole RRL-6 (table 2). Seven of these apparent-induced fractures were associated with impression-packer records with near-vertical fractures of a consistent orientation a few degrees east of north. These induced fractures were, therefore, orthogonal to the orientation of breakouts, which is consistent with the published conclusion that the basalt flows are subjected to nonequal compressional stresses, with the maximum principal stress directed along a north-south axis. An eighth set of near-vertical fractures at a depth of about 1017 m in borehole RRL-6 did not appear to have this orientation, but borehole-wall breakouts are apparent just above and below these fractures on the televiewer logs. If the impression-packer orientation is accepted, these breakouts also would deviate from the consistent east-west trend. However, if the breakouts are used to orient the data, this induced fracture would have the same orientation as the other seven. It was assumed that the impression-packer orientation for this fracture was in error, and that the induced fractures at a depth of about 1017 m in borehole RRL-6 had the same orientation as the other vertical fractures.

Table 2.--Depth and strike of induced fractures in boreholes RRL-6 and DC-4.

Depth (meters)	Fracture strike (degrees)
Borehole RRL-6	
1007.7	N28E
1016.8	N15E
1018.2	N15E
1104.8	N 8E
1108.7	N30W
1130.5	N22E
1188.9	N21W
1194.8	*
Borehole DC-4	
920.8	N18E
966.4	N23E
976.0	N 6W

* Impression-packer test not run.

Televiewer logs of the fractured intervals are compared to the impression-packer tracings in figures 34 to 44. The pre-fracture televiewer logs were expanded to match the post-fracture televiewer logs in order to facilitate comparison. Impression-packer tracings were rescaled to correspond with dimensions of the post-fracture televiewer logs. The televiewer produces an image of the borehole wall from the inside, whereas the impression packer is viewed looking from the outside. For this reason, the rescaled impression-packer tracings were made into transparencies, and their mirror image used in constructing figures 34 to 44. Comparison of the pre- and post-fracture televiewer logs indicate the increase in overall resolution of fine fractures that is possible when gain is independently adjusted for the local reflectivity of the borehole wall. Impression-packer tracings generally have a greater degree of resolution for very fine fractures, although some faint fractures are apparent in the televiewer logs that are not indicated on the impression-packer tracings. Some small differences between the televiewer and impression-packer results usually could be acccounted for by stretching and distortion in the flexible packer material during the removal of the soft rubber sheet with the impression from the packer surface. In those cases where the induced fracture is not indicated on either impression packer or televiewer logs, it is assumed that the attempted fracturing resulted in the opening of an existing fracture. In several cases (figs. 33 and 41), noticeable differences occurred in the character of natural fractures before and after hydraulic fracturing. Although there is some difference in resolution between the pre- and post-fracturing televiewer logs due to the different gains used, at least some of this difference may represent damage to the borehole wall produced by expansion and reduction of the fractures or by the seating of packers.

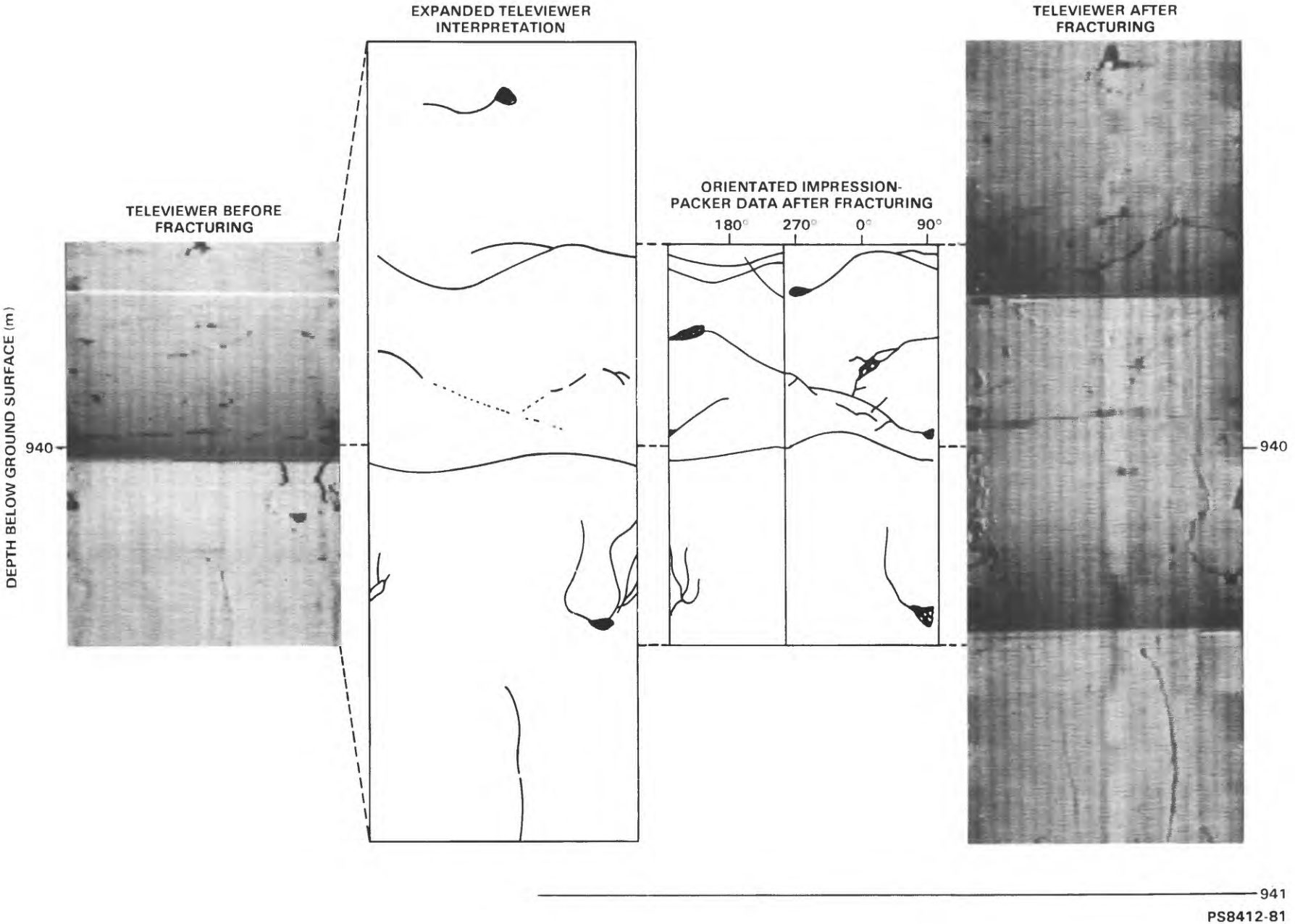

Figure 34. Televiewer logs obtained before and after hydraulic fracturing and post-fracture impression-packer tracing for fracture at a depth of about 940 meters in borehole RRL-6.

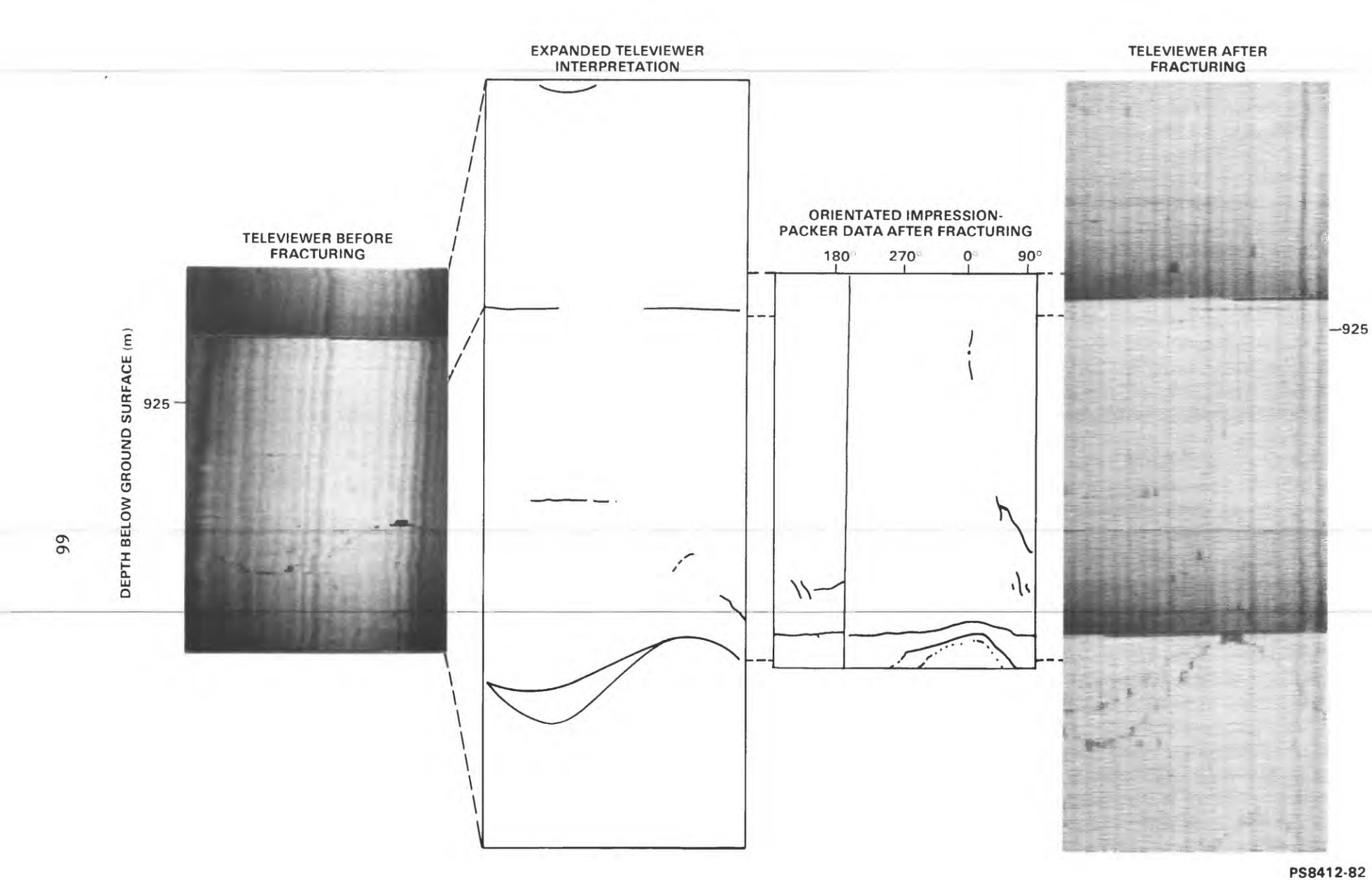

Figure 35. Televiewer logs obtained before and after hydraulic fracturing and post-fracture impression-packer tracing for fracture at a depth of about 1,008 meters in borehole RRL-6.

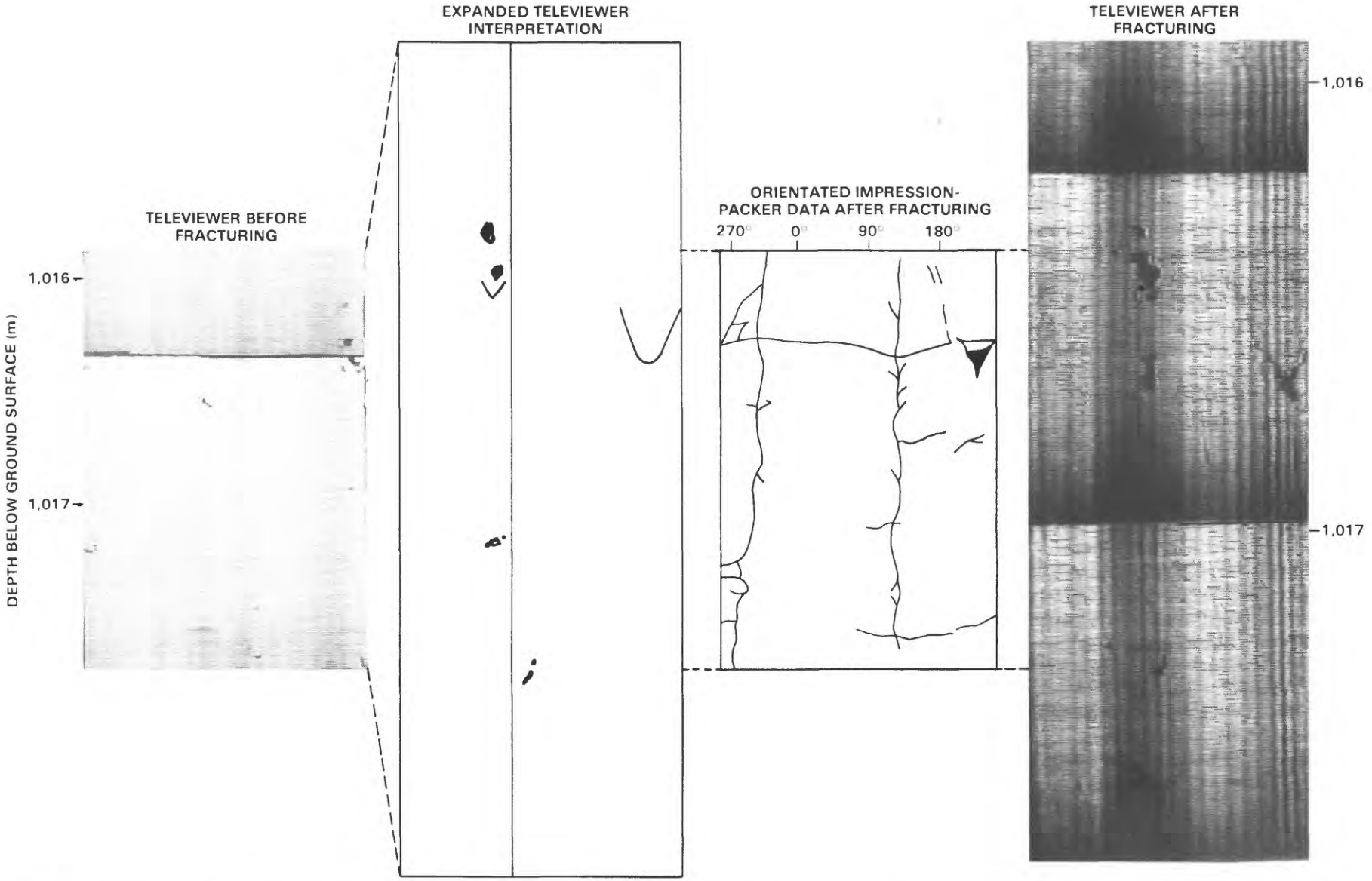

36. Televiewer logs obtained before and after hydraulic fracturing and post-fracture impression-packer tracing for induced fracture at a depth of about 1,017 meters in borehole RRL-6

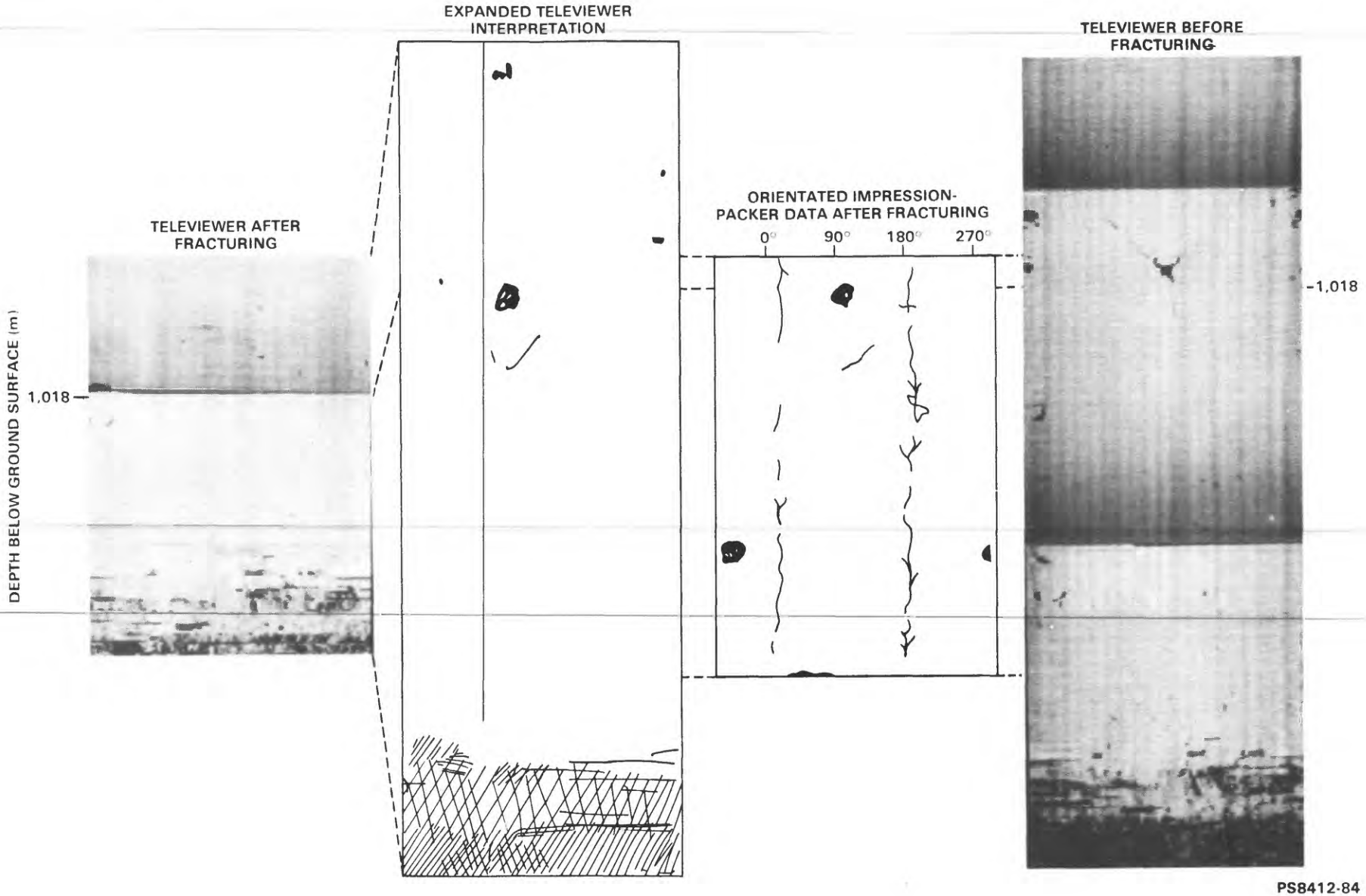

Figure 37. Televiewer logs obtained before and after hydraulic fracturing and post-fracture impression-packer tracing for induced fracture at a depth of about 1,018 meters in borehole RRL-6.

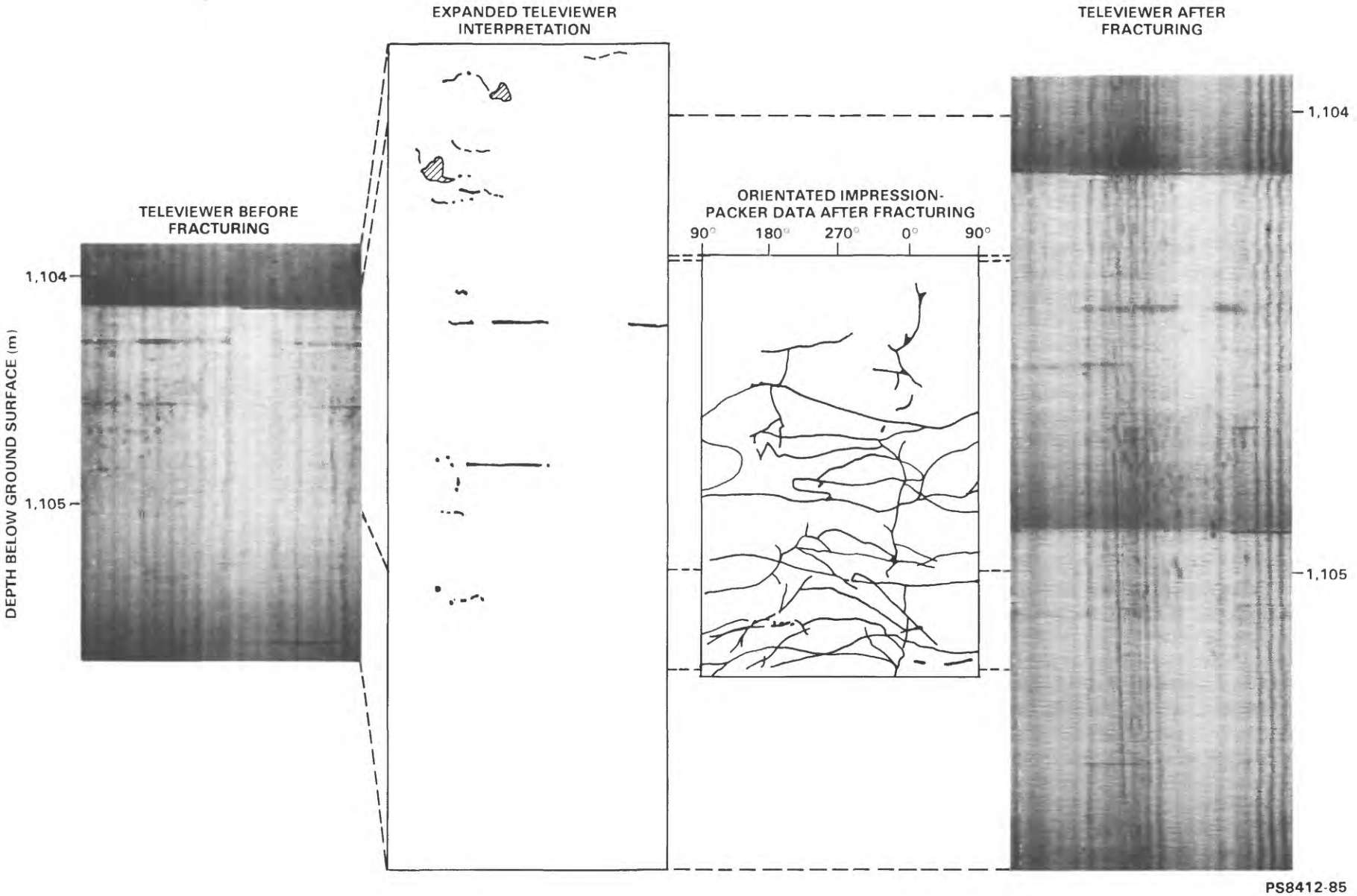

Figure 38. Televiewer logs obtained before and after hydraulic fracturing and post-fracture impression-packer tracing for induced fracture at a depth of about 1,105 meters in borehole RRL-6.

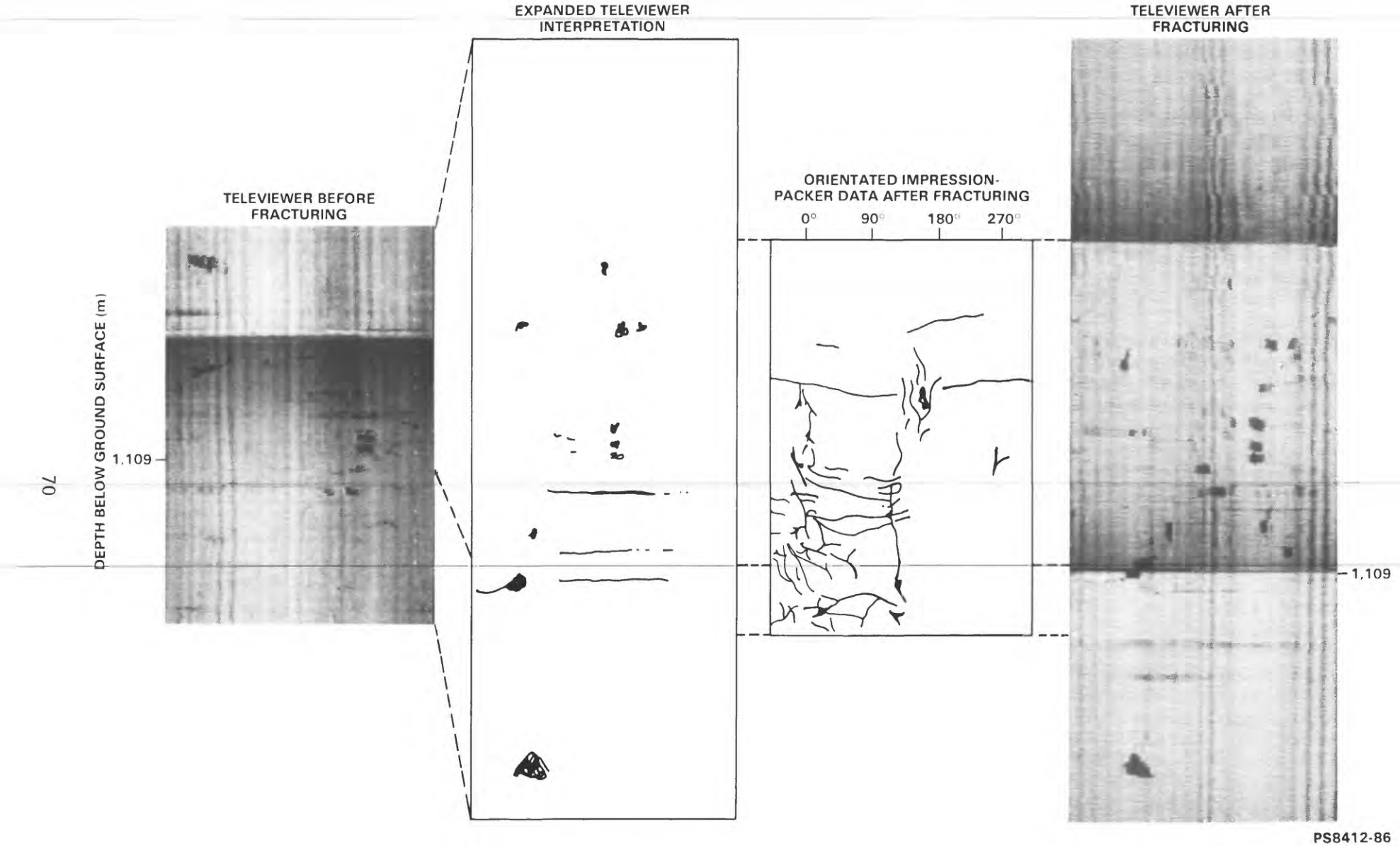

Figure 39. Televiewer logs obtained before and after hydraulic fracturing and post-fracture impression-packer tracing for induced fracture at a depth of about 1,109 meters in borehole RRL-6.

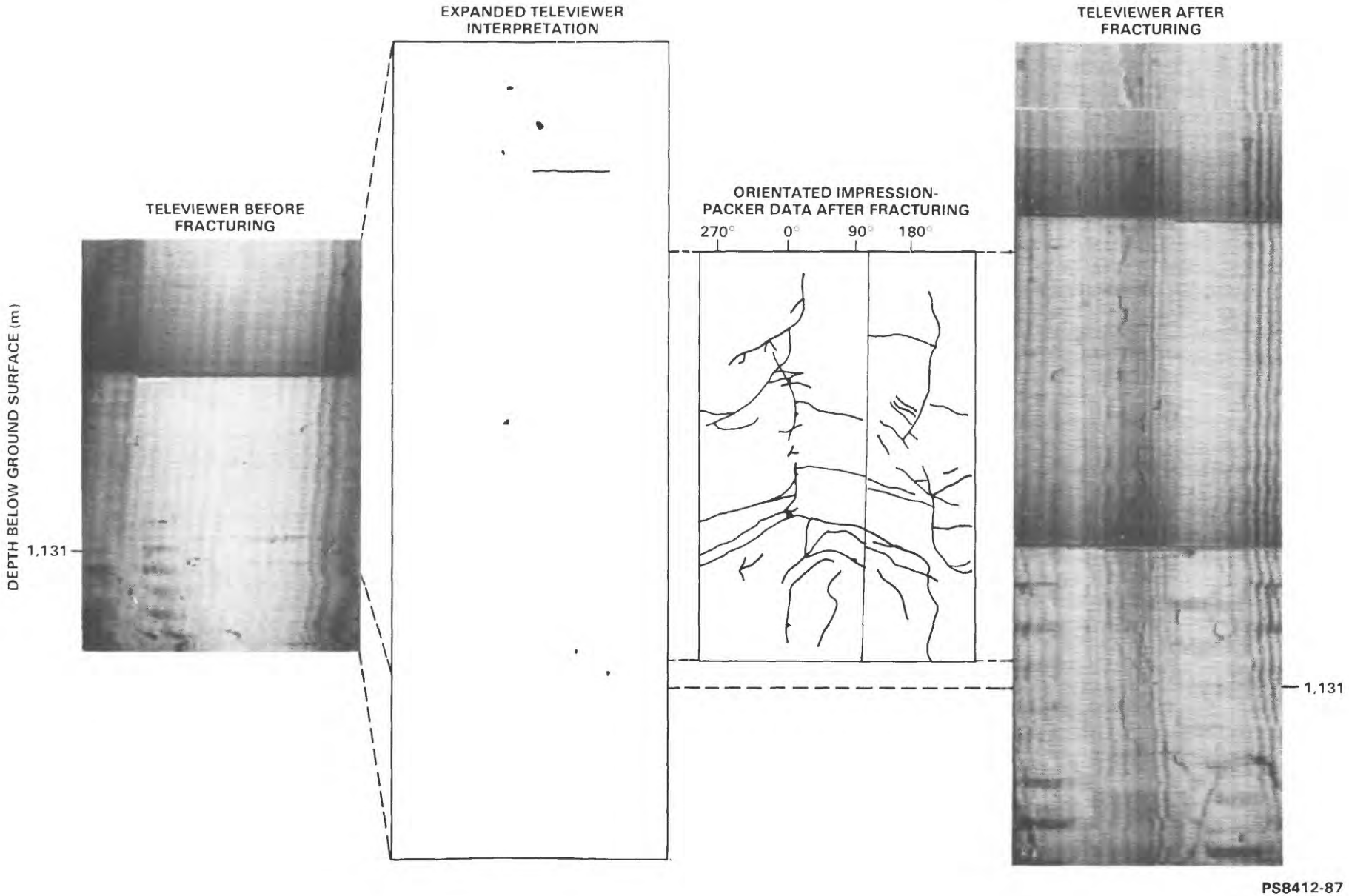

Figure 40. Televiewer logs obtained before and after hydraulic fracturing and post-fracture impression-packer tracing for induced fracture at a depth of about 1,131 meters in borehole RRL-6.

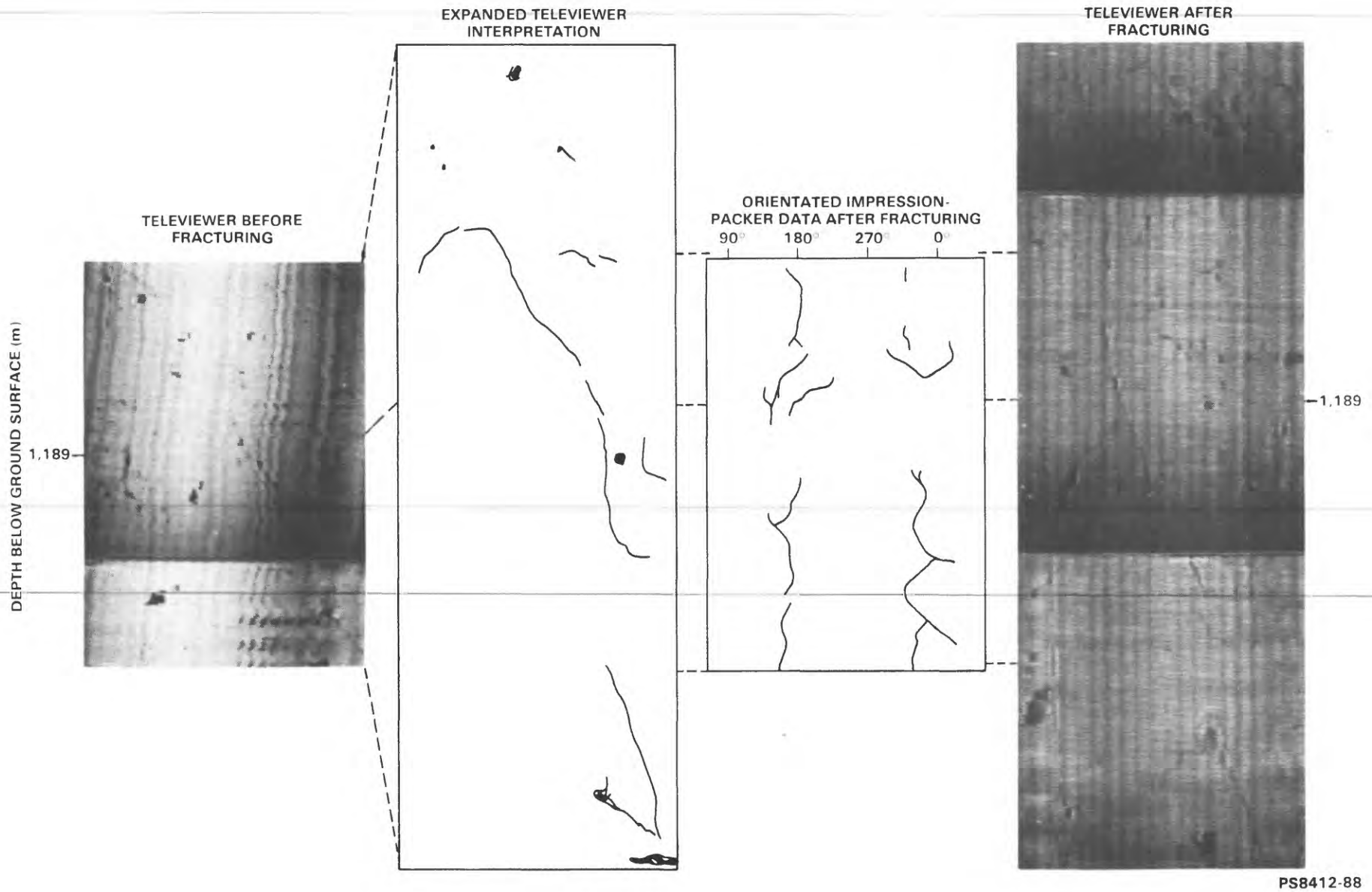

Figure 41. Televiewer logs obtained before and after hydraulic fracturing and post-fracture impression-packer tracing for induced fracture at a depth of about 1,189 meters in borehole RRL-6.

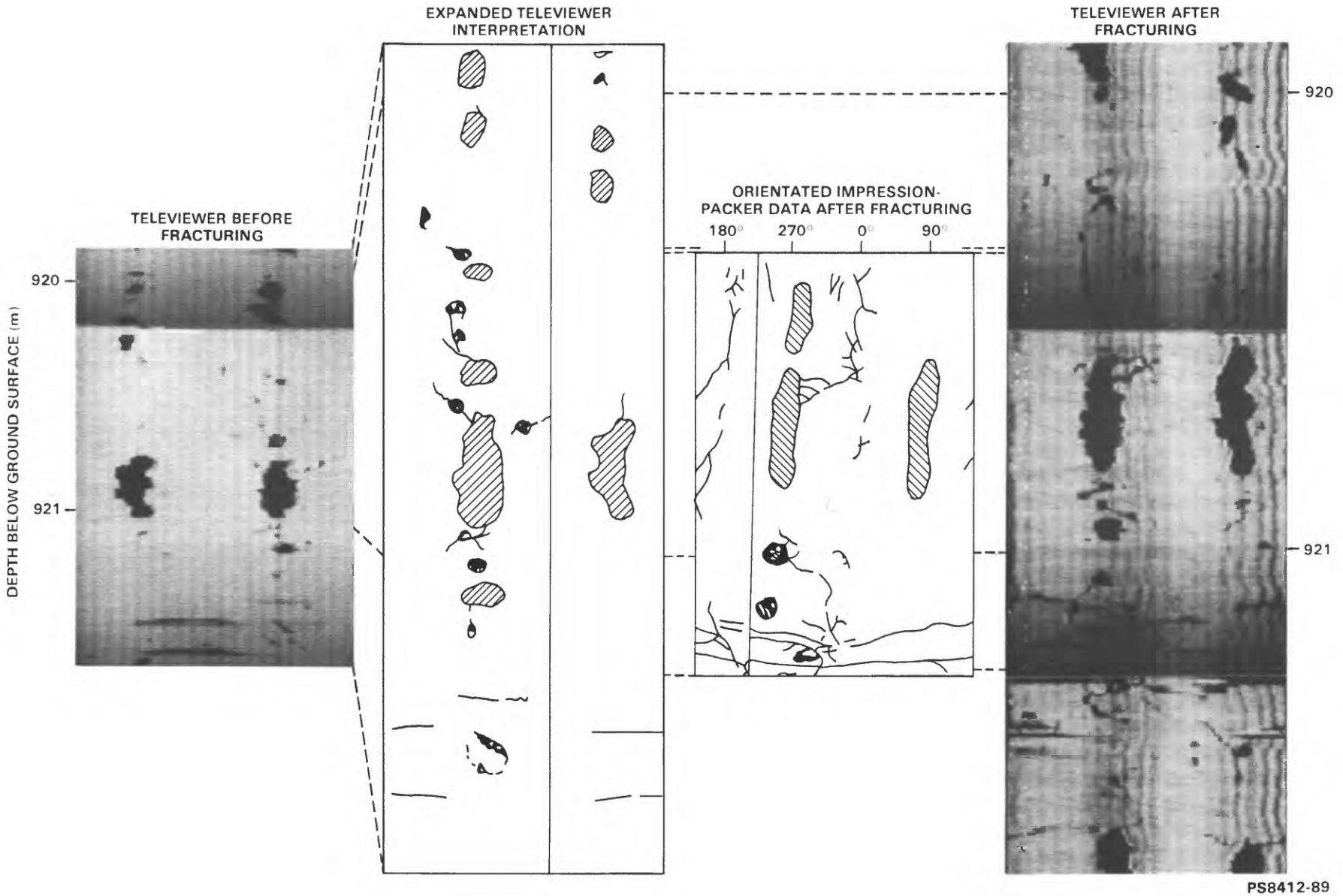

Figure 42. Televiewer logs obtained before and after hydraulic fracturing and post-fracture impression-packer tracing for induced fracture at a depth of about 921 meters in borehole DC-4.

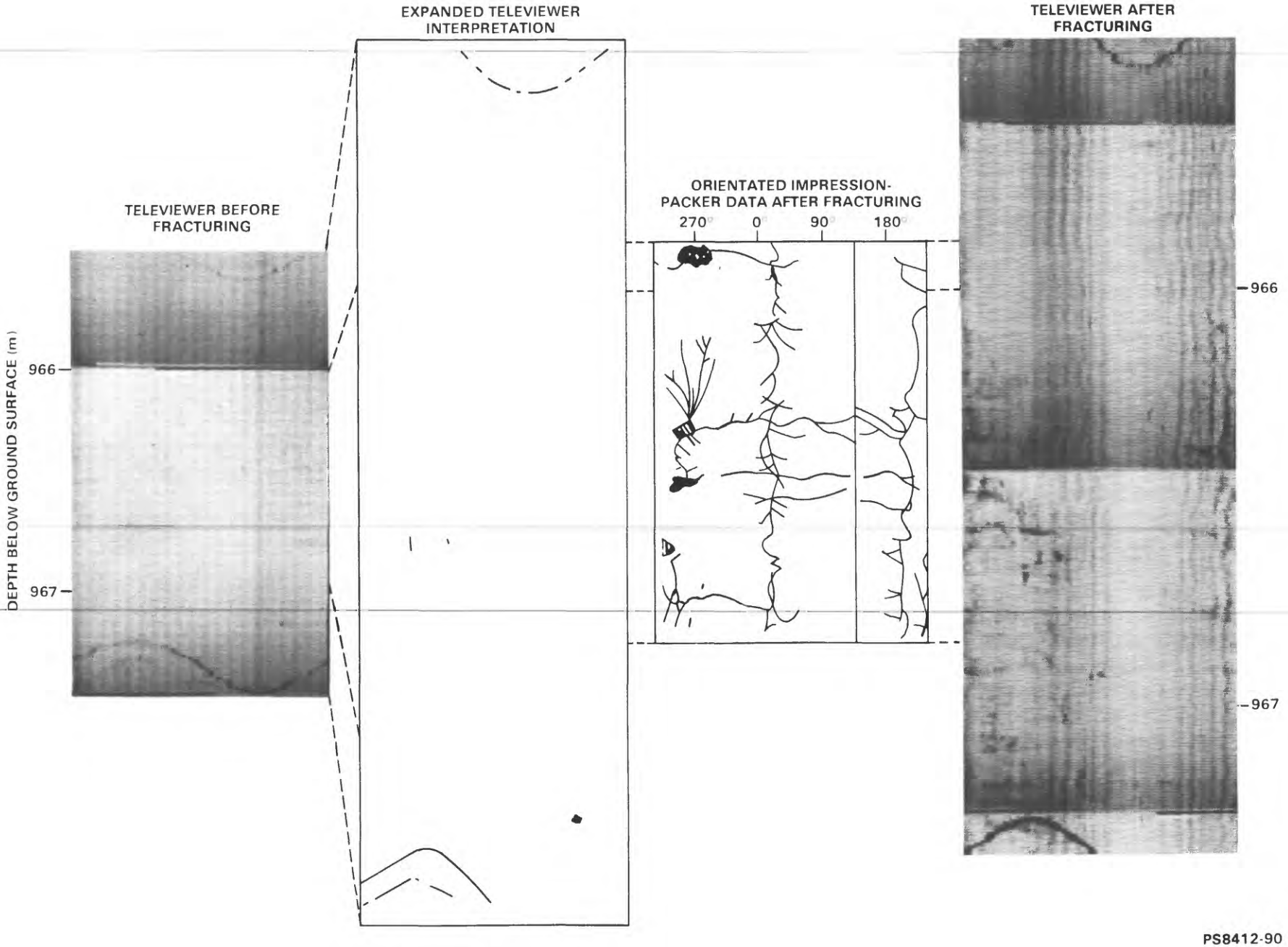

Figure 43. Televiewer logs obtained before and after hydraulic fracturing and post-fracture impression-packer tracing for induced fracture at a depth of about 966 meters in borehole DC-4.

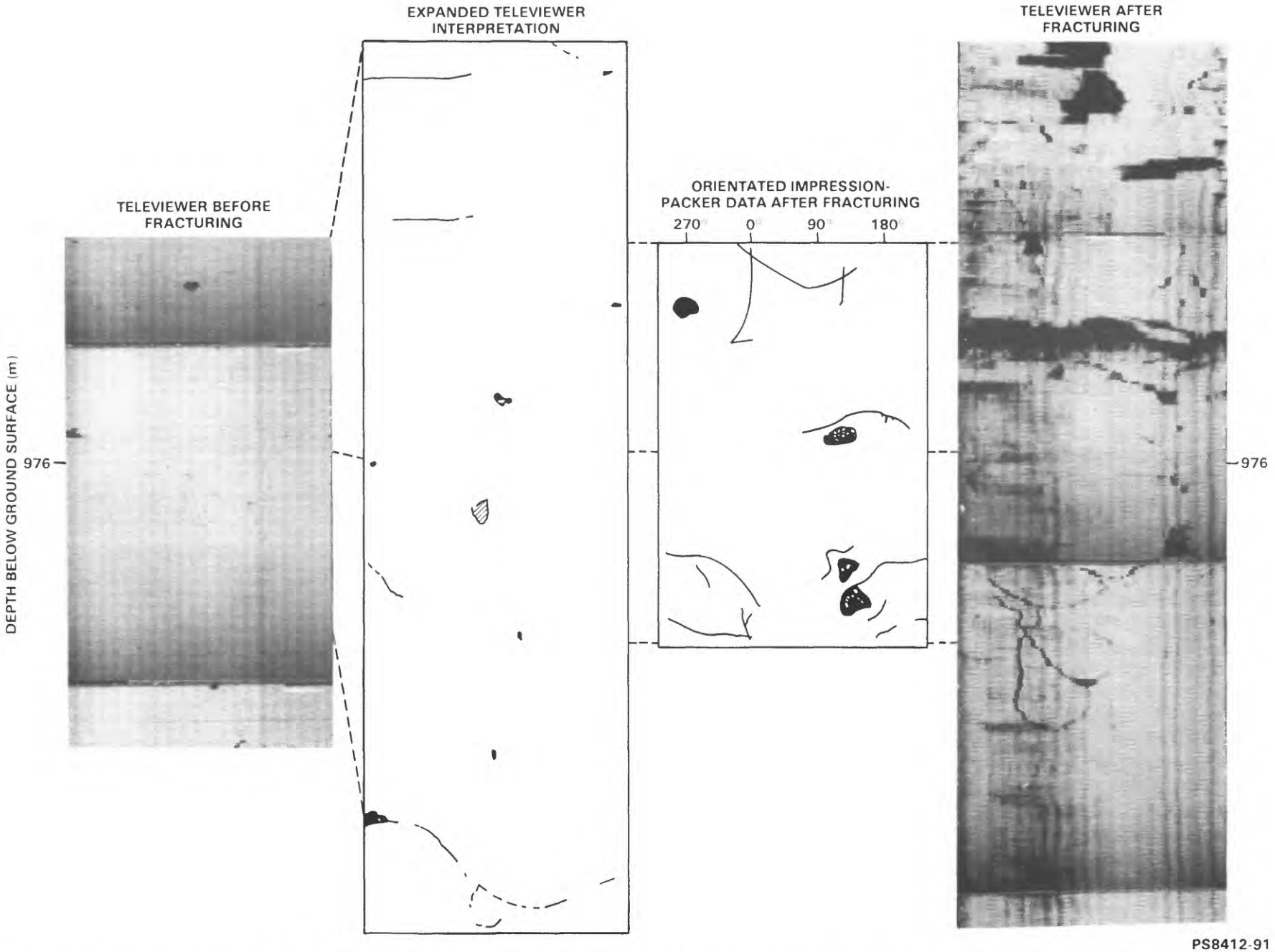

Figure 44. Televiewer logs obtained before and after hydraulic fracturing and post-fracture impression-packer tracing for induced fracture at a depth of about 976 meters in borehole DC-4.

ACOUSTIC-WAVEFORM LOGS

Acoustic-waveform logs were run in the Hanford boreholes in an effort to characterize fractures and unaltered rock located beyond the annulus of stress concentration around the boreholes. Various applications of acoustic-waveform logs in igneous and metamorphic rocks are described by Paillet (1980, 1983a, 1983b, and 1983c) and Paillet and White (1982). One of the primary applications of waveform logs is the interpretation of shear velocity. Acoustic transit-time logs are plots of the inverse of compressional velocity. The transit-time logs obtained during this study consistently showed that unaltered basalt of flow interiors was characterized by a transit-time of about 167 ± 3 μs/m, giving a compressional velocity of about 6.0 ± 0.1 km/s. Compressional and shear velocities for similar intervals of unaltered basalt were obtained from the digitized waveforms for comparison with the transit-time log. The waveforms were recorded with a 2-μs sampling rate, so that the seismic velocities determined from waveforms have somewhat less resolution than the compressional velocity determined from the transit-time log. Examples are given in figures 45 and 46. Two sets of waveforms at the near and far receivers corresponding to the interval of breakout-free and unfractured basalt at the top of figure 24 are shown in figure 45. The waveforms indicate the nature of the shear arrivals in the waveforms. Shear velocities generally are difficult to determine because they are superimposed on the earlier-arriving compressional wave. In the case of unfractured rock (fig. 45), shear arrivals could be picked by identifying the move-out in characteristic peaks and troughs in the wave signature, or by more sophisticated cross-correlation techniques, such as those described by Willis and Toksoz (1983) and Kimball and Marzetta (1984).

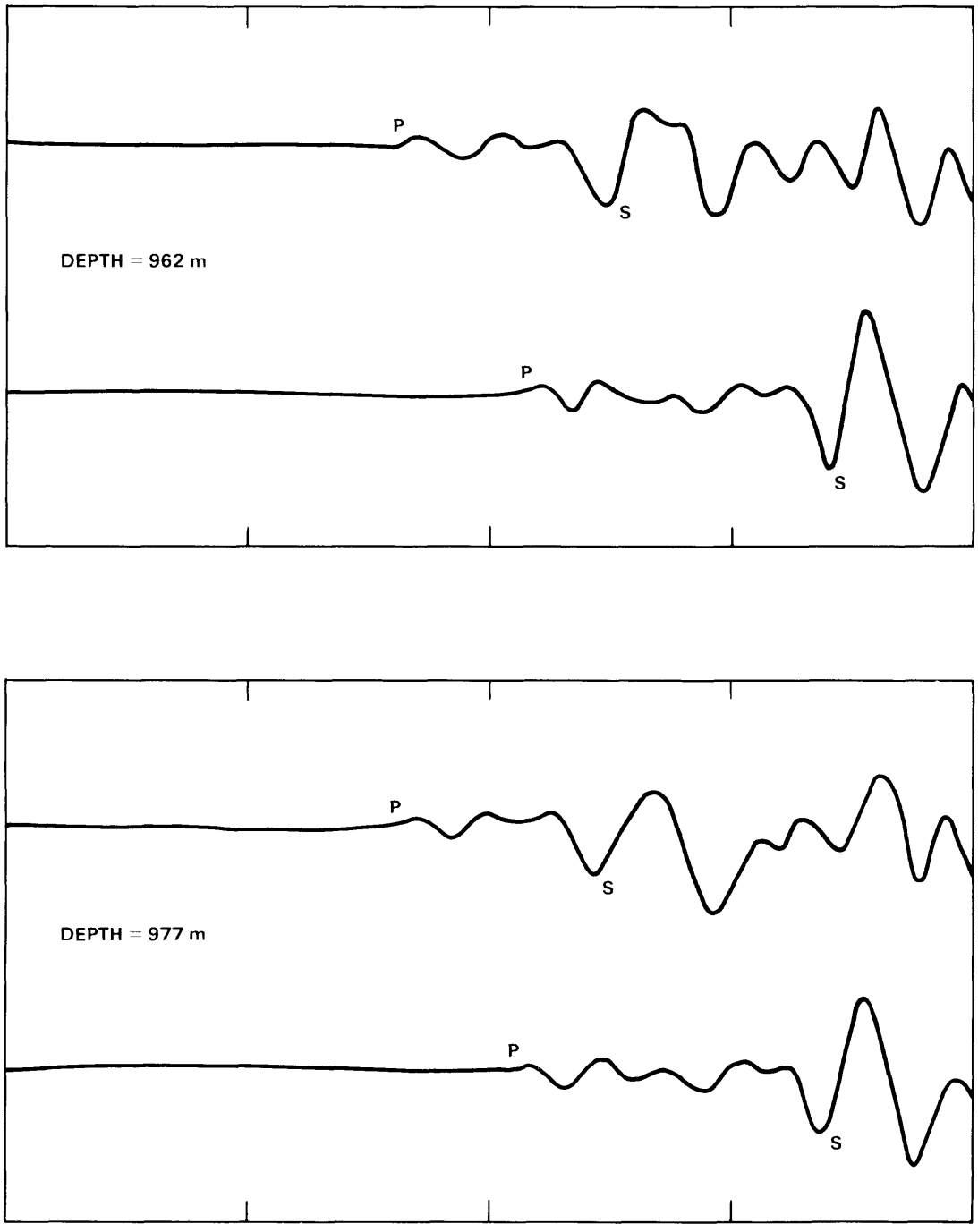

Figure 45. Diagrams showing representative samples of waveforms from unaltered and unfractured interior of flow illustrating character of shear-wave arrivals.

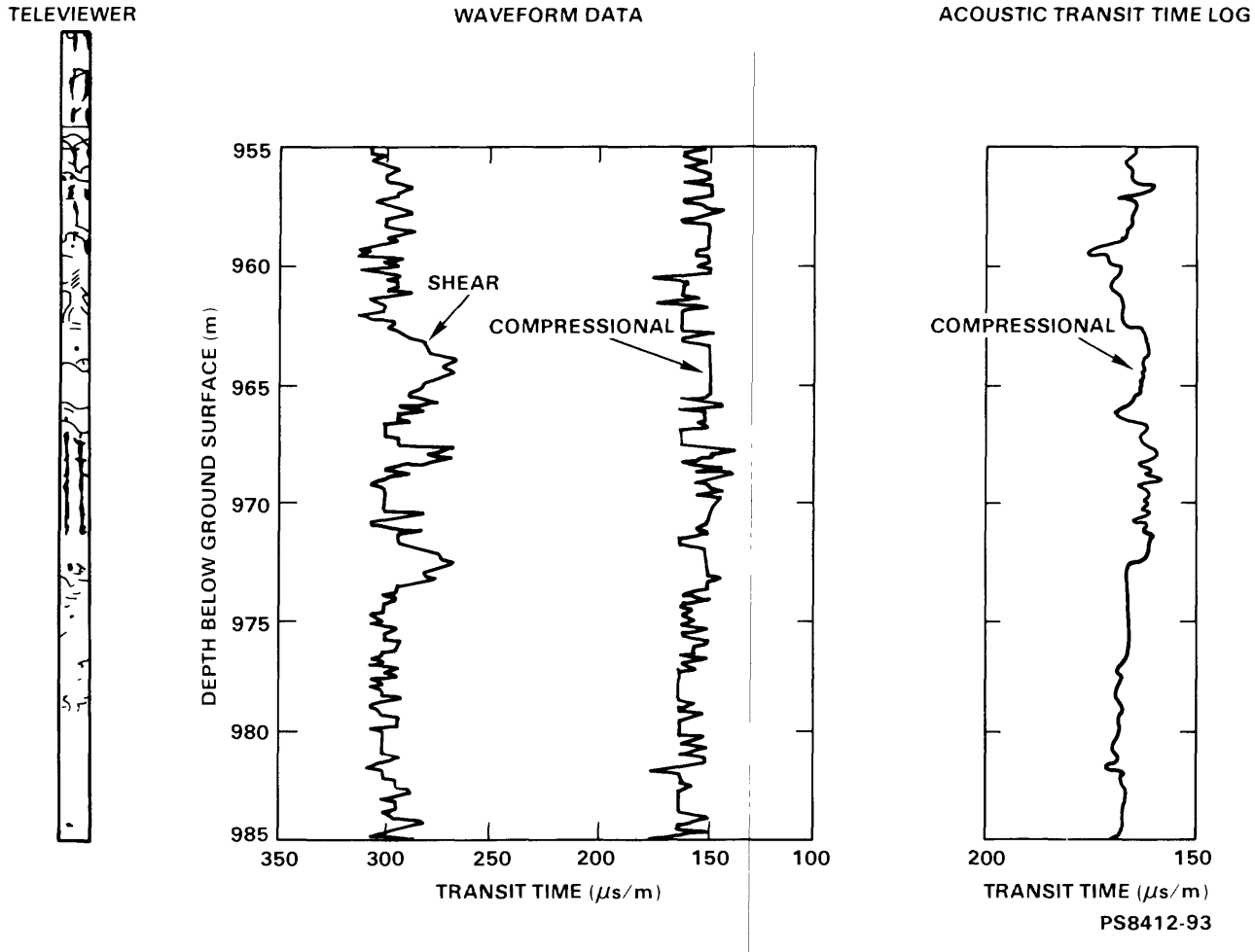

Figure 46. Televiewer log and diagrams showing example of seismic velocities picked from waveform records and acoustic transit-time log, borehole DC-4.

Shear velocities only could be recognized in the unaltered interiors of flows where shear waves propagate without much attenuation. Shear arrivals could not be measured in the interflows and altered flow tops. Shear attenuation could be substantial in these intervals because shear waves are not strongly excited when the Poisson ratio of rocks becomes large (White, 1965; Cheng and Toksoz, 1981).

The distribution of seismic velocities determined from the waveform logs are compared to the transit-time log for a representative interval of flow interior in borehole DC-4 in figure 46. Greater variability in the velocities determined from the waveforms indicates the somewhat lesser resolution imposed by the 2-μs sampling rate. The compressional velocity remains effectively constant throughout the prominent interval of nearly continuous borehole-wall breakouts at a depth of about 970 m. Computed shear velocities in this breakout zone appear to become somewhat faster, but inspection of the waveform data indicated this velocity could be induced by the effects of borehole-wall rugosity on the shear-velocity picking method, and did not represent a true increase in shear velocity.

Representative examples of the effect of lithology on the character of acoustic-waveform data are given in figures 47 to 49. Waveforms obtained for an interval in borehole DC-4 near and below at the bottom of the Cohassett flow are illustrated in figure 47. The interval of log shown in the figure begins in the interior of the flow beneath the Cohassett, extends through the altered and brecciated-flow top rock, and into the solid, unaltered basalt at the base of the Cohassett flow. This interval was selected for study to illustrate the effects of borehole-wall breakouts, vesicular rock, and unaltered-flow interior on waveform character. The large effect of the altered and brecciated-flow top on the waveforms is clearly indicated in figure 47. Waveform data for the unaltered-flow interiors at the top and bottom of the figure are extremely coherent by comparison. The interval of disturbed waveforms extends well below the flow top (Cross, 1983) in the published core description, but the much thinner interval, 985 to 987 m, of very attenuated acoustic signal seems to correspond very closely with the flow top in the core description.

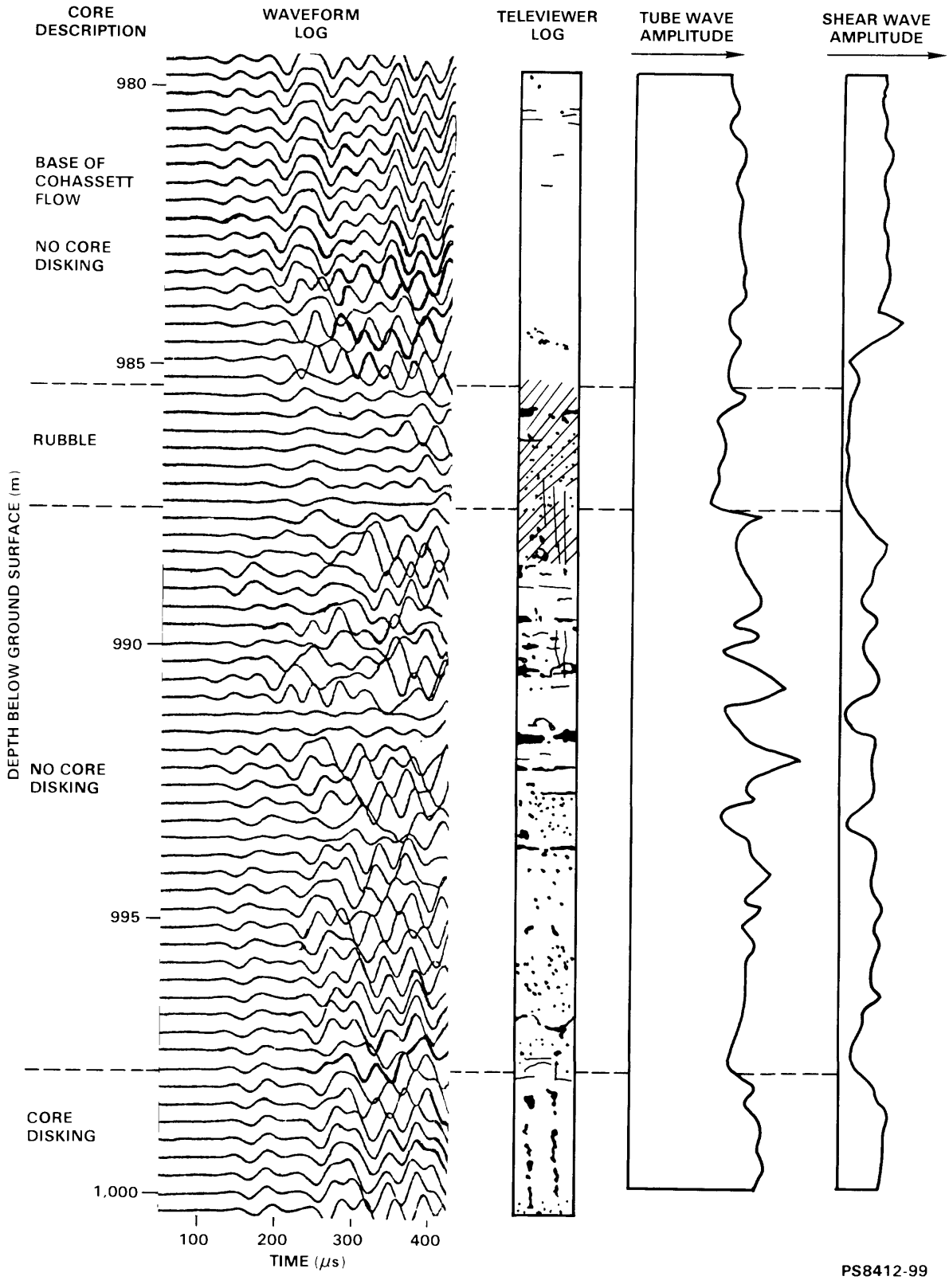

Figure 47. Acoustic-waveform, televiewer, and waveform-amplitude logs for a representative interval in borehole DC-4; waveforms indicate effects of borehole-wall breakouts, fractures, and altered flow tops on acoustic propagation.

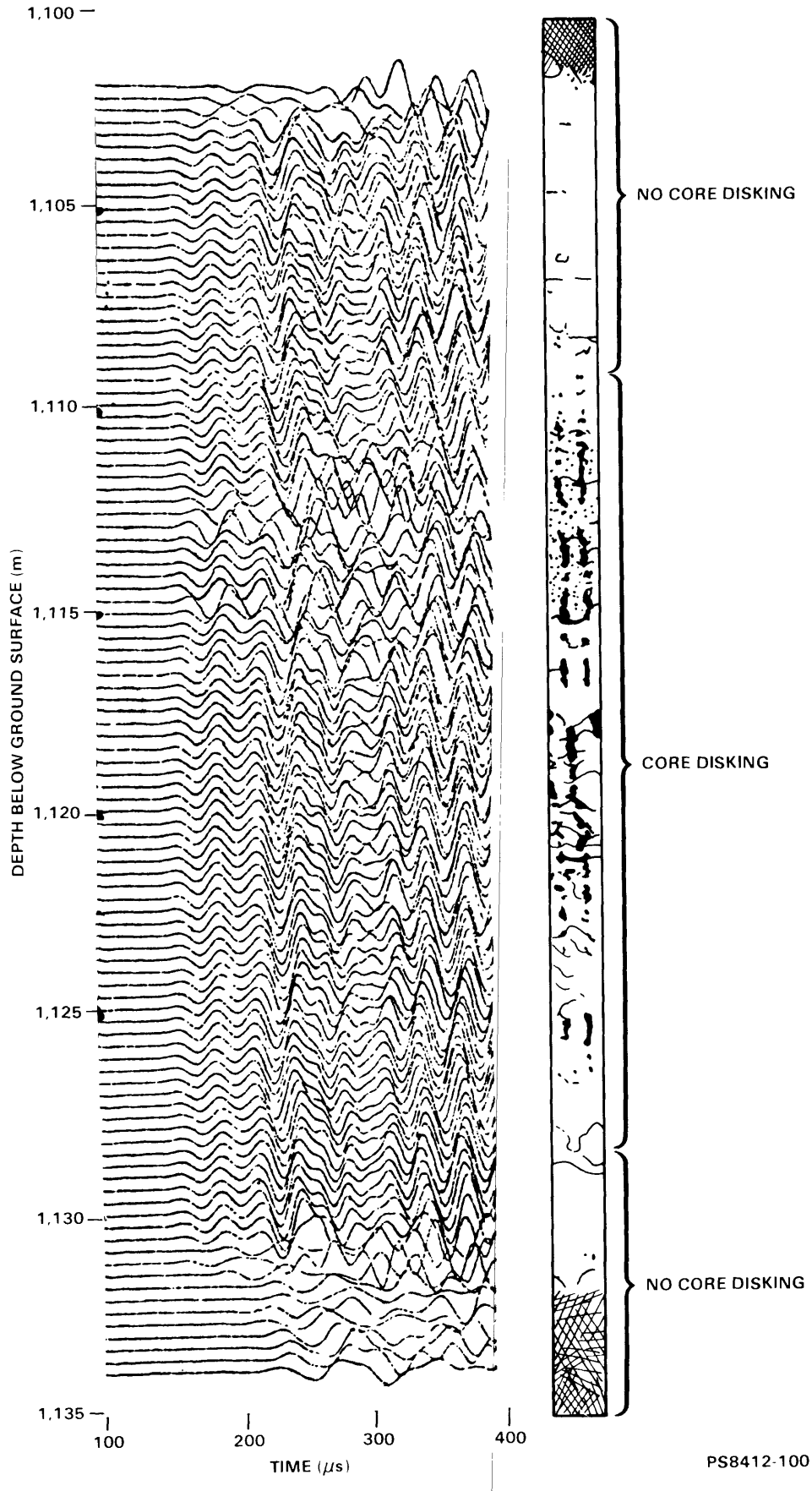

Figure 48. Waveform and televiewer logs for interval in borehole RRL-6; waveforms indicate effects of borehole-wall breakouts and vesicular zone on acoustic propagation along the borehole.

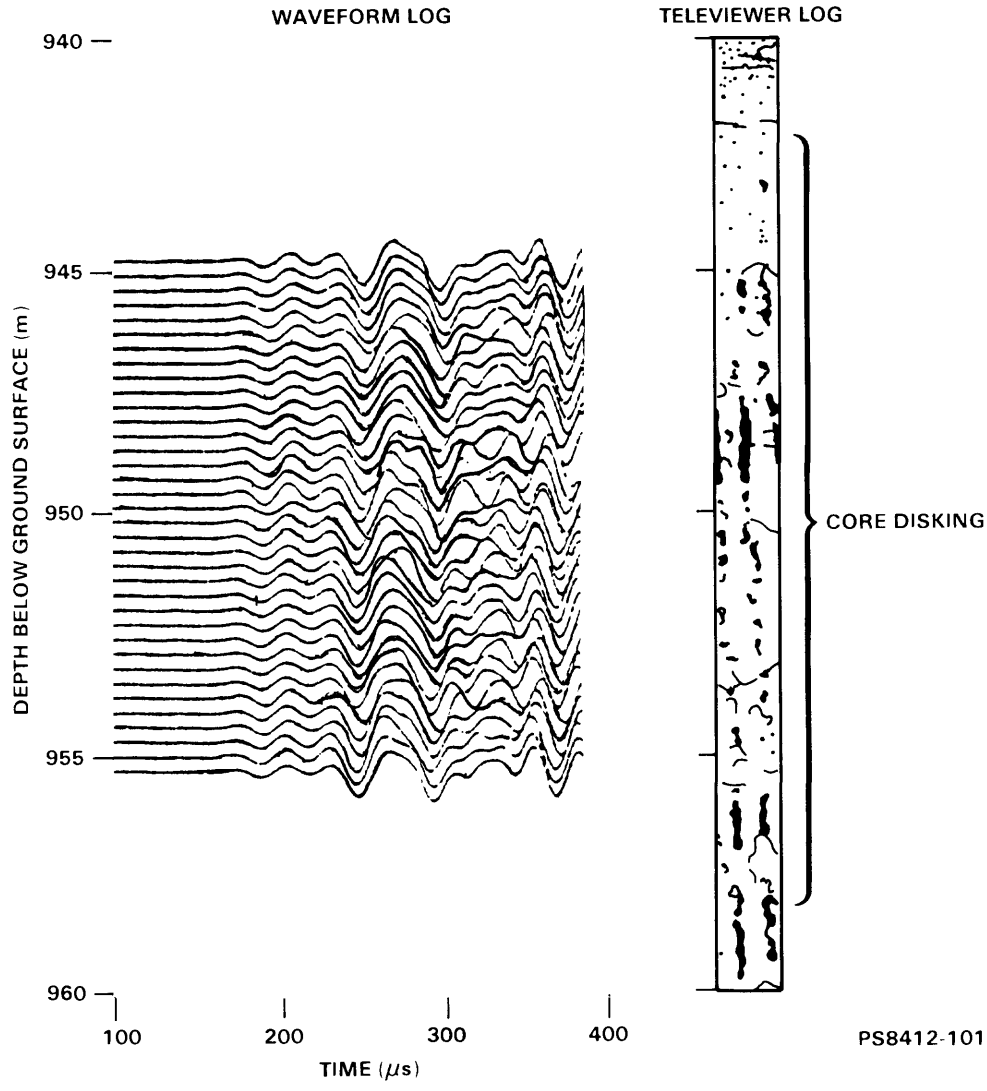

Figure 49. Waveform and televiewer logs for interval in borehole RRL-6; waveforms indicate effects of continuous and discontinuous borehole-wall breakouts on acoustic propagation along the borehole.

An especially important aspect of the data presented in figure 47 is the similarity of the waveforms near the top and bottom of the figure. The top of the figure corresponds to the base of the Cohassett flow, where the televiewer shows no sign of borehole-wall breakouts, and disking is not noted on core. The lower interval shows continuous breakouts that correspond very closely with the distribution of disking noted on the core description. Both continuous breakouts and continuous core disking extend above 1026 m, when the core depths are corrected to correspond with the U.S. Geological Survey logs. The waveforms for the intervals 1102 to 1108 m and 1116 to 1126 m appear nearly identical, and adjacent waveforms appear very coherent.

The effects of vesicular rock on the waveform logs is indicated by the interval just below 995 m in figure 47. The increasing porosity of the vesicular rock produces an increase in interval transit-time for both compressional and shear waves; however, it does not degrade the amplitude of the shear arrival away from the fractures as happens when there is a lack of interconnected pore space in the vesicular rock. Such unconnected pores do not allow for dissipation by flow through interconnections; therefore, they do not produce a pronounced increase in either compressional or shear-wave attenuation.

One of the conclusions presented by Paillet (1980, 1983b) in previous applications of waveform data to crystalline rock is the relationship between acoustic-waveform amplitude and borehole-wall permeability. This approach is based on the numerical results obtained by Rosenbaum (1974) and appears to involve the viscous-dissipation mechanism described for a generalized porous media by Biot (1956). Amplitude logs have been constructed for the waveform data presented in figure 47, and have been plotted next to the waveforms in that figure. The tube-wave amplitude log is based on the mean-square amplitude in a velocity window corresponding to the fundamental wave mode traveling along the borehole at a speed slightly less than the acoustic velocity of the borehole fluid (White, 1965). This mode apparently is sensitive to borehole-wall permeability, but can depend to a lesser extent on attenuation in the surrounding rock (Cheng and others, 1982). The tube-wave amplitude log appears virtually constant in the upper- and lower-flow interiors of figure 47. The very altered flow top (985 to 987 m) shows a nearly complete loss of shear amplitude, and a moderate decrease in tube-wave amplitude, which usually are caused by a lithologic effect associated with the very slow seismic velocities and substantial attenuation of the altered rock. The isolated lows in tube-wave amplitude that occur in the interval 990 to 995 m correspond with apparent fractures on the televiewer log. Such lows usually represent fracture permeability. Increases in tube-wave amplitude adjacent to these lows usually represent the effects of tube-wave reflection off fracture planes, although coherent reflections were not detected in visual inspection of the waveforms.

Two additional examples of waveform logs are given in figures 48 and 49. An interval in borehole RRL-6 with both vesicular rock (1110 to 1115 m) and extensive borehole-wall breakouts in the flow interior (1110 to 1125 m) is illustrated in figure 48. Waveforms for the flow interior appear very coherent except for two distinct anomalies at depth of about 1,113 and 1,115 m and a lower amplitude anomaly at a depth of 1,108 m. These anomalies are characteristic of fractures extending away from the borehole. Waveforms between these two anomalies have delayed arrivals due to the porosity of the vesicular rock, but have shear arrivals very similar in character to those of the unfractured rock above and below. Extensive borehole-wall breakouts in the interval from 1,117 to 1,125 m have very little effect on waveform coherence in comparison to the breakout-free intervals near the top and bottom of the flow.

An additional example of the ability of acoustic-waveform logs to investigate rock behind borehole-wall breakouts is shown in figure 49. The figure shows an interval in borehole RRL-6 containing a short section of continuous borehole-wall breakout, surrounded by a larger interval of discontinuous breakouts illustrating the nearly complete insensitivity of the compressional and shear arrivals to the presence of the breakouts. The one very small amplitude anomaly at a depth of 950 m probably is associated with the natural fracture indicated on the televiewer log at this depth.

SUMMARY

All televiewer and acoustic-waveform data presented here indicate the useful applications for acoustic logs in the characterization of the mechanical properties of rocks. The acoustic transit-time log provides an easy-to-run and very effective means for identifying unaltered interiors of flows. Perhaps the greatest problem noted here is the need to distinguish between the slow compressional velocities measured for unaltered but vesicular basalt, and the slow velocities and small amplitudes measured in the altered rock of flow tops and interflow deposits. Waveform logs appear to provide this distinction. Acoustic-waveform logs also provide the ability to investigate rock beyond the stress-concentration field around the immediate borehole wall, which appears to be especially important in cases such as this study where extensive intervals of borehole-wall breakout occur.

REFERENCES

Bell, J. S., and Gough, D. I., 1979, Northeast-southwest compressive stress in Alberta--Evidence from oil wells: Earth and Planetary Science Letters, v. 45, no. 2, p. 475-482.

Biot, M. A., 1956, Theory of propagation of elastic waves in a fluid-saturated porous solid, I--Low frequency range: Journal of the Acoustical Society of America, v. 28, no. 2, p. 168-178.

Chan, A. K., and Tsang, L., 1983, Propagation of acoustic waves in a fluid-filled borehole surrounded by a concentrically layered transversely isotropic formation: Journal of the Acoustical Society of America, v. 74, no. 5, p. 1605-1616.

Cheng, C. H., and Toksoz, M. N., 1981, Elastic wave propagation in a fluid-filled borehole and synthetic acoustic logs: Geophysics, v. 46, no. 7, p. 1042-1053.

Cheng, C. H., Toksoz, M. N., and Willis, M. E., 1982, Determination of in situ attenuation from full waveform acoustic logs: Journal of Geophysical Research, v. 87, no. B7, p. 5477-5484.

Cross, R. W., 1983, Deep borehole stratigraphic correlation charts and structure cross sections: Rockwell Hanford Operations Technical Report SD-BWI-DP-035, 130 p.

Davison, C. C., Keys, W. S., and Paillet, F. L., 1982, Use of borehole-geophysical logs and hydrologic tests to characterize crystalline rock for nuclear-waste storage, Whiteshell Nuclear Research Establishment, Manitoba, and Chalk River Nuclear Laboratory, Ontario, Canada: U.S. Department of Energy, issued by the U.S. Department of Commerce, National Technical Information Service, Report ONWI-418, 103 p.

Fordjor, C. K., Bell, J. S., and Gough, D. I., 1983, Breakouts in Alberta and stress in the North American plate: Canadian Journal of Earth Sciences, v. 20, no. 5, p. 1445-1455.

Gough, D. I., and Bell, J. S., 1981, Stress orientations from oil-well fractures in Alberta and Texas: Canadian Journal of Earth Sciences, v. 18, no. 2, p. 638-645.

Keys, W. S., and Sullivan, J. K., 1979, Role of borehole geophysics in defining the physical characteristics of the Raft River geothermal reservoir, Idaho: Geophysics, v. 64, no. 6, p. 1116-1141.

Kierstein, R. A., 1984, True location and orientation of fractures logged with the acoustic televiewer (including programs to correct fracture orientation): U.S. Geological Survey Water Resources Investigations Report 83-4275, 71 p.

Kimball, C. V., and Marzetta, T. L., 1984, Semblance processing of borehole acoustic array data: Geophysics, v. 49, no. 3, p. 274-281.

Lau, J. S. O., 1983, The determination of true orientations of fractures in rock cores: Canadian Geotechnical Journal, v. 20, no. 3, p. 221-227.

McGarr, A., and Gay, N. C., 1978, State of stress in the Earth's crust: Annual Review of Earth and Planetary Sciences, v. 6, p. 405-436.

Paillet, F. L., 1980, Acoustic propagation in the vicinity of fractures which interest a fluid-filled borehole: Society of Professional Well Log Analysts Annual Logging Symposium, 21st, Lafayette, La., Transactions, p. DD1-DD33.

----- 1983a, Acoustic character of hydraulic fractures in granite: Symposium on Rock Mechanics, 24th, American Institute of Mining, Metallurgical, and Petroleum Engineers, 1983, College Station, Tex., Proceedings, p. 327-334.

----- 1983b, Frequency and scale effects in the optimization of acoustic waveform logs: Society of Professional Well Log Analysts Annual Logging Symposium, 24th, Calgary, Alberta, Canada, 1983, Proceedings, p. U1-U25.

----- 1983c, Acoustic characterization of fracture permeability at Chalk River, Ontario: Canadian Geotechnical Journal, v. 20, no. 3, p. 468-476.

Paillet, F. L., and White, J. E., 1982, Acoustic normal modes in the borehole and their relationship to rock properties: Geophysics, v. 47, no. 8, p. 1215-1228.

Pickett, G. R., 1963, Acoustic character logs and their application in formation evaluation: Journal of Petroleum Technology, v. 15, no. 6, p. 659-667.

Plumb, R. A., 1982 Breakouts in the geothermal well, Auburn, N.Y.: EOS, Transactions, American Geophysical Union, v. 63, p. 1118.

Rosenbaum, J. H., 1974, Synthetic microseismograms--Logging in porous formations: Geophysics, v. 39, no. 1, p. 14-32.

Swanson, D. A., and others, 1979, Revisions in stratigraphic nomenclature of the Columbia River Basalt Group: U.S. Geological Survey Bulletin 1457-G, p. G1-G59.

White, J. E., 1965, Seismic waves--Radiation, transmission and attenuation: New York, McGraw-Hill, 380 p.

White, J. E., and Zechman, R. E., 1968, Computed response of an acoustic logging tool: Geophysics, v. 33, no. 2, p. 302-310.

Willis, M. E., and Toksoz, M. N., 1983, Automatic P and S velocity determination from full waveform digital acoustic logs: Geophysics, v. 48, no. 12, p. 1631-1644.

Zemanek, Joseph, and others, 1969, The borehole televiewer--A new logging concept for fracture location and other types of borehole inspection: Journal of Petroleum Technology, v. 21, no. 6, p. 762-774.

Zoback, M. D., and Haimson, B. C., 1982, Status of the hydraulic fracturing method for in situ stress measurements: Annual Symposium on Rock Mechanics 23rd, American Institute of Mining, Metallurgical and Petroleum Engineers, 1982, Berkeley, Calif., Proceedings, p. 143-156.

Zoback, M. D., Moos, Daniel, Matson, Larry, and Anderson, R. N., 1984, Wellbore breakouts and in situ stress: Journal of Geophysical Research, [in press].

Zoback, M. L., and Zoback, M. D., 1980, State of stress in the conterminous United States: Journal of Geophysical Research, v. 85, no. B12, p. 6113-6156.

☆U.S. GOVERNMENT PRINTING OFFICE:1986— 677-677 / 45104